The Role of Oxidative Stress in *C. elegans* Aging

Dissertation
Zur Erlangung des Grades
Doktor der Naturwissenschaften

Am Fachbereich Biologie
Der Johannes Gutenberg-Universität Mainz

Maike Thamsen
geb. am 4. Nov. 1980 in Rüsselsheim

Mainz, 2011

Tag der mündlichen Prüfung: 1. April 2011

TABLE OF CONTENTS

Index of Figures

Index of Tables

Contributions

The work described in this thesis represents peer-reviewed and published manuscripts (chapters 2 and 3), a submitted manuscript (chapter 4) and a published review (chapter 5). The work in chapter 2 was mainly done by the first author Caroline Kumsta. I did the ATP measurements and helped with the assessment of survival, movement and progeny production as well as the OxICAT experiments. The chaperone assay in chapter 3 was done by Fei Li and the measurement of GLN-3 by Caroline Kumsta. Chapter 4 has a shared co-first authorship with Daniela Knoefler, who did all Hyper experiments. Martin Koniczek developed the image quantification script for Hyper quantification. Ann-Kristin Diederich created the *daf-16* [*unc-54::HyPer*] strain. All work was performed under the guidance of Ursula Jakob.

Chapter 2 Effects of Oxidative Stress on Behavior, Physiology and the Redox Thiol Proteome of *Caenorhabditis elegans*

Caroline Kumsta, Maike Thamsen, Ursula Jakob

Manuscript	UJ (CK)
Figure 2-1	CK (**MT**)
Figure 2-2	CK
Figure 2-3	CK (**MT**)
Figure 2-4	CK
Figure 2-5	CK (**MT**)
Table 2-1	CK (**MT**)
Supplemental Figure 2-1	CK

Chapter 3 Is Overoxidation of Peroxiredoxin Physiolocially Significant?

Maike Thamsen, Caroline Kumsta, Fei Li, Ursula Jakob

Manuscript	UJ (**MT**)
Figure 3-1	**MT**/CK/FL
Figure 3-2	**MT**
Figure 3-3	**MT**

Chapter 4 Quantitative *In Vivo* Redox Sensors Uncover Oxidative Stress as an Early Event in Life

Daniela Knoefler*, Maike Thamsen*, Martin Koniczek, Ann-Kristin Diederich, Ursula Jakob

* authors contributed equally to this work

Manuscript	UJ (**MT**/DK)
Figure 4-1	**MT**
Figure 4-2	**MT**
Figure 4-3	**MT**
Figure 4-4	DK (MK)
Figure 4-5	DK (AKD/MK)
Table 4-1	**MT**
Table 4-2	**MT**
Supplemental Figure 4-1	DK (MK)
Supplemental Figure 4-2	DK
Supplemental Figure 4-3	DK (MK)
Supplemental Figure 4-4	DK (MK)
Supplemental Table 4-1	**MT**
Supplemental Table 4-2	**MT**
Supplemental Table 4-3	**MT**

Chapter 5 The Redoxome - Proteomic Analysis of Cellular Redox Networks

Maike Thamsen, Ursula Jakob

Manuscript	**MT** (UJ)
Figure 5-1	**MT** (UJ)
Figure 5-2	**MT** (UJ)
Figure 5-3	**MT** (UJ)

Abbreviations

°C	degrees Celsius
2D	two dimensional
ATP	adenosine triphosphate
BSA	bovine serum albumin
C. elegans	*Caenorhabditis elegans*
CGC	Caenorhabditis Genetics Center
CR	caloric restriction
CS	citrate synthase
Ctl	catalase
Cu	copper
CuCl2	copper chloride
Cys	cysteine
D. melanogaster	*Drosophila melanogaster*
Da	Dalton
DAB	denaturing alkylation buffer
Daf	defective dauer formation
DAz-2	4-(3-azidopropyl)cyclohexane-1,3-dione
DIGE	differential gel electrophoresis
DNA	deoxyribonucleic acid
DNPH	2,4-dinitrophenylhydrazine
DTT	dithiothreitol
Duox	dual oxidase
E. coli	*Escherichia coli*
EDTA	ethylenediaminetetraaetic acid
EFT	elongation factor
ETC	elctron transport chain
FOXO	forkhead box O
FUdR	fluorodeoxyuridine
g, mg, µg, ng	gram, milligram,microgram, nanogram
GAPDH	glyceraldehyde-3-phosphate dehydrogenase
GdnCl	guanidine hydrochloride
GLN-3	glutamine synthetase
Grx	glutaredoxin
GSH	glutathione
GSSG	oxidized glutathione
h	hour(s)
H_2O	water
H_2O_2	hydrogen peroxide
HPLC	high performance liquid chromatography
HSP	heat shock protein
IAM	iodoacetamide
IBP	irreversible biotinylation procedure
ICAT	isotope-coded affinity tag
IEF	isoelectric focusing
IGF-1	insulin-like growth factor 1

ILS	insulin-like signaling
IPG	immobilized pH gradient
JNK	c-Jun N-terminal kinase
kDa	kiloDalton
KH_2PO_4	monopotassium phosphate
l, ml, µl	liter, milliliter, microliter
LB	lysogenic broth
LC	liquid chromatography
let	lethal
M	molar
M, mM, µM, nM	molar, millimolar, micromolar, nanomolar
m, mm, µm, nm	meter, millimter, micrometer, nanometer
mA	milliampere
MAP kinase	mitogen-activated protein kinase
min	minute(s)
MLS	mean lifespan
mM	millimolar
MMTS	methyl methanethiosulfonate
Mn	manganese
MS	mass spectrometry
MSRA	methionine sulfoxide reductase A
N	nitrogen
n.d.	not determined
NADH	nicotinamide adenine dinucleotide
NADPH	nicotinamide adenine dinucleotide phosphate
NDPK	nucleoside diphosphate kinase
NF-kB	nuclear factor kappa B
NGM	nematode growth medium
$NO^{\bullet}$	nitric oxide
o/n	over night
O	oxygen
$O_2^{\bullet-}$	superoxide
$OH^{\bullet}$	hydroxyl radical
$ONOO^-$	peroxynitrite
PAB	polyadenylate binding protein
PCR	polymerase chain reaction
pI	isoelectric point
PKC	protein kinase C
PRDX-2	peroxiredin-2
prdx-2	peroxiredoxin-2 gene
PTEN	phosphate and tensin homolog
PUFA	polyunsaturated fatty acid
RNS	reactive nitrogen species
ROS	reactive oxygen species
RPL	large ribosomal protein
rpm	revolutions per minute
RPS	small ribosomal protein
RT	room temperature

SDS	sodium dodecyl sulfate
SE	standard error
SESN-1	sestrin
sesn-1	sestrin gene
S-NGM	super nematode growth medium
S-NO	S-nitrosylation
SO_2H	sulfinic acid
SO_3H	sulfonic acid
SOD	superoxide dismutase
SOH	sulfenic acid
Srx	sulfiredoxin
TBS	tris buffered saline
TCA	trichloroacetic acid
TCEP	tris(2-carboxyethyl)phosphine
Tris	tris(hydroxymethyl)aminomethane
Trx	thioredoxin
V, mV	Volt, millivolt
vol	volume
WT	wild type
YFP	yellow fluorescent protein
Zn	zinc

ABSTRACT

The free radical theory of aging postulates that aging is caused by damage induced by oxidative stress. Such stress is present when the production of reactive oxygen species (ROS) exceeds the cellular antioxidant capacity. Hydrogen peroxide (H_2O_2) is one of the most abundant ROS. It is produced as a by-product by several enzymes and acts as second messenger controlling the activity of numerous cellular pathways. To maintain H_2O_2 levels that are sufficiently high to allow signaling to occur, but low enough to prevent damage of cellular macromolecules, the production and removal of H_2O_2 must be tightly regulated.

When we investigated the effects of peroxide stress in the nematode *C. elegans*, we found that exogenous as well as endogenous peroxide stress causes age-related symptoms. We identified 40 target proteins of hydrogen peroxide that contain cysteines that get oxidized upon peroxide stress. Oxidation of redox-sensitive cysteines has been shown to regulate numerous cellular functions and likely contributes to the peroxide-mediated decrease in motility, fertility, growth rate and ATP levels. By monitoring the oxidation status of proteins over the lifespan of *C. elegans*, we discovered that many of the identified peroxide-sensitive proteins are heavily oxidized at distinct stages in life. As the free radical theory of aging predicts, we found oxidation to be significantly elevated in senescent worms. However, we were also able to identify numerous proteins that were significantly oxidized during the development of *C. elegans*. To investigate whether a correlation exists between developmental oxidative stress and lifespan, we monitored protein oxidation in long- and short-lived strains. We found that protein oxidation in short-lived *C. elegans* larvae was significantly increased. Additionally short-lived worms were incapable of recovering from the oxidative stress experienced during development which resulted in the inability to establish reducing conditions for the following reproductive phase. Long-lived *C. elegans*, on the other hand, did only experience a mild increase in protein oxidation in the developmental phase and were able to recover faster from oxidative stress than wild type worms.

Because many proteins that are sensitive to oxidation by H_2O_2 became oxidized in aging *C. elegans*, we monitored endogenous hydrogen peroxide concentrations over *C. elegans* lifespan and discovered that peroxide levels are significantly elevated in development. This suggests that the observed developmental protein oxidation is peroxide-mediated. The early onset of oxidative stress might be a result of increased metabolic activity in *C. elegans* development but could also represent the requirement of ROS dependent signaling events. Our results indicate that longevity is dependent on the worm's ability to cope with this early boost of oxidants.

1 OVERVIEW

1.1 Introduction

1.1.1 Why do we age?

To explain why we age, we first have to define what aging is. Aging can be described as the process of continuously growing older with a steady increase in mortality rate (Neafsey *et al.*, 1988). Aging is associated with a progressive physiological decline, including loss of fertility, viability and memory as well as a susceptibility to age-related diseases. But what exactly causes aging on a molecular level? The number of theories in aging research is overwhelming. One of the most popular theories is the free radical theory of aging, which claims that the accumulation of damage caused by reactive oxygen species (ROS) over time causes aging (see 1.1.2) (Harman, 1956). Other theories propose that hormonal regulation (Hammerman, 1987; Ho *et al.*, 1987; Sonntag *et al.*, 1999), accumulation of mutations (Szilard, 1959; Gensler & Bernstein, 1981) or metabolic rate (Pearl, 1928; Lints, 1989) determine life expectancy.

One of the aging theories that received more attention than others is the theory that accumulation of mutations in DNA is the cause of aging (Szilard, 1959; Gensler & Bernstein, 1981). It has been shown in many organisms that the extent of DNA mutations increases with age (Martin *et al.*, 1985; Lu *et al.*, 2004). It is, however, not clear if this is the cause or a consequence of aging. The mutation accumulation theory is supported by the fact that many diseases, which cause premature aging like Hutchinson-Gilford syndrome, have a defect in the DNA repair system as underlying cause (Martin & Oshima, 2000). If an accumulation of mutations causes aging, an increased mutation rate should thus accelerate aging while a decreased mutation rate should slow aging down. *In vivo* evidence, however, did not support these assumptions; neither increased mutation rates caused by radiation nor decreased levels of mutations by overexpressing genes involved in DNA repair mechanisms had any influence on lifespan (de Magalhaes, 2005).

Extending lifespan by hormonal therapies (e.g., growth hormone) is a popular anti-aging treatment. However, research studies in which the otherwise declining hormone levels were maintained, led to contradictory results. In humans, elevated growth hormone levels lead to healthier appearances but, on the downside, also correlate with increased risk of cancer (Blackman *et al.*, 2002; Liu *et al.*, 2007). In addition, an age-prolonging effect has never been shown. Studies in mice, which also investigated the anti-aging properties of

growth hormones yielded in equally conflicting results (Khansari & Gustad, 1991; Coschigano *et al.*, 2000; Laron, 2005).

The "rate of living theory" was proposed by Raymond Pearl in 1928 (Pearl, 1928). Based on the observation that small animals have higher metabolic rates than large animals and that the lifespan of smaller animals is usually shorter compared to large animals (Rubner, 1908), he suggested that lifespan is inversely proportional to an organism's metabolic rate. Although being the most popular aging theory for several decades, evidence to support the rate of living theory is scarce. Fruit-flies, nematodes and other organisms have a temperature-dependent lifespan (Lamb, 1968; Klass, 1977; Conti *et al.*, 2006). A lower cultivation temperature leads to a lower metabolic rate and therefore, as the theory claims, to an extension in lifespan. The rate of living theory does, however, not explain why animals, like rats and bats, which have comparable metabolic rates, differ dramatically in life span (Brunet-Rossinni & Austad, 2004). It has also been shown that long-lived mutants of several organisms including *C. elegans* do not have lowered metabolic rates (Braeckman *et al.*, 2002; Hulbert *et al.*, 2004; Hulbert *et al.*, 2007). Also not in agreement with the rate of living theory is that regular exercise which increases metabolic rate does not result in reduction of lifespan (Holloszy *et al.*, 1985; Pahor & Carbonin, 1995).

The free radical theory of aging provides a possible mechanism for aging on a molecular level. As most of the work presented here aims to connect oxidative stress with aging, the main proposition of this theory, this theory will be discussed in detail below.

1.1.2 The free radical theory of aging

Reactive oxygen species, like hydrogen peroxide (H_2O_2), superoxide ($O_2^{\bullet -}$), and hydroxyl radicals ($OH^{\bullet}$), are natural by-products of metabolism and can cause damage to basically all cellular macromolecules including DNA, proteins and lipids. The free radical theory of aging, which was postulated by Denham Harman in 1956, hypothesizes that the cellular accumulation of damaged macromolecules is the cause of aging (Harman, 1956).

1.1.2.1 Origin of reactive oxygen species

ROS have multiple intracellular sources with oxidative phosphorylation in the mitochondria being one of the main producers of oxidants (Lambert & Brand, 2009). Oxygen functions as the final electron acceptor in the electron transport chain (ETC), which is located in the inner membrane of mitochondria and is used to generate ATP. It is estimated that approximately 1% of the consumed oxygen is converted into ROS (Chance *et al.*, 1979;

Hansford *et al.*, 1997). ROS generation happens when electrons, which are transferred between the different complexes of the ETC, leak directly to oxygen in a process that results in the production of superoxide (Kowaltowski *et al.*, 2009). In addition to the components of the ETC, several enzymes also directly produce either superoxide or hydrogen peroxide in the cell. NADPH oxidases, for instance, are commonly expressed in macrophages and generate superoxide when stimulated by the engulfment of pathogenic bacteria (Jones, 1994). Hydrogen peroxide is generated as a by-product of numerous oxidases, including monoamine oxidase, xanthine oxidase and P450 oxidase (Lee *et al.*, 1977; Maker *et al.*, 1981; Meunier *et al.*, 2004).

The toxicity of reactive oxygen species depends largely on their reactivity with different kinds of cellular macromolecules, their reaction products and the cellular location where they are generated. While superoxide is thought to be limited to the site of its production, hydrogen peroxide readily diffuses through membranes and thus easily reaches different cells and organelles (Gus'kova *et al.*, 1984; Bienert *et al.*, 2006). Intracellular superoxide gets rapidly converted to hydrogen peroxide by superoxide dismutases (SODs) (see 1.1.2.3). It can however also react with nitric oxide ($NO^{\bullet}$) to form reactive nitrogen species (RNS) (Pryor & Squadrito, 1995). Superoxide itself is not very reactive but it has been shown to interact with and destroy iron-sulfur clusters of certain enzymes (Benov, 2001). Similar to superoxide, hydrogen peroxide is rather un-reactive. However, interaction with Fenton reagents rapidly convert H_2O_2 into highly reactive hydroxyl radicals (Winterbourn, 1995) which are extremely damaging and react instantaneously with DNA, lipids and proteins (Cheng *et al.*, 2002).

1.1.2.2 Damage caused by reactive oxygen species

Excessive ROS production or the inability of cells to adequately detoxify ROS leads to oxidative stress conditions, which are characterized by the disruption of the reducing environment of the cell. The transition into a more oxidizing environment is hazardous for many cellular components (Figure 1-1). In proteins, the sulfur-containing side chains of cysteine and methionine make these amino acids the most vulnerable to oxidative modifications (Davies, 2005). Methionine is easily oxidized to methionine sulfoxide (-SO) or methionine sulfone (-SOO). The thiol group in cysteines is oxidized to sulfenic acid (-SOH), which, due to its unstable nature, is either further oxidized to the irreversible sulfinic ($-SO_2H$) or sulfonic acid ($-SO_3H$), or forms reversible disulfide bonds (-S-S-) with nearby cysteine residues. The amino acids arginine, lysine, proline and threonine are prone to carbonylation,

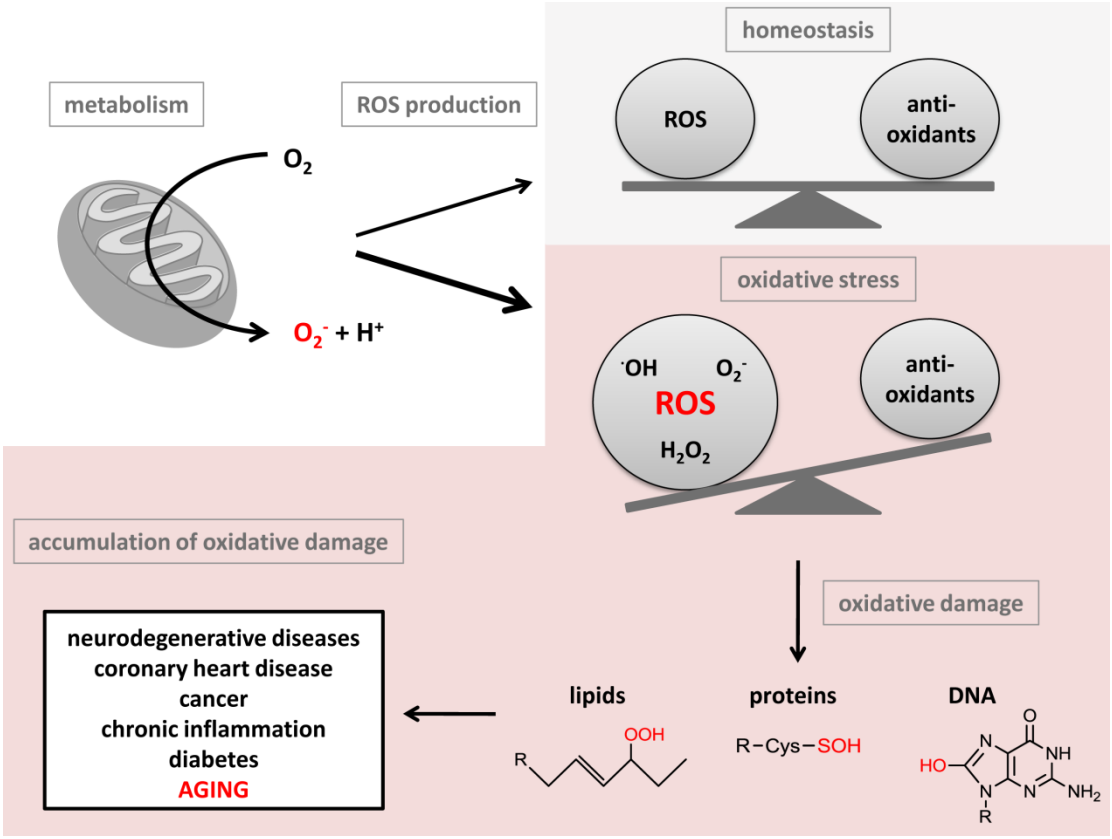

Figure 1-1 Origin and consequence of oxidative stress
Reactive oxygen species are by-products of normal metabolism. They are continuously detoxified by antioxidant systems to maintain cellular homeostasis. Oxidative stress occurs if the antioxidant defense can no longer contain the amount of ROS produced. Oxidative stress causes accumulating damage to DNA, lipids and proteins, and is thought to be involved in the development of numerous diseases and in aging (Essick & Sam, 2010).

the introduction of carbon monoxide, which often marks the protein for degradation by proteolysis (Nystrom, 2005).

In addition to causing oxidative damage to proteins, oxidative stress also affects DNA and lipids. Damage to DNA includes strand breakage and modification of bases and deoxyribose (Cooke *et al.*, 2003). The most common base modification, the formation of 8-hydroxy-2-deoxyguanosine, is a biomarker of oxidative stress (Shigenaga & Ames, 1991). Oxidative modification of lipids involves predominantly poly-unsaturated fatty acids (PUFA) in cell and organelle membranes, which are prone to peroxidation (Gardner, 1989).

Considering the numerous cellular points of attack, it is not surprising that oxidative stress interferes with many basic functions of a cell, including DNA replication, cell division, membrane integrity and cell signaling (Davies, 2000). To prevent oxidative damage every organism that is exposed to oxygen possesses a highly effective antioxidant machinery, designed to detoxify ROS and repair the damage.

1.1.2.3 Cellular antioxidant defense

Cells have a machinery of antioxidant proteins and mechanisms to combat oxidative stress and sustain the reducing environment of the cell. Most organisms invest large amounts of energy into their antioxidant defense system, illustrating its importance for maintaining proper cellular functions. Numerous enzymes catalytically remove ROS. Superoxide is eliminated by superoxide dismutases (SODs), which dismute superoxide into H_2O_2 and O_2 (Fridovich, 1995). SODs are present in all subcellular locations that produce superoxide and include Mn-SOD in mitochondria and Cu/Zn-SOD in cytoplasm and the extracellular space. Hydrogen peroxide which is produced by SODs and other enzymes (see 1.1.2.1) is detoxified by catalases and peroxidases such as peroxiredoxin and glutathione peroxidase. Catalases directly decompose hydrogen peroxide to water and oxygen. They have very high turnover numbers, which enable the enzymes to quickly remove large amounts of hydrogen peroxide (Chelikani *et al.*, 2004). Since the active site requires two H_2O_2 molecules, however, low concentrations of H_2O_2 negatively affect the detoxification ability of catalases. Peroxiredoxins, in contrast, are capable of removing hydrogen peroxide even when the oxidant is present at very low concentrations. They utilize active site cysteines to reduce H_2O_2 (Figure 1-2) (Hall *et al.*, 2009), which are, particularly in eukaryotic peroxiredoxins, highly prone to overoxidation. Overoxidation of the active site cysteine leads to the formation of sulfinic acid, which causes the inactivation of peroxiredoxins at high hydrogen peroxide concentrations (Rhee *et al.*, 2005). This inactivation of peroxiredoxins is thought be of physiological significance, as it allows transient ROS signaling to take place ("flood-gate theory") (Biteau *et al.*, 2003; Wood *et al.*, 2003). Specific sulfinic acid reductases called sulfiredoxins have been identified, which use ATP hydrolysis to reduce the overoxided cysteine and reactivate the peroxidase function of peroxiredoxins (Biteau *et al.*, 2003).

In addition to the aforementioned enzymatic antioxidants, numerous non-enzymatic systems play an important role in the cellular antioxidant defense as well. One of the most important non-enzymatic antioxidants is glutathione, a tripeptide that carries a free thiol group on a cysteine residue, which is used to directly reduce substrates (Mari *et al.*, 2009). Many other small molecule antioxidants are nutrients, which are often taken up with food. These include vitamin E, a lipid soluble vitamin which protects membranes from oxidative damage and vitamin C, which, among other functions, keeps iron and copper in their reduced state (Truscott, 2001).

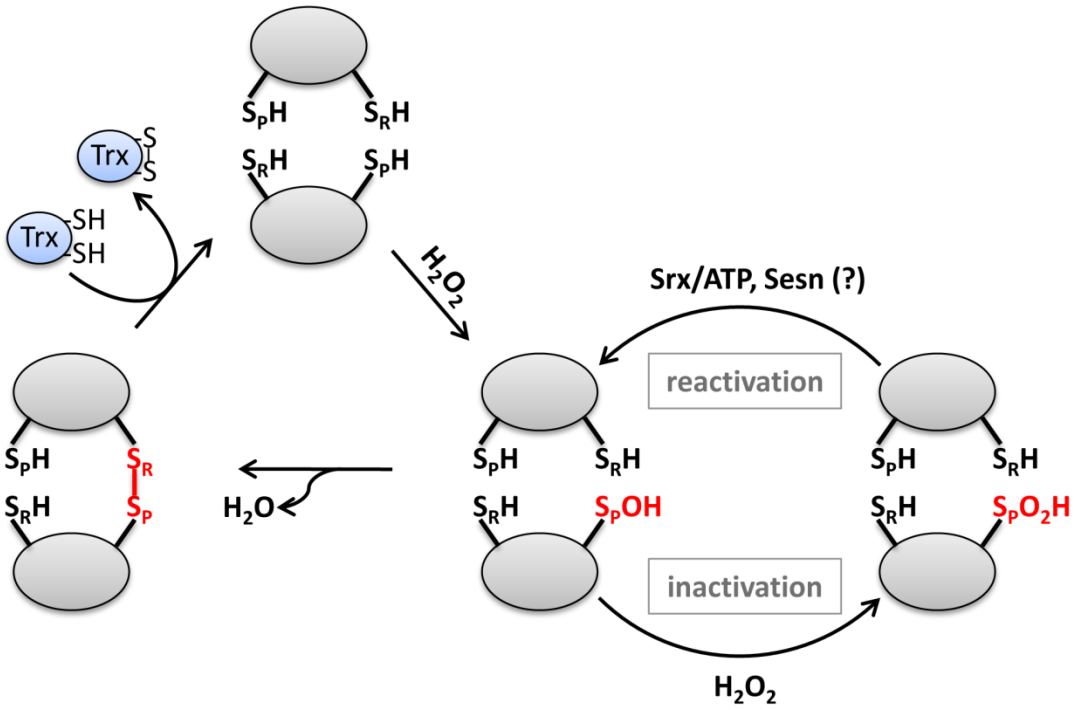

Figure 1-2 Catalytic cycle of peroxiredoxin
Peroxiredoxins are peroxidases that detoxify hydrogen peroxide and other peroxides. Typical 2-Cys peroxiredoxins contain two highly conserved cysteines. The peroxidatic cysteine (SP) reacts with hydrogen peroxide and forms a cysteine sulfenic acid (SOH) which gets attacked by the free thiol group of the resoving cysteine (SR) of another peroxiredoxin molecule. The two cysteines form a disulfide bond. The peroxiredoxin dimer gets separated by reduction of the disulfide bond by thioredoxin (Trx) or another reducing equivalent. Before the disulfide bond forms the sulfenic acid of the peroxidatic cysteine can get further oxidized by another hydrogen peroxide molecule to form cysteine sulfinic acid (SO2H). This happens more frequently if cellular peroxide concentrations are elevated. The overoxidation to cysteine sulfinic acid inactivates the peroxidase function of peroxiredoxin and is not reversible by reduction through thioredoxin. Two enzymes have been reported to reverse peroxiredoxin overoxidation. While sulfiredoxin (Srx) has been shown to have cysteine sulfinic acid reductase activity, research that tried to connect sestrin (Sesn) to the reduction of overoxidized peroxiredoxins is conflicting.

1.1.2.4 Studies to test the free radical theory of aging

It has been shown in many organisms that oxidative modifications of DNA, proteins and lipids increase with age (Pratico, 2002; Van Remmen *et al.*, 2003; Chakravarti & Chakravarti, 2007). Especially mitochondria, the organelles with the highest ROS production, are prone to oxidative damage (Van Remmen & Richardson, 2001). While the level of oxidatively modified DNA increases with age in both nucleus and mitochondria, mitochondrial DNA shows higher levels of oxidative damage than nuclear DNA (Van Remmen *et al.*, 2003). As organisms age, oxidative damage also increases in lipids, due to peroxidation, and in proteins causing malfunction and degradation (Pratico, 2002; Stadtman, 2006). If the free radical theory is accurate, it can be postulated that organisms with less

oxidative damage should live longer while animals with elevated levels of damage should live shorter. A straightforward way to experimentally test this correlation between oxidative stress and aging involves manipulation of ROS production, detoxification or the extent of oxidative damage, and determination of the effects on lifespan. A different approach is to monitor long- or short-lived mutants for either altered ROS concentrations, antioxidant capacity or oxidative damage to macromolecules.

By using these experimental approaches, extensive correlative evidence supporting the free radical theory of aging has been accumulated; fruit flies that overexpress cytoplasmic Cu/Zn-SOD and catalase, for instance, have a lifespan extension of over 30% and show less oxidative damage to proteins than wild type flies (Orr & Sohal, 1994). Female and male mice overexpressing catalase in mitochondria show an extension of lifespan as well as less oxidative damage to DNA (Schriner *et al.*, 2005). Long-lived mutant strains of *C. elegans* and *D. melanogaster* have been shown to produce elevated levels of antioxidant enzymes (Rose, 1989; Larsen, 1993; Hari *et al.*, 1998). Fruit flies that overexpress methionine sulfoxide reductase A (MSRA), an enzyme that re-reduces oxidized methionine residues, have an extended lifespan while MSRA knockout mice suffer from a shortened lifespan (Moskovitz *et al.*, 2001; Ruan *et al.*, 2002).

In contrast to these studies that support the free radical theory of aging, several other studies did not find a correlation between oxidative damage, antioxidant activity and lifespan. Nutritional supplementation with antioxidants was long thought to promote healthy aging but studies using controlled supplementation with various antioxidants did not report any conclusive results on lifespan extending or health promoting effects in humans (Bjelakovic *et al.*, 2004; Lee *et al.*, 2005; Pham & Plakogiannis, 2005) or other organisms (Morley & Trainor, 2001; Keaney *et al.*, 2004; Bass *et al.*, 2007). Furthermore, deletion of one or several of the known SOD genes in *C. elegans* has little or no effect on prolonging lifespan (Doonan *et al.*, 2008; Van Raamsdonk & Hekimi, 2009) and mice that overexpress different combinations of Mn-SOD, Cu/Zn-SOD and catalase do not experience any lifespan extension (Perez *et al.*, 2009). Also not in agreement with the free radical theory of aging is the fact that physical exercise, which is undeniable health promoting, causes production of free radicals and should therefore, according to the free radical theory of aging, shorten lifespan (Konig *et al.*, 2001). Despite the extensive research on the influence of ROS, oxidative stress and antioxidant capacity on aging and lifespan, the jury is still out on the question whether accumulation of oxidative damage is cause or consequence of aging.

1.1.3 *C. elegans* as model organism for aging research

Caenorhabditis elegans is a well-established model organism, which was introduced by Sydney Brenner in 1974 (Brenner, 1974). Its small size and low demands make the maintenance of *C. elegans* easy and inexpensive. *C. elegans* feed on bacteria, which can be spread on plates as food source. *C. elegans* hermaphrodites propagate by self-fertilization, which is convenient for growing large isogenic populations. Due to its transparent nature *C. elegans* is also well suited for experiments that involve imaging analysis.

Studying aging in *C. elegans* is advantageous because of its well-understood development, its short lifespan, the availability of established long- and short-lived mutant strains and the morphological and physiological signs that accompany its aging process, including arrested fertility, impaired movement and decreased pharyngeal pumping hindered feeding (Figure 1-3). The average lifespan of a worm is highly dependent on the cultivation temperature and ranges from about 20 days at 15°C to 10 days at 25°C.

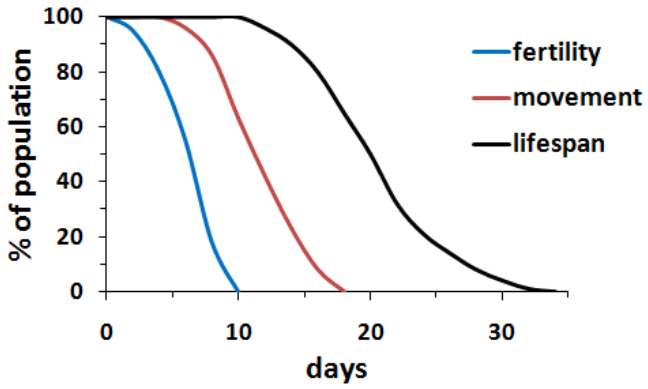

Figure 1-3 Aging and age-related characteristics in *C. elegans*
The average lifespan of *C. elegans* is approximately 20 days at a cultivation temperature of 15°C. Fertility declines rapidly after worms reach adulthood and the egg-laying-phase ceases after 10 days at the latest. Decline in motility precedes death. Worms stop to move in a fast sinusoidal manner usually between day 10 and 15 of adulthood.

The generation of a synchronized population of worms, which is important for aging research, is simple and involves treatment of worms with alkaline hypochloride, which kills worms but leaves eggs unaffected (Sulston, 1988). The eggs will hatch and generate an age-matched population of worms. *C. elegans* goes through four larval stages (L1 to L4) before reaching adulthood. If food is scarce, *C. elegans* enters a dauer stage between the larval stages L2 and L3, which is a very resistant, non-reproductive stage that allows worms to survive for many months (Burnell *et al.*, 2005). *C. elegans* is also a popular organism for caloric restriction studies, where a ~30% reduction in food intake leads to lifespan extensions of up to 50% (Lakowski & Hekimi, 1998).

A major regulator of aging and lifespan in *C. elegans* and other organisms is the insulin/IGF-1 signaling pathway, which is extremely conserved and very well studied in

worms (Kenyon, 2001). Signaling through the insulin/IGF-1 receptor leads to the phosphorylation of the FOXO transcription factor DAF-16, which results in its inactivation. Dephosphorylation of DAF-16, which occurs when insulin/IGF-1 signaling is inhibited leads to its activation. Active DAF-16 translocates into the nucleus where it promotes transcription of genes involved in stress defense like Mn-SOD, catalase and glutathione S-transferase (McElwee *et al.*, 2003). Therefore, deletion of the insulin/IGF-1 receptor *daf-2* in *C. elegans* leads to a lifespan that is twice as long as that of wild type worms while deletion of *daf-16* shortens *C. elegans* lifespan significantly (Figure 1-4) (Kenyon *et al.*, 1993).

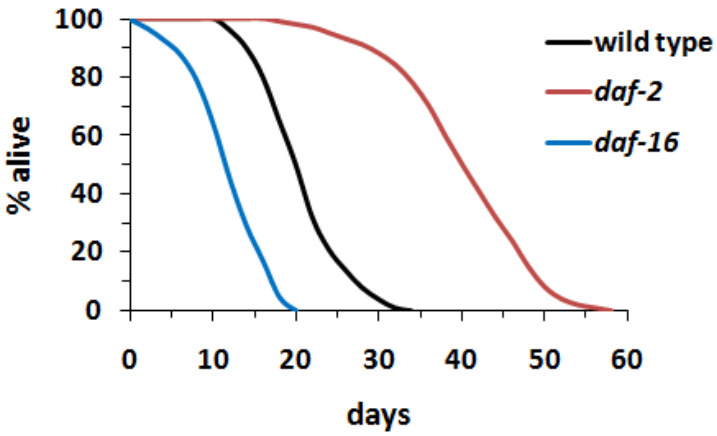

Figure 1-4 Lifespan of insulin/ IGF-1 signaling mutants
Knockout of the FOXO transcription factor DAF-16 in *C. elegans* leads to a substantially decreased lifespan. Knockout of the insulin/IGF-1 receptor DAF-2 leads to a 2-fold extension of lifespan in *C. elegans* (Kenyon et al., 1993).

1.1.4 Monitoring oxidative stress *in vivo*

To correlate oxidative stress to the aging process, techniques are necessary to measure cellular production of reactive oxygen species and oxidatively modified macromolecules. *In vivo* measurement of free radicals is challenging due to their short-lived nature and high reactivity. A common approach is the use of fluorescent dyes for the measurement of hydrogen peroxide levels in isolated mitochondria (Murphy, 2009). Due to the non-specificity of the dyes and the non-physiological conditions, however, this approach is thought to be not entirely reliable and might not reflect mitochondrial ROS production *in vivo*. A new opportunity emerged with the introduction of the hydrogen peroxide specific sensor protein HyPer, which allows measurement of hydrogen peroxide concentrations *in vivo* in real time (Belousov et al., 2006). In HyPer, the hydrogen peroxide sensing domain of OxyR is fused to the yellow fluorescent protein (YFP) and allows ratiometric detection of intracellular hydrogen peroxide levels. Our lab constructed transgenic worms, which express HyPer in the body wall muscle thus allowing muscle cell specific detection of hydrogen peroxide levels (see chapter 4).

A different approach to assess oxidative stress involves methods that measure oxidative damage. One such assay is, for instance, the comet assay, which determines DNA oxidation by utilizing the disorganized nature of damaged DNA (Singh et al., 1988). A popular method to detect lipid peroxidation is by iodine liberation using the oxidizing capacity of lipid peroxides (Halliwell & Chirico, 1993). A variety of different methods exist to detect oxidatively damaged proteins. One very common method measures protein carbonylation by the specific reaction of protein carbonyls with 2,4-dinitrophenylhydrazine (DNPH) and subsequent visualization using western blot analysis with anti-DNPH antibodies (Nakamura & Goto, 1996). These carbonylation measurements have, however, significant limitations since they are not suited to quantify the extent of protein oxidation, are often unable to identify the modified proteins and do not allow to make predictions about whether the oxidative modification will affect the function of the protein. Our lab has recently developed a new mass spectrometric technique called OxICAT, which precisely quantifies the oxidation status of redox-sensitive protein thiols *in vivo*, using this information as sensitive read-out for the presence of increased ROS levels. Redox sensitive proteins contain cysteines that are prone to oxidation and work as sensors of oxidative stress. The oxidation of redox-sensitive cysteines often regulates the activity of proteins. By using OxICAT, we are able to identify oxidation-sensitive proteins and their affected cysteines and predictions can be made about the extent to which the activity of proteins and the pathway they are part of is altered (Leichert et al., 2008).

1.1.4.1 Monitoring thiol oxidation using OxICAT

The thiol trapping technique OxICAT is based on the labeling of free thiol groups with isotope-coded affinity tag (ICAT) (Gygi *et al.*, 1999). The ICAT tag contains an iodoacetamide group that irreversibly alkylates free thiols in cysteines, a linker region that is available in a light isoform (^{12}C-ICAT) and a 9 Da heavier isoform (^{13}C-ICAT), which makes them distinguishable using mass spectrometry, and a cleavable biotin tag. By using OxICAT, the simultaneous quantification of the *in vivo* oxidation state of hundreds of proteins is possible.

To monitor thiol oxidation in proteins of *C. elegans*, we extracted proteins using acid precipitation, which stops all thiol-disulfide exchange reactions and prevents non-specific air-oxidation during sample preparation. The labeling steps are done successively; in the first step all free thiols, i.e., *in vivo* reduced cysteines, are labeled with light ICAT (Figure 1-5). Then, all *in vivo* oxidized thiols are reduced using the reductant tris(2-carboxy-ethyl)phosphine (TCEP) and subsequently labeled with heavy ICAT. Proteins are digested

with trypsin, ICAT labeled peptides are purified using the biotin affinity tag and high performance liquid chromatography (HPLC) and mass spectrometry (MS) are performed to separate peptides by mass and time of elution. Partially oxidized peptides, whose cysteine are labeled either with light ICAT (i.e, *in vivo* reduced) or with heavy ICAT (*in vivo* oxidized), will elute at the same time but with a mass difference of 9 Da or multiples of 9 Da depending on the number of oxidized cysteines in the peptide. The intensity of the light and heavy peak allows the use of a ratiometric quantification of the *in vivo* oxidation status of the peptide. The peptides are identified by performing MS/MS analysis.

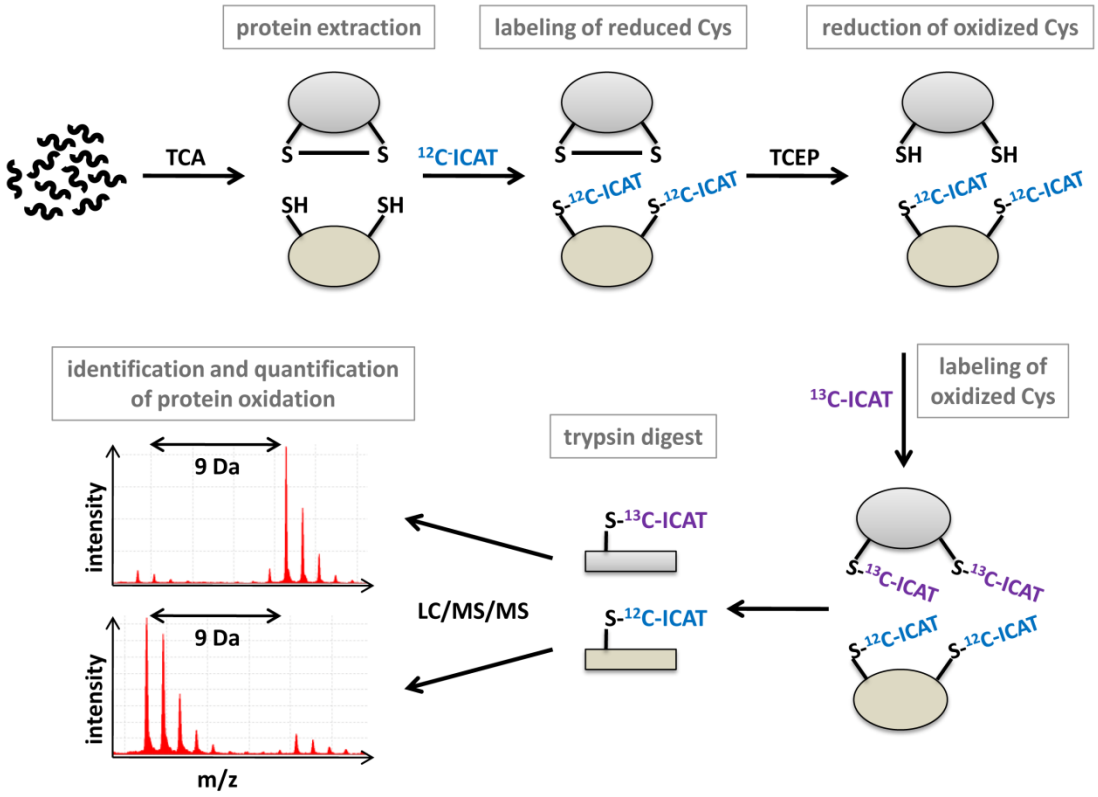

Figure 1-5 Using OxICAT to identify oxidized proteins
The thiol trapping technique OxICAT is used to identify and quantify oxidative thiol modifications in proteins. Proteins are extracted using whole worm lysates of *C. elegans* with trichloroacetic acid (TCA) precipitation. Free cysteine thiols get irreversibly labeled with light ^{12}C-ICAT. Subsequently all oxidized cysteines are reduced with the reductant TCEP and then labeled with heavy ^{13}C-ICAT. LC/MS is performed after trypsin digest of proteins and purification of all ICAT labeled peptides. Heavy ^{13}C-ICAT labeled peptides with cysteines that were oxidized are 9 Da heavier than light ^{12}C-ICAT labeled, formerly reduced peptides. Upon the intensity of the light and heavy peaks, the oxidation of each peptide can be quantified. Using MS/MS analysis the peptides are identified and assigned to the according proteins.

1.2 Objective

The aim of my thesis was to study the role of oxidative stress in aging with the main objective being to use quantitative redox proteomics as read-out for the onset and extent of cellular oxidative stress conditions. By comparison with short- and long-lived mutants of *C. elegans*, we wanted to test the free radical theory of aging and investigate whether a correlation exists between oxidative stress and lifespan.

Oxidation of proteins often affects the thiol-containing amino acid cysteine. It has been shown that cysteine oxidation does not occur randomly; instead it is a very selective process, which particularly affects redox-regulated proteins (Nishimura *et al.*, 1976; Le Moan *et al.*, 2006). Rapid oxidation of their cysteine residues under conditions of increased ROS levels affects the function of these proteins, and thus the function of the pathway that the proteins are part of. Therefore the identification of redox-regulated proteins as well as understanding how altered ROS levels will change their function will help elucidate how ROS affect signaling pathways, metabolism and cellular antioxidant systems and ultimately reveal the role that reactive oxygen species play in aging.

A well-known redox-regulated protein is the peroxidase peroxiredoxin. It contains a redox-sensitive cysteine, whose oxidation status regulates the function of the protein. One of our goals was to investigate the role of cysteine oxidation in *C. elegans* peroxiredoxin-2 (PRDX-2). It has been shown in other organisms that overoxidation of peroxiredoxin's peroxidatic cysteine to sulfinic acid leads to a switch from peroxidase to chaperone function (Kumsta & Jakob, 2009). The protein thus has the potential to protect other proteins in conditions of oxidative stress. Besides investigating the relevance of peroxiredoxin's different functions in *C. elegans,* we were also interested in the role of PRDX-2 in aging. Being one of the major antioxidant enzymes, PRDX-2 should have a substantial influence on lifespan. Indeed it has been shown that a knockout of PRDX-2 leads to a temperature dependent decrease in lifespan (Olahova *et al.*, 2008). We wanted to investigate the effect of a *prdx-2* knockout further, by examining if the endogenous peroxide stress causes physiological and behavioral changes that are also observed in aging and identify proteins that are affected by peroxide stress and possibly lead to the shortened lifespan.

The redox proteomic technique OxICAT allows identification of proteins that are prone to oxidation including their affected cysteines. OxICAT is also used for the quantification of overall protein thiol oxidation which provides an insight into general cellular redox homeostasis. To evaluate the role of hydrogen peroxide in aging we wanted to identify proteins that become oxidized by peroxide stress and compare them to proteins

that are affected by aging. With the identification of oxidation-sensitive proteins insight is gained into signaling pathways and cellular processes that are targets of oxidative stress.

The investigation of overall redox conditions at different stages of *C. elegans* lifespan allows determination of onset and extent of oxidative stress in aging. According to the free radical theory of aging thiol oxidation should increase in aging *C. elegans* and also short-lived worms should experience higher levels of oxidation than long-lived worms. Our goal was to examine oxidative stress levels and thiol oxidation in wild-type *C. elegans* as well as the short-lived strain *daf-16* and the long-lived strain *daf-2* and see if oxidation levels correlate with their lifespan. Besides the assessment of temporal changes of protein oxidation in *C. elegans*, the evaluation of spatial aspects of oxidative stress was of further interest. With the analysis of expression sites of oxidation-sensitive proteins the identification of cells and tissues in *C. elegans* that are particularly prone to oxidation is possible.

1.3 Results

1.3.1 Hydrogen peroxide stress causes progeric phenotypes in *C. elegans*

As a first assessment to investigate the impact of oxidative stress on *C. elegans*, we exposed a synchronized population of wild type worms at the L4 larval stage to a short-term peroxide treatment and monitored worms for the remainder of their life. The oxidative stress treatment consisted of a 30 min incubation of worms in either 6 or 10 mM H_2O_2. This short-term oxidative stress treatment was found to be non-lethal and does not affect the mean lifespan of wild type *C. elegans* (Fig. 2-1A). It does, however, cause severe behavioral and physiological symptoms, which include limited movement, a decline in progeny production and pharyngeal pumping and decreased growth rate and ATP levels (Fig. 2-1B-G). We found that worms recover within 2 to 3 days after the oxidative insult, suggesting that effective antioxidant defense and cellular repair systems exist, which eliminate excessive ROS and repair the oxidative damage. One of the systems that appear to be involved in the regeneration of worms is peroxiredoxin-2, which is a highly abundant protein and plays a major role in the detoxification of hydrogen peroxide. We found that deletion of *C. elegans* PRDX-2 leads to changes that are very similar to the changes observed in peroxide-treated worms, including a temperature-dependent shortening of lifespan, decreased growth rate and pharyngeal pumping as well as a reduced brood size and ATP levels (Fig. 2-2; Fig. 3-2). These physiological changes are very similar to the changes observed in senescent worms

(Huang *et al.*, 2004; Houthoofd *et al.*, 2005) suggesting that at least some of these changes might be due to the accumulation of intracellular peroxide.

1.3.2 Identification of hydrogen peroxide sensitive target proteins

To identify cellular targets of hydrogen peroxide that might cause the oxidative stress-mediated phenotypes that we observed, we conducted OxICAT experiments with wild type and *prdx-2* deletion worms before and after hydrogen peroxide treatment. The goal was to find proteins which contain redox-sensitive cysteines that are specifically oxidized upon stress treatment. We were able to identify 40 proteins with highly redox-sensitive cysteines. Proteins that were affected were found to be involved in motility and ATP metabolism as well as in protein translation and cellular homeostasis (Fig. 2-5; Table2-1), suggesting that at least some of the changes that we observed are caused by the oxidative modification of key proteins. The wide range of peroxide sensitive proteins that we identified also revealed that peroxide stress affects many different cellular functions and pathways.

1.3.3 Reduction of overoxidized peroxiredoxin *in vivo*

We could show that deletion of PRDX-2 in *C. elegans* eliminated the worm's ability to recover from exogenous oxidative stress treatment. At the same time, however, we observed that PRDX-2 is rapidly overoxidized by this treatment, suggesting that its peroxidase activity is quickly inactivated. To assess whether the regeneration of *C. elegans* from oxidative stress correlates to the recovery of reduced, peroxidase-active PRDX-2 or requires the chaperone function of this enzyme (Jang *et al.*, 2004), we monitored the recovery of reduced PRDX-2 after oxidative stress treatment *in vivo*. Reduced and overoxidized peroxiredoxin can be separated by 2D gel electrophoresis due to their differences in isoelectric points. We found that over 50% of PRDX-2 molecules were overoxidized upon oxidative stress treatment and recovery proceeded very slowly (Fig. 3-2A). After 22 hours a third of PRDX-2 was still in the overoxidized state.

Sulfiredoxin is an enzyme found in many organisms, which functions as a reductase of overoxidized peroxiredoxin (Biteau *et al.*, 2003). *C. elegans* does not possess a sulfiredoxin homolog, which either indicates that other proteins might take over the function of sulfiredoxin or that the overoxidation of peroxiredoxin is not physiologically relevant in *C. elegans*. One other group of proteins, which has been suggested to replace sulfiredoxins in organisms lacking this enzyme, are sestrins, a family of highly conserved proteins that are

upregulated under oxidative stress conditions in *C. elegans* and other organisms (Budanov *et al.*, 2004). We found that *C. elegans* encodes one sestrin homolog, SESN-1, whose existence might explain the lack of sulfiredoxin. We tested recovery of reduced peroxiredoxin after oxidative stress treatment in a *sesn-1* deletion strain. Against our expectations, *sesn-1* mutant worms did not exhibit significantly increased levels of overoxidized PRDX-2 nor was the ability to regenerate reduced peroxiredoxin inhibited (Fig. 3-2B). These results suggested that *C. elegans* SESN-1 is not involved in the reduction of overoxidized PRDX-2. The inability of sestrins to recover reduced peroxiredoxins also agreed with recent work by Woo *et al*., who found no sulfinic acid reductase activity for sestrin in cell cultures (Woo et al., 2009).

1.3.4 Physiological role of peroxiredoxin overoxidation

To investigate the connection between oxidative stress, peroxide detoxification and aging, we monitored the overoxidation of peroxiredoxin in an untreated, synchronized population of *C. elegans*. We were unable to detect a significant amount of overoxidized peroxiredoxin at any time point in *C. elegans* lifespan (Fig. 3-3A) suggesting that under normal physiological conditions, *C. elegans* is not exposed to peroxide concentrations that are high enough to cause PRDX-2 overoxidation. The *sesn-1* deletion strain showed comparable results (Fig. 3-3B). These results suggest that overoxidation of *C. elegans* peroxiredoxin does not occur to a significant extent *in vivo* implying that the chaperone activity exerted by overoxidized PRDX-2 (Fig. 3-1) does not play a significant physiological role in *C. elegans*.

1.3.5 Establishing a thiol oxidation baseline in *C. elegans*

To determine onset, extent and targets of reactive oxygen species during the lifespan of *C. elegans*, we first established a thiol oxidation baseline, which was generated by determining the overall thiol oxidation in young adult wild type worms. The oxidation status of proteins was quantified by performing OxICAT analysis on a synchronized population of worms cultivated at 15°C on day 2 of adulthood. The redox status of 170 thiol-containing peptides was analyzed. We found that the majority of identified protein thiols showed a very low oxidation of less than 20% (Fig. 4-1; Suppl. Table 4-1). Analysis of the subcellular localization of the identified proteins revealed that cytosolic, mitochondrial and nuclear proteins were largely reduced while most of the highly oxidized proteins belonged to the category of secreted proteins, known to be stabilized by disulfide bonds (Fig. 4-1; Suppl. Table 4-1) (Moir & Mao, 1990).

1.3.6 Biphasic pattern of thiol oxidation in aging *C. elegans*

After we determined the baseline thiol oxidation state in young adult worms, we evaluated when and to what extent proteins become oxidized during the lifespan of *C. elegans*. We therefore monitored the oxidation of the previously identified protein at 5 different time points by subjecting them to OxICAT analysis. The early developmental stage L2 and the last developmental stage L4 represent pre-reproductive stages. Thiol oxidation at day 2 of adulthood, which previously served as baseline, represents fertile adult worms, while samples taken at day 8 and at day 15 should provide insight into the oxidation level in aging worms. At day 8 of adulthood most worms have stopped reproduction whereas at day 15, advanced aging can be observed as a severe decline in movement in the majority of worms.

We quantified the oxidation state of the identified proteins and clustered the proteins into groups according to their oxidation profile. The majority or proteins did not significantly alter their redox status throughout the lifespan of *C. elegans* (Fig. 4-2, clusters 1 to 3; Suppl. Table 4-2). A subset of proteins (30%), however, showed dramatic changes in their oxidation state when tested at different times during *C. elegans'* lifespan (Fig. 4-2, clusters 4 to 8; Suppl. Table 4-2). While only a few proteins followed the prediction of the free radical theory of aging with a steady increase in oxidation (Fig. 4-2, cluster 4; Table 4-1A, Suppl. Table 4-2), the majority of proteins showed increased oxidation in two separate phases of *C. elegans* lifespan (Fig. 4-2, cluster 5 to 8; Table 4-1B, Suppl. Table 4-2). Thiol oxidation was significantly increased in late development, dropped to low levels in the reproductive phase of early adulthood and increased again in aging worms. While the observation that thiol oxidation increases in aging worms agrees well with the free radical theory of aging and might be connected to oxidative stress conditions in old worms, occurrence of oxidized proteins during development has not been observed before.

1.3.7 Correlation between thiol oxidation and aging

To investigate if the oxidative stress levels in *C. elegans* larvae and aged worms are altered in long- and short-lived worms, we determined thiol oxidation levels in *C. elegans* mutants, defective in the evolutionarily conserved insulin/IGF-1 signaling pathway. Differences in protein oxidation levels in the three strains, wild type, short-lived *daf-16* and long-lived *daf-2*, were first noticeable in the last developmental stage L4, which was also the first phase of elevated thiol oxidation levels that were observed in wild type worms (Fig 4-3; Suppl. Table 4-3). Protein oxidation was significantly increased at this stage in wild type

worms and approximately 50% of the identified protein thiols were oxidized more than 15%. In contrast, proteins in the long-lived *daf-2* deletion strain stayed in their reduced state and were significantly less oxidized than in wild type worms. The opposite effect was seen in worms lacking DAF-16. 60% of proteins showed elevated oxidation at the larval stage L4.

In wild type worms it was also observed that thiol oxidation levels drop rapidly when worms reach adulthood and the reproductive phase. In contrast, short-lived *daf-16* deletion worms were not capable to fully recover from the developmental increase in protein oxidation and displayed elevated thiol oxidation during the reproductive phase (Fig 4-3; Suppl. Table 4-3). *Daf-2* knockout worms were again able to remain their low thiol oxidation levels in fertile young adult worms. A steady increase in the concentration of thiol oxidation with advancing age, as detected on day 8 and day 15 of adulthood in wild type *C. elegans*, was also observed in worms lacking DAF-16. Long-lived *daf-2* worms experienced only a minor increase in thiol oxidation. The results obtained in long-and short-lived worms suggest that the extent of oxidation during early adulthood, and the ability to recover from developmental oxidative stress might be determinants of lifespan.

1.3.8 Hydrogen peroxide, a possible cause of thiol oxidation

Many of the oxidation-sensitive proteins that we identified with our OxICAT screen were identified before as being sensitive to hydrogen peroxide-mediated thiol oxidation. To directly investigate if hydrogen peroxide production is the cause of the observed thiol oxidation in L4 larvae and senescent worms, we expressed the peroxide-specific sensor protein HyPer in the body wall muscle cells of *C. elegans*, which we knew from OxICAT studies accumulates oxidized protein thiols. We monitored endogenous hydrogen peroxide production over the lifespan of wild type *C. elegans* and found that peroxide production is indeed significantly increased in developmental stages (Fig. 4-4). In the reproductive phase of *C. elegans* peroxide levels are very low and increase slowly as worms grow older. These results are in excellent agreement with our OxICAT studies and suggest that endogenous hydrogen peroxide production is responsible for the increased protein oxidation observed in development and old worms. To correlate endogenous peroxide production to *C. elegans* lifespan, we measured hydrogen peroxide levels in the long- and short lived strains *daf-2* and *daf-16* and further confirmed our OxICAT results. We found decreased hydrogen peroxide levels in worms lacking DAF-2 and increased levels in *daf-16* deletion worms starting in late development, suggesting a correlation between endogenous hydrogen peroxide levels early in life and lifespan (Fig. 4-5).

1.4 Discussion

To evaluate the role of oxidative stress in the development of age-related characteristics, it is important to determine which reactive oxygen species are involved, when the onset of oxidative stress occurs and to what extent ROS accumulates in cells and tissues. We addressed these questions by a combination of physiological studies and proteomic OxCIAT experiments. We first investigated the impact of hydrogen peroxide stress on *C. elegans* and realized that peroxide stress, caused either by exogenous treatment with hydrogen peroxide or endogenously through the loss of the peroxidase PRDX-2, leads to physiological changes highly reminiscent of aging *C. elegans*. While young worms are able to recover from a short period of peroxide stress, *C. elegans* lacking either PRDX-2 or catalase-2 (CTL-2), the two major peroxide detoxifying enzymes, exhibit a progeric phenotype resulting in a shortened lifespan (Petriv & Rachubinski, 2004; Olahova *et al.*, 2008). These results suggest that hydrogen peroxide plays a distinct role in aging. The inability to control intracellular peroxide levels seems to cause physiological changes that accelerate aging. The search for target proteins of hydrogen peroxide revealed that proteins involved in numerous cellular activities including protein translation, cellular homeostasis as well as motility and energy metabolism were affected by thiol oxidation. Oxidation of cysteine residues did not affect all proteins equally; instead specific cysteine residues appeared to be prone to oxidation by hydrogen peroxide suggesting a connection with redox-regulatory mechanisms. The finding that several of the affected cysteines are highly conserved indicates that those residues are important for protein function or structure. Their oxidation might be a regulatory mechanism which likely affects the activity of the protein.

Proteins involved in protein translation including numerous ribosomal proteins as well as elongation factors were especially affected by peroxide stress. Oxidative modification of selective cysteines in these proteins might interfere with their function leading to decreased protein expression in conditions that are very likely to produce oxidatively damaged proteins. The down-regulation of non-essential cellular functions in stress conditions allows organisms to save energy that can instead be utilized for antioxidant defense mechanisms. Reversible thiol modifications ensure that proteins can recover their function after redox conditions are restored.

Overoxidation of peroxiredoxins is one example of regulation of protein function by oxidative modification. The inactivation of peroxiredoxins by oxidation of the conserved peroxidatic cysteine has been discussed as regulatory mechanism that might allow hydrogen peroxide signaling to occur under conditions of high ROS levels (Wood *et al.*, 2003). This

model was supported by the finding that sulfiredoxins exist, which specifically reduce overoxidized peroxiredoxins, thus re-activating their peroxidase function. It came as a surprise to realize that numerous organisms including *C. elegans* lack a sulfiredoxin homolog. This raised the question as to how these organisms deal with peroxiredoxin overoxidation? One possibility is that sestrins are able to reduce overoxidized peroxiredoxins as was reported by Budanov and coworkers (Budanov *et al.*, 2004). We explored this possibility and found that in *C. elegans*, peroxiredoxin regeneration occurs independent of sestrin. The reduction of overoxidized peroxiredoxin was a very slow process, suggesting that *C. elegans* lacks a system for the regeneration of peroxiredoxins. It is thus possible that under physiological conditions, *C. elegans* does not encounter peroxide concentrations that cause significant overoxidation of peroxiredoxin and therefore do not need a specific reduction system. Our results, which we obtained by monitoring peroxiredoxin overoxidation in wild type worms over their lifespan, agreed with this hypothesis. At no point during the lifespan of *C. elegans* did we observe significant levels of overoxidized peroxiredoxin suggesting that *C. elegans* does not require a reductase for overoxidized peroxiredoxin. This also indicates a minor role for the reported activation of peroxiredoxin's chaperone function in *C. elegans* and possibly other organisms lacking sulfiredoxin.

The existence of peroxidases like peroxiredoxin assures a tight regulation of cellular hydrogen peroxide concentrations. We were able to show the importance of hydrogen peroxide detoxification for longevity with the short-lived *C. elegans* mutant *daf-16*, which revealed elevated hydrogen peroxide levels as well as increased thiol oxidation starting in late development. In contrast, the long-lived *daf-2* strain was able to rapidly detoxify developmentally occurring hydrogen peroxide and showed only a slight elevation of thiol oxidation. This result suggests that the ability of worms to recover from the early oxidative insult might influence their lifespan. The role of hydrogen peroxide in aging was further confirmed as we found many proteins to get oxidized in aging *C. elegans* that were shown to be peroxide-sensitive in our previous OxICAT screen.

Other recently conducted studies, which focused on finding characteristics that influence aging, support the theory of an early lifespan determination (Dillin *et al.*, 2002; Ben-Zvi *et al.*, 2009; Sun *et al.*, 2009). It has, for instance, been shown that the decline of protein homeostasis (i.e., proteostasis) starts in young adult worms long before signs of aging appear. Extending proteostasis by the overexpression of DAF-16 extends the lifespan (Ben-Zvi *et al.*, 2009). We observed that protein thiol oxidation occurs before the collapse of the proteostasis. Oxidized proteins often form high molecular weight aggregates which, if

not removed by the proteasome, disturb many cellular functions (Bader & Grune, 2006). Therefore the elevated protein oxidation in late development of *C. elegans* might be involved in the early dysfunction of proteostasis.

The most likely cause for the increased peroxide production in *C. elegans* development is the high metabolic rate that has been reported for larval stages (Wadsworth & Riddle, 1989; Kowaltowski *et al.*, 2009). A higher metabolic rate will likely result in elevated ROS production in the mitochondria. We were able to show that the insulin/IGF-1 signaling pathway is involved in this early onset of oxidative stress and activation of the transcription factor DAF-16 is needed for the establishment of reducing conditions in the fertile phase of *C. elegans*. Our data suggests that DAF-16-mediated protein expression is important in the late developmental phase. In early development no connection between peroxide production as well as thiol oxidation and lifespan is present indicating that DAF-16 is inactive at this stage possibly to allow signaling mediated by reactive oxygen species.

Our studies strongly support the idea that hydrogen peroxide is one of the key players in lifespan determination and should be differentiated from other reactive oxygen species like superoxide. While deletion of hydrogen peroxide detoxifying enzymes causes accelerated aging (Petriv & Rachubinski, 2004; Olahova *et al.*, 2008), deletion of one or more of the five different superoxide dismutases has failed to influence aging in *C. elegans* (Doonan *et al.*, 2008; Van Raamsdonk & Hekimi, 2009). Although cellular superoxide is thought to get rapidly converted into hydrogen peroxide by SODs, superoxide does not seem to play the same role in aging as hydrogen peroxide.

Our findings agree well with the free radical theory of aging which predicts that aging occurs due to oxidative damage caused by reactive oxygen species. We could show that peroxide stress causes accelerated aging and is involved in the development of age-related phenotypes. We furthermore showed that protein thiol oxidation increases with age, as predicted by this theory, and is correlated to longevity. However, as can be seen on the example of hydrogen peroxide, reactive oxygen species do not only cause damage but also have essential physiological functions. Hydrogen peroxide plays an important role as a second messenger and has been shown to be involved in cellular processes like cell proliferation, activation of lymphocytes and apoptosis where it functions in the activation of transcription factors, signal transduction and regulation of other processes (Schreck *et al.*, 1991; Bae *et al.*, 1997; Song & Lee, 2003; Stone & Yang, 2006).

The somewhat surprising result that lifespan determination might be dependent on the extent of oxidative stress that *C. elegans* is exposed to as early as in development agrees

with the concept of mitochondrial hormesis (i.e., mitohormesis), which suggests that temporary elevated ROS levels induce the synthesis of antioxidant enzymes that have a long-lasting health-promoting effect (Schulz *et al.*, 2007). Mitohormesis can also explain why physical exercise, which causes production of ROS due to increased respiration, has a positive effect on health (Ristow *et al.*, 2009).

1.5 Outlook

The redox-proteomic technique OxICAT has great potential in aging research. Now that we have identified target proteins of hydrogen peroxide in *C. elegans*, it would also be worthwhile to determine target proteins of other reactive oxygen or nitrogen species and to determine whether these oxidants play a role in aging as well. It would be worthwhile to conduct further investigation of the correlation between thiol oxidation and lifespan in mammalian model organisms. OxICAT is well suited to measure protein oxidation levels in mammalian cells. To further pinpoint sites of ROS production and oxidative damage, organ-specific quantification of protein oxidation is possible. Using a mammalian system, investigation of thiol oxidation in age-related diseases that are linked to oxidative stress, like neurodegenerative disorders including Alzheimer's and Parkinson's, type-2 diabetes and cardiovascular disorders, is possible (Essick & Sam, 2010). Oxidative stress is also involved in the development of many cancers, like leukemia and prostate cancer (Khandrika *et al.*, 2009; Visconti & Grieco, 2009). OxICAT would allow the identification of target proteins that are involved in the development of these diseases.

Nowadays techniques like quantitative real-time PCR and microarrays can be performed with single worms. This allows, for instance, investigation of factors in an isogenic population of *C. elegans*, which can lead to large differences in lifespans of single worms. The hydrogen peroxide sensor HyPer also allows quantification of hydrogen peroxide levels in single worms. With new techniques that allow rescuing worms after imaging, hydrogen peroxide concentration can be measured throughout a worm's lifespan. By choosing an adequate promoter HyPer can also be expressed ubiquitously, allowing the assessment of peroxide levels in the whole worm, or in defined cells and organs only, making it possible to evaluate site-specific hydrogen peroxide production. Analysis of spatial and temporal aspects of ROS production will improve our understanding of the role of reactive oxygen species in aging.

1.6 References

Bader N & Grune T (2006) Protein oxidation and proteolysis. *Biol Chem* **387**, 1351-1355.

Bae YS, Kang SW, Seo MS, Baines IC, Tekle E, Chock PB & Rhee SG (1997) Epidermal growth factor (EGF)-induced generation of hydrogen peroxide. Role in EGF receptor-mediated tyrosine phosphorylation. *J Biol Chem* **272**, 217-221.

Bass TM, Weinkove D, Houthoofd K, Gems D & Partridge L (2007) Effects of resveratrol on lifespan in Drosophila melanogaster and *Caenorhabditis elegans*. *Mech Ageing Dev* **128**, 546-552.

Belousov VV, Fradkov AF, Lukyanov KA, Staroverov DB, Shakhbazov KS, Terskikh AV & Lukyanov S (2006) Genetically encoded fluorescent indicator for intracellular hydrogen peroxide. *Nat Methods* **3**, 281-286.

Ben-Zvi A, Miller EA & Morimoto RI (2009) Collapse of proteostasis represents an early molecular event in *Caenorhabditis elegans* aging. *Proc Natl Acad Sci U S A* **106**, 14914-14919.

Benov L (2001) How superoxide radical damages the cell. *Protoplasma* **217**, 33-36.

Bienert GP, Schjoerring JK & Jahn TP (2006) Membrane transport of hydrogen peroxide. *Biochim Biophys Acta* **1758**, 994-1003.

Biteau B, Labarre J & Toledano MB (2003) ATP-dependent reduction of cysteine-sulphinic acid by S. cerevisiae sulphiredoxin. *Nature* **425**, 980-984.

Bjelakovic G, Nikolova D, Simonetti RG & Gluud C (2004) Antioxidant supplements for prevention of gastrointestinal cancers: a systematic review and meta-analysis. *Lancet* **364**, 1219-1228.

Blackman MR, Sorkin JD, Munzer T, Bellantoni MF, Busby-Whitehead J, Stevens TE, Jayme J, O'Connor KG, Christmas C, Tobin JD, Stewart KJ, Cottrell E, St Clair C, Pabst KM & Harman SM (2002) Growth hormone and sex steroid administration in healthy aged women and men: a randomized controlled trial. *JAMA* **288**, 2282-2292.

Braeckman BP, Houthoofd K & Vanfleteren JR (2002) Assessing metabolic activity in aging *Caenorhabditis elegans*: concepts and controversies. *Aging Cell* **1**, 82-88; discussion 102-103.

Brenner S (1974) The genetics of *Caenorhabditis elegans*. *Genetics* **77**, 71-94.

Brunet-Rossinni AK & Austad SN (2004) Ageing studies on bats: a review. *Biogerontology* **5**, 211-222.

Budanov AV, Sablina AA, Feinstein E, Koonin EV & Chumakov PM (2004) Regeneration of peroxiredoxins by p53-regulated sestrins, homologs of bacterial AhpD. *Science* **304**, 596-600.

Burnell AM, Houthoofd K, O'Hanlon K & Vanfleteren JR (2005) Alternate metabolism during the dauer stage of the nematode *Caenorhabditis elegans*. *Exp Gerontol* **40**, 850-856.

Chakravarti B & Chakravarti DN (2007) Oxidative modification of proteins: age-related changes. *Gerontology* **53**, 128-139.

Chance B, Sies H & Boveris A (1979) Hydroperoxide metabolism in mammalian organs. *Physiol Rev* **59**, 527-605.

Chelikani P, Fita I & Loewen PC (2004) Diversity of structures and properties among catalases. *Cell Mol Life Sci* **61**, 192-208.

Cheng FC, Jen JF & Tsai TH (2002) Hydroxyl radical in living systems and its separation methods. *J Chromatogr B Analyt Technol Biomed Life Sci* **781**, 481-496.

Conti B, Sanchez-Alavez M, Winsky-Sommerer R, Morale MC, Lucero J, Brownell S, Fabre V, Huitron-Resendiz S, Henriksen S, Zorrilla EP, de Lecea L & Bartfai T (2006) Transgenic mice with a reduced core body temperature have an increased life span. *Science* **314**, 825-828.

Cooke MS, Evans MD, Dizdaroglu M & Lunec J (2003) Oxidative DNA damage: mechanisms, mutation, and disease. *FASEB J* **17**, 1195-1214.

Coschigano KT, Clemmons D, Bellush LL & Kopchick JJ (2000) Assessment of growth parameters and life span of GHR/BP gene-disrupted mice. *Endocrinology* **141**, 2608-2613.

Davies KJ (2000) Oxidative stress, antioxidant defenses, and damage removal, repair, and replacement systems. *IUBMB Life* **50**, 279-289.

Davies MJ (2005) The oxidative environment and protein damage. *Biochim Biophys Acta* **1703**, 93-109.

de Magalhaes JP (2005) Open-minded scepticism: inferring the causal mechanisms of human ageing from genetic perturbations. *Ageing Res Rev* **4**, 1-22.

Dillin A, Hsu AL, Arantes-Oliveira N, Lehrer-Graiwer J, Hsin H, Fraser AG, Kamath RS, Ahringer J & Kenyon C (2002) Rates of behavior and aging specified by mitochondrial function during development. *Science* **298**, 2398-2401.

Doonan R, McElwee JJ, Matthijssens F, Walker GA, Houthoofd K, Back P, Matscheski A, Vanfleteren JR & Gems D (2008) Against the oxidative damage theory of aging: superoxide dismutases protect against oxidative stress but have little or no effect on life span in *Caenorhabditis elegans*. *Genes Dev* **22**, 3236-3241.

Essick EE & Sam F (2010) Oxidative stress and autophagy in cardiac disease, neurological disorders, aging and cancer. *Oxid Med Cell Longev* **3**, 168-177.

Fridovich I (1995) Superoxide radical and superoxide dismutases. *Annu Rev Biochem* **64**, 97-112.

Gardner HW (1989) Oxygen radical chemistry of polyunsaturated fatty acids. *Free Radic Biol Med* **7**, 65-86.

Gensler HL & Bernstein H (1981) DNA damage as the primary cause of aging. *Q Rev Biol* **56**, 279-303.

Gus'kova RA, Ivanov, II, Kol'tover VK, Akhobadze VV & Rubin AB (1984) Permeability of bilayer lipid membranes for superoxide (O2-.) radicals. *Biochim Biophys Acta* **778**, 579-585.

Gygi SP, Rist B, Gerber SA, Turecek F, Gelb MH & Aebersold R (1999) Quantitative analysis of complex protein mixtures using isotope-coded affinity tags. *Nat Biotechnol* **17**, 994-999.

Hall A, Karplus PA & Poole LB (2009) Typical 2-Cys peroxiredoxins--structures, mechanisms and functions. *FEBS J* **276**, 2469-2477.

Halliwell B & Chirico S (1993) Lipid peroxidation: its mechanism, measurement, and significance. *Am J Clin Nutr* **57**, 715S-724S; discussion 724S-725S.

Hammerman MR (1987) Insulin-like growth factors and aging. *Endocrinol Metab Clin North Am* **16**, 995-1011.

Hansford RG, Hogue BA & Mildaziene V (1997) Dependence of H2O2 formation by rat heart mitochondria on substrate availability and donor age. *J Bioenerg Biomembr* **29**, 89-95.

Hari R, Burde V & Arking R (1998) Immunological confirmation of elevated levels of CuZn superoxide dismutase protein in an artificially selected long-lived strain of Drosophila melanogaster. *Exp Gerontol* **33**, 227-237.

Harman D (1956) Aging: a theory based on free radical and radiation chemistry. *J Gerontol* **11**, 298-300.

Ho KY, Evans WS, Blizzard RM, Veldhuis JD, Merriam GR, Samojlik E, Furlanetto R, Rogol AD, Kaiser DL & Thorner MO (1987) Effects of sex and age on the 24-hour profile of growth hormone secretion in man: importance of endogenous estradiol concentrations. *J Clin Endocrinol Metab* **64**, 51-58.

Holloszy JO, Smith EK, Vining M & Adams S (1985) Effect of voluntary exercise on longevity of rats. *J Appl Physiol* **59**, 826-831.

Houthoofd K, Fidalgo MA, Hoogewijs D, Braeckman BP, Lenaerts I, Brys K, Matthijssens F, De Vreese A, Van Eygen S, Munoz MJ & Vanfleteren JR (2005) Metabolism, physiology and stress defense in three aging Ins/IGF-1 mutants of the nematode *Caenorhabditis elegans*. *Aging Cell* **4**, 87-95.

Huang C, Xiong C & Kornfeld K (2004) Measurements of age-related changes of physiological processes that predict lifespan of *Caenorhabditis elegans*. *Proc Natl Acad Sci U S A* **101**, 8084-8089.

Hulbert AJ, Clancy DJ, Mair W, Braeckman BP, Gems D & Partridge L (2004) Metabolic rate is not reduced by dietary-restriction or by lowered insulin/IGF-1 signalling and is not correlated with individual lifespan in Drosophila melanogaster. *Exp Gerontol* **39**, 1137-1143.

Hulbert AJ, Pamplona R, Buffenstein R & Buttemer WA (2007) Life and death: metabolic rate, membrane composition, and life span of animals. *Physiol Rev* **87**, 1175-1213.

Jang HH, Lee KO, Chi YH, Jung BG, Park SK, Park JH, Lee JR, Lee SS, Moon JC, Yun JW, Choi YO, Kim WY, Kang JS, Cheong GW, Yun DJ, Rhee SG, Cho MJ & Lee SY (2004) Two enzymes in one; two yeast peroxiredoxins display oxidative stress-dependent switching from a peroxidase to a molecular chaperone function. *Cell* **117**, 625-635.

Jones OT (1994) The regulation of superoxide production by the NADPH oxidase of neutrophils and other mammalian cells. *Bioessays* **16**, 919-923.

Keaney M, Matthijssens F, Sharpe M, Vanfleteren J & Gems D (2004) Superoxide dismutase mimetics elevate superoxide dismutase activity *in vivo* but do not retard aging in the nematode *Caenorhabditis elegans*. *Free Radic Biol Med* **37**, 239-250.

Kenyon C (2001) A conserved regulatory system for aging. *Cell* **105**, 165-168.

Kenyon C, Chang J, Gensch E, Rudner A & Tabtiang R (1993) A *C. elegans* mutant that lives twice as long as wild type. *Nature* **366**, 461-464.

Khandrika L, Kumar B, Koul S, Maroni P & Koul HK (2009) Oxidative stress in prostate cancer. *Cancer Lett* **282**, 125-136.

Khansari DN & Gustad T (1991) Effects of long-term, low-dose growth hormone therapy on immune function and life expectancy of mice. *Mech Ageing Dev* **57**, 87-100.

Klass MR (1977) Aging in the nematode *Caenorhabditis elegans*: major biological and environmental factors influencing life span. *Mech Ageing Dev* **6**, 413-429.

Konig D, Wagner KH, Elmadfa I & Berg A (2001) Exercise and oxidative stress: significance of antioxidants with reference to inflammatory, muscular, and systemic stress. *Exerc Immunol Rev* **7**, 108-133.

Kowaltowski AJ, de Souza-Pinto NC, Castilho RF & Vercesi AE (2009) Mitochondria and reactive oxygen species. *Free Radic Biol Med* **47**, 333-343.

Kumsta C & Jakob U (2009) Redox-regulated chaperones. *Biochemistry* **48**, 4666-4676.

Lakowski B & Hekimi S (1998) The genetics of caloric restriction in *Caenorhabditis elegans*. *Proc Natl Acad Sci U S A* **95**, 13091-13096.

Lamb MJ (1968) Temperature and lifespan in Drosophila. *Nature* **220**, 808-809.

Lambert AJ & Brand MD (2009) Reactive oxygen species production by mitochondria. *Methods Mol Biol* **554**, 165-181.

Laron Z (2005) Do deficiencies in growth hormone and insulin-like growth factor-1 (IGF-1) shorten or prolong longevity? *Mech Ageing Dev* **126**, 305-307.

Larsen PL (1993) Aging and resistance to oxidative damage in *Caenorhabditis elegans*. *Proc Natl Acad Sci U S A* **90**, 8905-8909.

Le Moan N, Clement G, Le Maout S, Tacnet F & Toledano MB (2006) The Saccharomyces cerevisiae proteome of oxidized protein thiols: contrasted functions for the thioredoxin and glutathione pathways. *J Biol Chem* **281**, 10420-10430.

Lee H, Carlson JD, McMahon KK, Moyer TP & Fischer AG (1977) Xanthine oxidase: a source of hydrogen peroxide in bovine thyroid glands. *Life Sci* **20**, 453-458.

Lee IM, Cook NR, Gaziano JM, Gordon D, Ridker PM, Manson JE, Hennekens CH & Buring JE (2005) Vitamin E in the primary prevention of cardiovascular disease and cancer: the Women's Health Study: a randomized controlled trial. *JAMA* **294**, 56-65.

Leichert LI, Gehrke F, Gudiseva HV, Blackwell T, Ilbert M, Walker AK, Strahler JR, Andrews PC & Jakob U (2008) Quantifying changes in the thiol redox proteome upon oxidative stress *in vivo*. *Proc Natl Acad Sci U S A* **105**, 8197-8202.

Lints FA (1989) The rate of living theory revisited. *Gerontology* **35**, 36-57.

Liu H, Bravata DM, Olkin I, Nayak S, Roberts B, Garber AM & Hoffman AR (2007) Systematic review: the safety and efficacy of growth hormone in the healthy elderly. *Ann Intern Med* **146**, 104-115.

Lu T, Pan Y, Kao SY, Li C, Kohane I, Chan J & Yankner BA (2004) Gene regulation and DNA damage in the ageing human brain. *Nature* **429**, 883-891.

Maker HS, Weiss C, Silides DJ & Cohen G (1981) Coupling of dopamine oxidation (monoamine oxidase activity) to glutathione oxidation via the generation of hydrogen peroxide in rat brain homogenates. *J Neurochem* **36**, 589-593.

Mari M, Morales A, Colell A, Garcia-Ruiz C & Fernandez-Checa JC (2009) Mitochondrial glutathione, a key survival antioxidant. *Antioxid Redox Signal* **11**, 2685-2700.

Martin GM & Oshima J (2000) Lessons from human progeroid syndromes. *Nature* **408**, 263-266.

Martin GM, Smith AC, Ketterer DJ, Ogburn CE & Disteche CM (1985) Increased chromosomal aberrations in first metaphases of cells isolated from the kidneys of aged mice. *Isr J Med Sci* **21**, 296-301.

McElwee J, Bubb K & Thomas JH (2003) Transcriptional outputs of the *Caenorhabditis elegans* forkhead protein DAF-16. *Aging Cell* **2**, 111-121.

Meunier B, de Visser SP & Shaik S (2004) Mechanism of oxidation reactions catalyzed by cytochrome p450 enzymes. *Chem Rev* **104**, 3947-3980.

Moir DT & Mao JI (1990) Protein secretion systems in microbial and mammalian cells. *Bioprocess Technol* **9**, 67-94.

Morley AA & Trainor KJ (2001) Lack of an effect of vitamin E on lifespan of mice. *Biogerontology* **2**, 109-112.

Moskovitz J, Bar-Noy S, Williams WM, Requena J, Berlett BS & Stadtman ER (2001) Methionine sulfoxide reductase (MsrA) is a regulator of antioxidant defense and lifespan in mammals. *Proc Natl Acad Sci U S A* **98**, 12920-12925.

Murphy MP (2009) How mitochondria produce reactive oxygen species. *Biochem J* **417**, 1-13.

Nakamura A & Goto S (1996) Analysis of protein carbonyls with 2,4-dinitrophenyl hydrazine and its antibodies by immunoblot in two-dimensional gel electrophoresis. *J Biochem* **119**, 768-774.

Neafsey PJ, Boxenbaum H, Ciraulo DA & Fournier DJ (1988) A Gompertz age-specific mortality rate model of aging, hormesis, and toxicity: fixed-dose studies. *Drug Metab Rev* **19**, 369-401.

Nishimura JS, Mitchell T & Matula JM (1976) Inactivation of Escherichia coli succinic thiokinase by selective oxidation of thiol groups by permanganate. *Biochem Biophys Res Commun* **69**, 1057-1064.

Nystrom T (2005) Role of oxidative carbonylation in protein quality control and senescence. *EMBO J* **24**, 1311-1317.

Olahova M, Taylor SR, Khazaipoul S, Wang J, Morgan BA, Matsumoto K, Blackwell TK & Veal EA (2008) A redox-sensitive peroxiredoxin that is important for longevity has tissue- and stress-specific roles in stress resistance. *Proc Natl Acad Sci U S A* **105**, 19839-19844.

Orr WC & Sohal RS (1994) Extension of life-span by overexpression of superoxide dismutase and catalase in Drosophila melanogaster. *Science* **263**, 1128-1130.

Pahor M & Carbonin P (1995) Exercise intensity and longevity in men. *JAMA* **274**, 1132-1133.

Pearl R (1928) *The rate of living, being an account of some experimental studies on the biology of life duration*. New York,: A.A. Knopf.

Perez VI, Bokov A, Van Remmen H, Mele J, Ran Q, Ikeno Y & Richardson A (2009) Is the oxidative stress theory of aging dead? *Biochim Biophys Acta* **1790**, 1005-1014.

Petriv OI & Rachubinski RA (2004) Lack of peroxisomal catalase causes a progeric phenotype in *Caenorhabditis elegans*. *J Biol Chem* **279**, 19996-20001.

Pham DQ & Plakogiannis R (2005) Vitamin E supplementation in cardiovascular disease and cancer prevention: Part 1. *Ann Pharmacother* **39**, 1870-1878.

Pratico D (2002) Lipid peroxidation and the aging process. *Sci Aging Knowledge Environ* **2002**, re5.

Pryor WA & Squadrito GL (1995) The chemistry of peroxynitrite: a product from the reaction of nitric oxide with superoxide. *Am J Physiol* **268**, L699-722.

Rhee SG, Yang KS, Kang SW, Woo HA & Chang TS (2005) Controlled elimination of intracellular H(2)O(2): regulation of peroxiredoxin, catalase, and glutathione peroxidase via post-translational modification. *Antioxid Redox Signal* **7**, 619-626.

Ristow M, Zarse K, Oberbach A, Kloting N, Birringer M, Kiehntopf M, Stumvoll M, Kahn CR & Bluher M (2009) Antioxidants prevent health-promoting effects of physical exercise in humans. *Proc Natl Acad Sci U S A* **106**, 8665-8670.

Rose MR (1989) Genetics of increased lifespan in Drosophila. *Bioessays* **11**, 132-135.

Ruan H, Tang XD, Chen ML, Joiner ML, Sun G, Brot N, Weissbach H, Heinemann SH, Iverson L, Wu CF & Hoshi T (2002) High-quality life extension by the enzyme peptide methionine sulfoxide reductase. *Proc Natl Acad Sci U S A* **99**, 2748-2753.

Rubner M (1908) *Das Problem der Lebensdauer und seine Beziehungen zu Wachstum und Ernährung*. München,: Oldenbourg.

Schreck R, Rieber P & Baeuerle PA (1991) Reactive oxygen intermediates as apparently widely used messengers in the activation of the NF-kappa B transcription factor and HIV-1. *EMBO J* **10**, 2247-2258.

Schriner SE, Linford NJ, Martin GM, Treuting P, Ogburn CE, Emond M, Coskun PE, Ladiges W, Wolf N, Van Remmen H, Wallace DC & Rabinovitch PS (2005) Extension of murine life span by overexpression of catalase targeted to mitochondria. *Science* **308**, 1909-1911.

Schulz TJ, Zarse K, Voigt A, Urban N, Birringer M & Ristow M (2007) Glucose restriction extends *Caenorhabditis elegans* life span by inducing mitochondrial respiration and increasing oxidative stress. *Cell Metab* **6**, 280-293.

Shigenaga MK & Ames BN (1991) Assays for 8-hydroxy-2'-deoxyguanosine: a biomarker of *in vivo* oxidative DNA damage. *Free Radic Biol Med* **10**, 211-216.

Singh NP, McCoy MT, Tice RR & Schneider EL (1988) A simple technique for quantitation of low levels of DNA damage in individual cells. *Exp Cell Res* **175**, 184-191.

Song JJ & Lee YJ (2003) Catalase, but not MnSOD, inhibits glucose deprivation-activated ASK1-MEK-MAPK signal transduction pathway and prevents relocalization of Daxx: hydrogen peroxide as a major second messenger of metabolic oxidative stress. *J Cell Biochem* **90**, 304-314.

Sonntag WE, Lynch CD, Cefalu WT, Ingram RL, Bennett SA, Thornton PL & Khan AS (1999) Pleiotropic effects of growth hormone and insulin-like growth factor (IGF)-1 on biological aging: inferences from moderate caloric-restricted animals. *J Gerontol A Biol Sci Med Sci* **54**, B521-538.

Stadtman ER (2006) Protein oxidation and aging. *Free Radic Res* **40**, 1250-1258.

Stone JR & Yang S (2006) Hydrogen peroxide: a signaling messenger. *Antioxid Redox Signal* **8**, 243-270.

Sulston J (1988) *The Nematode Caenorhabditis elegans*: Cold Spring Harbor.

Sun L, Sadighi Akha AA, Miller RA & Harper JM (2009) Life-span extension in mice by preweaning food restriction and by methionine restriction in middle age. *J Gerontol A Biol Sci Med Sci* **64**, 711-722.

Szilard L (1959) On the Nature of the Aging Process. *Proc Natl Acad Sci U S A* **45**, 30-45.

Truscott TG (2001) Synergistic effects of antioxidant vitamins. *Bibl Nutr Dieta*, 68-79.

Van Raamsdonk JM & Hekimi S (2009) Deletion of the mitochondrial superoxide dismutase sod-2 extends lifespan in *Caenorhabditis elegans*. *PLoS Genet* **5**, e1000361.

Van Remmen H, Hamilton ML & Richardson A (2003) Oxidative damage to DNA and aging. *Exerc Sport Sci Rev* **31**, 149-153.

Van Remmen H & Richardson A (2001) Oxidative damage to mitochondria and aging. *Exp Gerontol* **36**, 957-968.

Visconti R & Grieco D (2009) New insights on oxidative stress in cancer. *Curr Opin Drug Discov Devel* **12**, 240-245.

Wadsworth WG & Riddle DL (1989) Developmental regulation of energy metabolism in *Caenorhabditis elegans*. *Dev Biol* **132**, 167-173.

Winterbourn CC (1995) Toxicity of iron and hydrogen peroxide: the Fenton reaction. *Toxicol Lett* **82-83**, 969-974.

Woo HA, Bae SH, Park S & Rhee SG (2009) Sestrin 2 is not a reductase for cysteine sulfinic acid of peroxiredoxins. *Antioxid Redox Signal* **11**, 739-745.

Wood ZA, Poole LB & Karplus PA (2003) Peroxiredoxin evolution and the regulation of hydrogen peroxide signaling. *Science* **300**, 650-653.

2 EFFECTS OF OXIDATIVE STRESS ON BEHAVIOR, PHYSIOLOGY, AND THE REDOX THIOL PROTEOME OF *CAENORHABDITIS ELEGANS*

Caroline Kumsta[1], Maike Thamsen[1], Ursula Jakob[1,2]

Antioxid Redox Signal., *in press*

[1]Department of Molecular, Cellular, and Developmental Biology and [2]Program in Cellular and Molecular Biology, University of Michigan, Ann Arbor, MI, USA

2.1 Abstract

Accumulation of reactive oxygen species has been implicated in various diseases and aging. However, the precise physiological effects of accumulating oxidants are still largely undefined. Here, we applied a short-term peroxide stress treatment to young *Caenorhabditis elegans* and measured behavioral, physiological, and cellular consequences. We discovered that exposure to peroxide stress causes a number of immediate changes, including loss in mobility, decreased growth rate, and decreased cellular ATP levels. These alterations, which are highly reminiscent of changes in aging animals, are fully reversible, suggesting the presence of effective antioxidant systems in young *C. elegans*. One of these antioxidant systems involves the highly abundant protein peroxiredoxin 2 (PRDX-2), whose gene deletion causes phenotypes symptomatic of chronic peroxide stress and shortens lifespan. Applying the quantitative redox proteomic technique OxICAT to oxidatively stressed wild-type and *prdx-2* deletion worms, we identified oxidation-sensitive cysteines in 40 different proteins, including proteins involved in mobility and feeding (*e.g.,* MYO-2, LET-75), protein translation and homeostasis (*e.g.,* EFT-1, HSP-1), and ATP regeneration (*e.g.,* NDPK). The oxidative modification of some of these redox-sensitive cysteines may contribute to the physiological and behavioral changes observed in oxidatively stressed animals.

2.2 Introduction

Reactive oxygen species (ROS), like superoxide radicals ($O_2\bullet^-$) and hydrogen peroxide (H_2O_2), occur during normal metabolism, often because of incomplete electron transfer within the respiratory chain (Apel & Hirt, 2004). To cope with these oxidants, cells harbor ROS-detoxifying enzymes and redox-balancing systems to maintain the appropriate reducing potential (Deneke, 2000). When ROS concentrations exceed the antioxidant capacity of the cell, severe DNA, lipid, and protein damage can occur and organisms suffer from a condition termed oxidative stress (Imlay, 2003). The damaging effects of accumulating ROS have been implicated in neurodegenerative

diseases, cancer, atherosclerosis, diabetes, and heart disease (Finkel & Holbrook, 2000; Aliev *et al.*, 2002). However, the specific physiological consequences of oxidative stress conditions in higher eukaryotes remain largely unknown.

The predominant cellular targets of ROS are the amino acids of proteins. Side chain modifications, which include oxidation of cysteines and methionines as well as carbonylation reactions, often cause the inactivation of the affected proteins (Stadtman, 2001). This oxidative inactivation of specific cellular proteins has been proposed to constitute one of the major mechanisms that links oxidative stress to loss of critical physiological functions (Sohal, 2002). Although the damaging effects of ROS have long been recognized, the pivotal role that specific reactive oxygen species play in the post-translational regulation of redox-sensitive proteins has only recently started to emerge (Paulsen & Carroll). ROS were found to reversibly modify structurally and functionally important cysteines in numerous redox-sensitive proteins. These thiol modifications often cause profound functional changes in proteins involved in transcription, translation, metabolism, stress protection, signal transduction, and apoptosis, and these changes contribute to or may even cause the immediate and long-term responses of organisms to oxidative stress (Brandes *et al.*, 2009).

Several different proteomic techniques have been established with the goals of identifying redox-sensitive proteins in eukaryotic tissues and understanding the effects of oxidative stress in greater detail (Paulsen & Carroll). However, most of these methods have limitations, including the inability to identify the redox-sensitive cysteine(s) and, even more importantly, to precisely quantify the extent of oxidative thiol modifications. While identification of the redox-sensitive cysteine is crucial in evaluating how oxidative modification might affect the structure and function of the respective protein, determination of the extent of oxidative modification is essential in determining whether or not these oxidative modifications are physiologically relevant. We have recently developed a quantitative thiol trapping technology, termed OxICAT, which enables us to determine the precise oxidation status of hundreds of cellular proteins in a single experiment (Leichert *et al.*, 2008). By using OxICAT, we identified several novel redox-sensitive *Escherichia coli* proteins, which were found to play pivotal roles in the oxidative stress resistance of bacteria. We have now decided to use this methodology to gain insights into the physiological and redox proteomic effects of oxidative stress in higher eukaryotes.

Here, we exposed synchronized young wild-type *Caenorhabditis elegans* on day 0 of adulthood to a short treatment with hydrogen peroxide and monitored subsequent behavior and physiology. Although most animals eventually recovered from this oxidative stress regimen, they first reacted with dramatic behavioral changes, including nearly complete loss of mobility and

reduction in growth rate and cellular ATP levels. OxICAT analysis revealed a number of physiologically relevant eukaryotic target proteins, which harbor highly conserved cysteines that significantly change their redox status upon oxidative stress treatment. These included proteins involved in muscle contraction, feeding behavior, and ATP regeneration. Identification of these redox-regulated proteins substantially increased our understanding of redox-regulated responses in eukaryotes and will form the foundation for future studies aimed to understand the physiological consequences of oxidative stress in aging and disease.

2.3 Materials and Methods

2.3.1 Strains and culture conditions

The Bristol strain N2 (wild-type), and the original isolate VC289 *prdx-2*(gk169)II were provided by the CGC. The *prdx-2* strain was backcrossed three times to strain N2. Strains were maintained and cultured under standard conditions using *E. coli* OP50 as a food source.

2.3.2 Oxidative stress treatment

Synchronized worms at day 0 of adulthood were collected by centrifugation in M9 medium and washed. 100 µl of worms (~ 30,000 worms) were incubated in 2 ml M9 with the indicated concentration of H_2O_2 at room temperature in a rotating roller drum for 30 min. After treatment, the worms were collected by centrifugation and the oxidant was washed away with M9 medium. The animals were seeded on fresh NGM plates and immediately singled. Singling and scoring was performed blinded for the day 0 evaluation.

2.3.3 Lifespan, movement, and brood size analysis

All behavioral studies were conducted, scored, and statistically analyzed as previously described (Huang *et al.*, 2004). Details are found in Supplemental Materials and Methods (see 2.8).

2.3.4 ATP measurements

100 µl of synchronized young adults were treated with the indicated concentrations of H_2O_2 in 1.8 ml of M9 media for 30 min. After the treatment, worms were washed with M9 medium, shock frozen in liquid N2, thawed, transferred into boiling 4 M Guanidinium-HCl, and boiled for 15 min. After centrifugation (30 min, 4°C, 13,200 x g), the protein concentration of the supernatant was determined using the BioRad assay (Bio-Rad Laboratories). Samples were diluted 1:200 into ATP buffer (40 mM HEPES-KOH, 4 mM $MgSO_4$, pH 7.8) and mixed with the same volume of assay buffer containing 200 nM luciferase (Roche), 140 µM luciferin (Biotium Inc.), 0.1 mg/ml BSA, 200 mM

KH_2PO_4, 50 mM glycylglycine, 0.4 mM EDTA, pH 7.8. Chemiluminescence was measured using a FLUOstar Omega (BMG Labtech). ATP concentrations were determined according to an ATP standard curve and normalized over protein content.

2.3.5 Sample preparation for OxICAT

To prepare protein extracts for the redox proteomic analysis, 50–100 µl stress-treated worms were harvested onto 10% (w/v) trichloracetic acid (TCA), shock frozen in liquid nitrogen to induce breaking and lysis, after thawing they were homogenized for 2 min with Power Gen 125 (Fisher Scientific). The TCA-treated protein extract from *C. elegans* was centrifuged (13,000 x g, 4°C, 30 min) and the resulting pellet was washed once with 500 µl 10% (w/v) TCA and once with 200 µl 5% (w/v) TCA. The supernatant was completely removed and the sample was transferred to the anaerobic chamber for the first OxICAT alkylation step. All subsequent steps of the OxICAT labeling were performed according to the published protocol (Leichert *et al.*, 2008). Mass spectrometery was performed at the Michigan Proteome Consortium. Data analysis was conducted as described (Leichert *et al.*, 2008).

2.4 Results

2.4.1 Peroxide treatment leads to reversible behavioral defects in *C. elegans*

The cellular accumulation of reactive oxygen species has been attributed to many different physiological and pathological alterations, yet the precise effects that sublethal concentrations of oxidants such as H_2O_2 exert on the physiology of multicellular organisms have not been well defined. We therefore decided to investigate the effects of specific oxidants on the behavior and redox proteome of *C. elegans*. We chose *C. elegans* because it is a very well characterized organism that can be easily synchronized, and it has a multitude of age-related behavioral traits, such as mobility, brood size, and pharyngeal pumping, that can be quantitatively assessed along with size and lifespan. In previous oxidative stress resistance tests in *C. elegans*, the minimal lethal oxidant concentrations have been determined, but investigations of physiological effects and/or potential recovery have remained relatively unexplored (Larsen, 1993).

We initiated our studies by exposing synchronized *C. elegans* on day 0 of adulthood to different H_2O_2 concentrations for 30 min. We then removed the oxidant and monitored immediate and long-term behavior. Our goal was to find oxidant concentrations that affect the majority of the worm population without killing them; this information would be used for subsequent quantitative redox proteomic analysis to reveal oxidative stress-specific target proteins in *C. elegans*. We found

that short-term exposure of *C. elegans* to 6 or 10 mM H_2O_2 fulfills these criteria. These treatments are non-lethal (survival rate >95% compared to control group) and do not affect the mean lifespan of the organism (Fig. 2-1A). At the same time, they cause very distinct behavioral defects in the majority of animals. The most obvious and immediate effects of H_2O_2 treatment that we observed were mobility defects, which were expressed as decreased thrashing in H_2O_2-supplemented liquid media (data not shown). This movement defect remained after washing the worms and seeding them on oxidant-free food plates. We found that highly impaired movement, ranging from no movement to slow and uncoordinated motility, occurred in about 20% of the worms treated with 6 mM H_2O_2 and in about 60% of worms treated with 10 mM H_2O_2 (Fig. 2-1B). Importantly, within less than 48 h after treatment, the vast majority of worms regained fast, sinusoidal body movement, which they maintained until the typical age-related motility decline set in (Fig. 2-1B). This result suggests that young worms have effective antioxidant systems that reverse the effects of exogenous oxidative stress and promote their recovery.

Another consequence of exposing *C. elegans* to H_2O_2 stress was a significant reduction in the total progeny production. This decrease was not due to differences in the length of the fertile period but instead due to a severe decline in egg production in the first three days after the oxidative stress treatment (Fig. 2-1C). As observed with the mobility defects, the animals recovered from the H_2O_2 treatment and showed a progeny production very similar to the progeny production of the control group after 72 h (Fig. 2-1C). In addition, we found that peroxide-treated animals showed reduced pharyngeal pumping (Fig. 2-1D), a significant decrease in body length (Fig. 2-1E), and a significantly reduced growth rate (Fig. 2-1F).

Peroxide stress has been shown to lead to a massive decline in intracellular ATP levels due to the oxidative inactivation of key enzymes involved in energy generating pathways, *i.e.,* glyceraldehyde-3-phosphate dehydrogenase and ATP synthases (Hyslop *et al.*, 1988). Because decreased ATP levels might explain at least some of the observed behavioral changes in *C. elegans*, we measured intracellular ATP concentrations after 30 min of exposure to peroxide stress. As shown in Fig. 2-1G, we found that peroxide-treated worms do indeed suffer from a significant drop in intracellular ATP levels. These results suggest that a change in the cellular energy charge might be at least in part responsible for some of the behavioral changes observed in peroxide-treated worms.

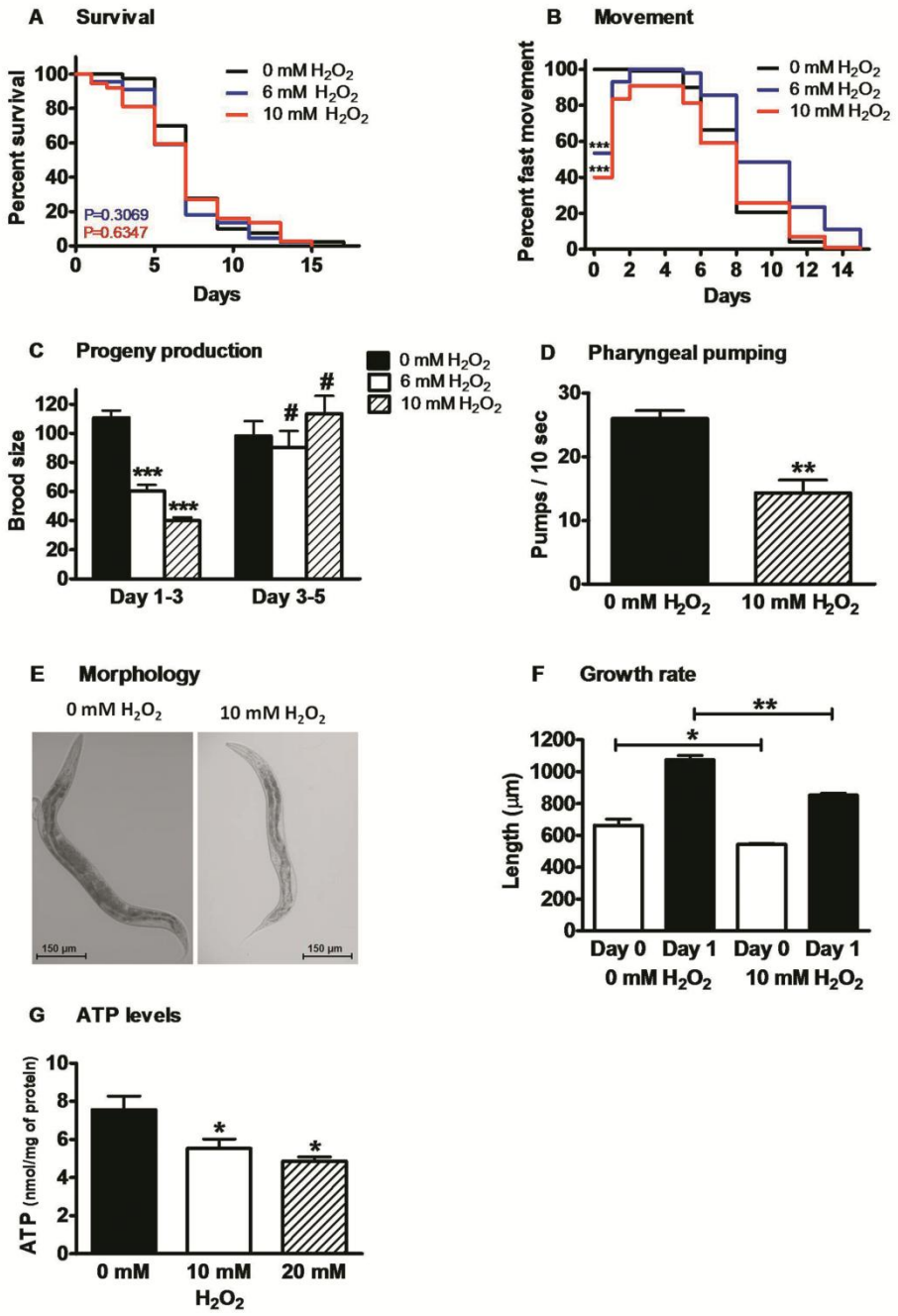

Figure 2-1 Short term H_2O_2 treatment causes reversible behavioral defects in *C. elegans*
Synchronized wild-type *C. elegans* at day 0 of adulthood were treated with 0, 6, or 10 mM H_2O_2 for 30 min in liquid M9 media. Then, the oxidant was removed and 50 worms per treatment were singled and scored for (**A**) survival and lifespan, (**B**) fast movement, (**C**) progeny production, (**D**) pharyngeal pumping (day 1), (**E**) morphology (day 1), and (**F**) growth rate (from day 0 to day 1 of adulthood) at 25°C. (**G**) To determine intracellular ATP levels, 100 µl of worms were treated with the indicated concentrations of H_2O_2 for 30 min, and ATP levels were measured before and after oxidative stress treatment. As seen in (**A**), no significant difference in the mean lifespan of oxidatively stressed worms was observed in five independent experiments. A representative life span is shown here with P = 0.3069, χ^2 1.044 for 6 mM H_2O_2 and P = 0.6347, χ^2 2.258 for 10 mM H_2O_2 in comparison with the control group (0 mM H_2O_2) (non-parametric log rank test). The movement plot shown in (**B**) is an average of at least three independent experiments and the direct comparison by repeated measures ANOVA and Bonferroni post hoc test reveals a difference in the movement behavior on day 0 after the oxidative stress treatment ($P < 0.001$). The symbols above the bars in (**C**-**G**) represent the P values obtained using t-test or 1-way ANOVA : # > 0.05, * < 0.05, ** < 0.01, *** < 0.001.

2.4.2 Peroxiredoxin-2 promotes recovery from peroxide stress-induced motility and egg-laying defects

One important player in the H_2O_2 detoxification system of *C. elegans* is the 2-Cys peroxiredoxin PRDX-2 (Olahova *et al.*, 2008), a highly abundant protein that constitutes about 0.5% of the total *C. elegans* proteome (Suppl. Fig. 2-1). Deletion of *prdx-2* has been shown to increase the sensitivity of *C. elegans* towards exogenous peroxide treatment and to cause a significant decrease in the lifespan of these worms, especially at lower cultivation temperatures (Olahova *et al.*, 2008) (Fig. 2-2B). Moreover, the phenotypes of *prdx-2* mutant worms, especially after the larval stages (Isermann *et al.*, 2004; Olahova *et al.*, 2008), were highly reminiscent of the behavioral changes that we observed when we treated wild-type strains with hydrogen peroxide (Fig. 2-2C–F). Adult *prdx-2* deletion strains show a reduced brood size, and remain significantly smaller during their adult lifespan. These results not only indicate that *prdx-2* worms suffer from endogenous oxidative stress but suggest that short-term peroxide treatment can be used to mimic reversible peroxide stress *in vivo*.

To assess the effects of exogenous oxidative stress in worms lacking PRDX-2, we exposed synchronized *prdx-2* mutant worms on day 0 of adulthood to our short-term peroxide stress treatment. Although we did not detect any change in the mean adult lifespan, we did notice a reproducible increase in the initial mortality rate and a decreased minimal lifespan (Fig. 2-3A). This result suggests that lack of PRDX-2 might lead to a prolonged period of peroxide stress in worms, which leads to early death in a susceptible subfraction of the animals. We also analyzed movement and progeny production of *prdx-2* mutants upon peroxide treatment. Although exogenous peroxide stress treatment caused only a slight but reproducibly more severe immediate motility defect in the *prdx-2* mutant strain as compared to wild-type *C. elegans* (compare Fig. 2-1B with Fig. 2-3B), recovery in the 10 mM H_2O_2-treated group was severely impaired in the mutant worms, with many worms never regaining their original mobility (Fig. 2-3B). These results suggest that lack of PRDX-2 lengthens the exposure of cellular macromolecules to the damaging effects of peroxide stress. Very similar results were obtained when we analyzed the effects of peroxide stress on the progeny production of *prdx-2* worms; brood size dropped to less than 20% of the values obtained in the untreated *prdx-2* mutants and never recovered (Fig. 2-3C). In contrast to mobility, progeny production and pharyngeal pumping of *prdx-2* worms, which were all additionally affected by exogenous oxidative stress treatment (Fig. 2-3B-D), neither size, growth rate nor intracellular ATP levels of *prdx-2* mutant animals were further reduced

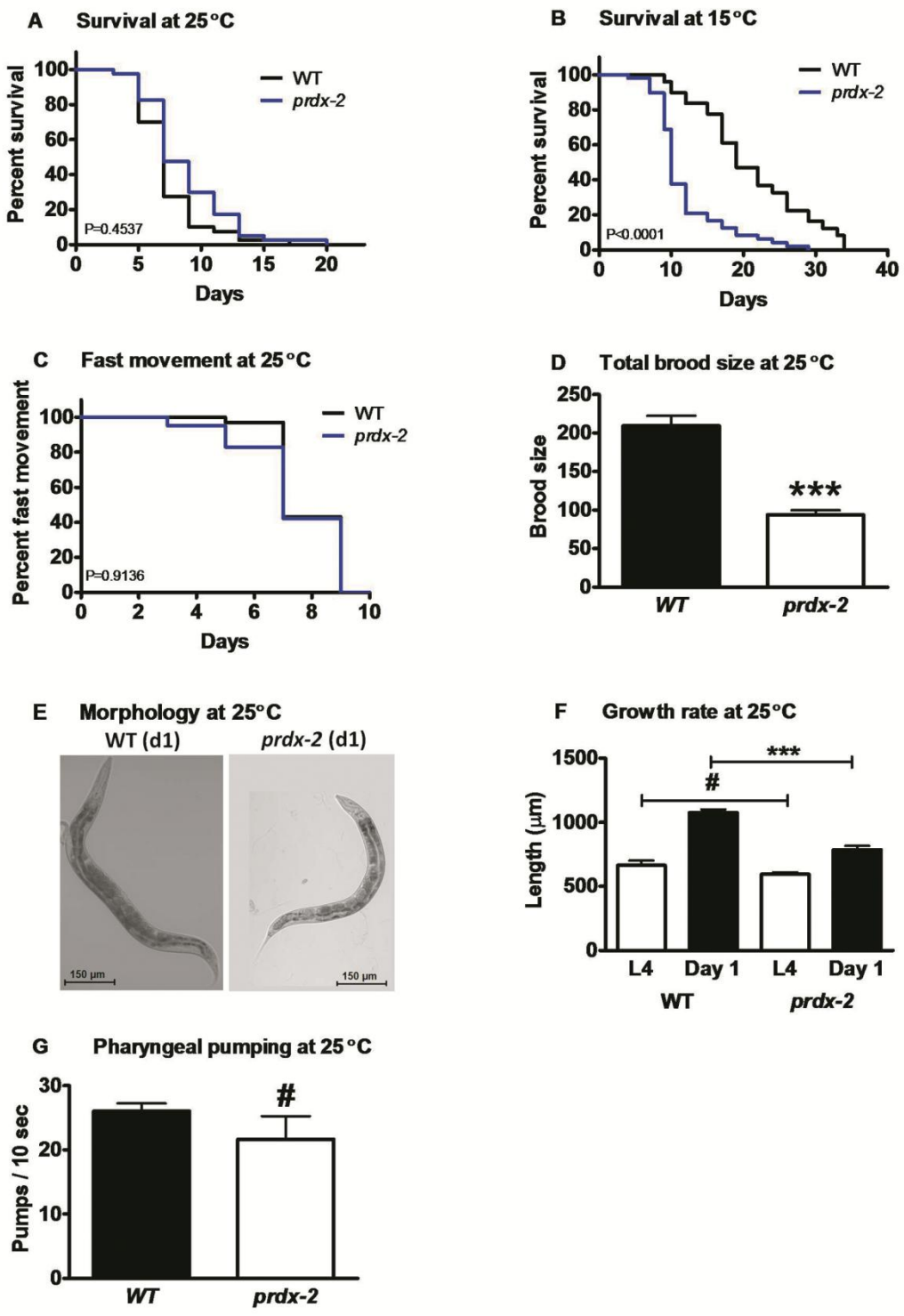

Figure 2-2 Phenotypes of *prdx-2* deletion mutants

Synchronized wild type and *prdx-2* mutant worms (n=50) were singled and scored for (**A, B**) survival at 25°C and 15°C (**C**) fast movement at 25°C and (**D**) progeny production at 25°C. The *prdx-2* mutants are significantly short-lived (P < 0.001) at 15°C (**B**) but not at 25°C (P=0.4537) (**A**). There is no difference in the fast movement span at 25°C (P=0.9136) (**C**) and in the pharyngeal pumping rate on day 1 at 25°C (P=0.2668) (**G**), but *prdx-2* worms produce fewer offspring (P < 0.001) (**D**). Worms were imaged on day 0 and on day 1 after oxidative stress treatment to assess morphology (day 1) at 25°C (**E**) and growth rate from L4 stage to day 1 of adulthood (**F**). The symbols above the bars represent the p-values obtained: # > 0.05, * < 0.05, *** < 0.001. Similar results were obtained in at least three independent experiments.

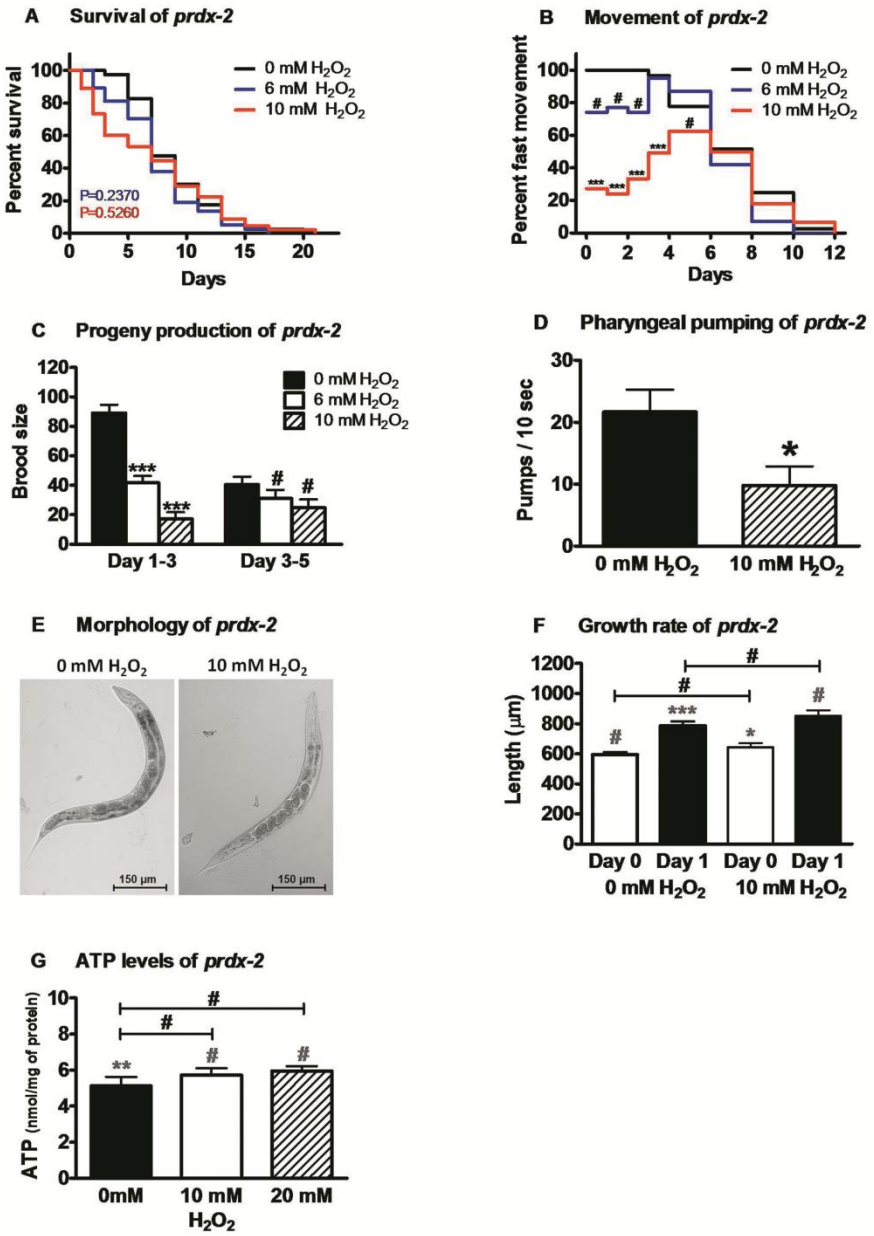

Figure 2-3 Recovery from exogenous H_2O_2 stress is mediated by PRDX-2

Synchronized *prdx-2 C. elegans* (day 0 of adulthood) were incubated with 0, 6, or 10 mM H_2O_2 as in Fig. 1. Then, the oxidant was removed and 50 worms per treatment were singled and scored for (**A**) survival and lifespan, (**B**) fast movement, (**C**) progeny production, (**D**) pharyngeal pumping (day 1), (**E**) morphology (day 1), and (**F**) growth rate (from day 0 to day 1 of adulthood) at 25°C. (**G**) To determine intracellular ATP levels, 100 µl of worms were treated with the indicated concentrations of H_2O_2 for 30 min, and ATP levels were measured before and after oxidative stress treatment. As seen in (**A**), no significant difference in the mean lifespan of oxidatively stressed worms was observed in four independent experiments. A representative life span is shown here with P = 0.2370, χ^2 1.3990 for 6 mM H_2O_2 and P = 0.5260, χ^2 0.4020 for 10 mM H_2O_2 in comparison with the control group (0 mM H_2O_2) (non-parametric log rank test). The movement plot shown in (**B**) is an average of at least three independent experiments and the direct comparison by repeated measures ANOVA and Bonferroni post hoc test reveals a difference in the movement behavior on day 0 through day 3 after the oxidative stress treatment with 10 mM H_2O_2 (P < 0.001) but not with 6 mM H_2O_2. The symbols above the bars in (**C**-**G**) represent the P values obtained using t-test or 1-way ANOVA: # > 0.05, * < 0.05, ** < 0.01, *** < 0.001. The additional symbols (light gray) above the bars in (**F-G**) represent the P values obtained for the comparison of *prdx-2* worms and the respective wild-type worms presented in Fig. 1F and 1G using 2- way ANOVA and Bonferroni post hoc test: # > 0.05, * < 0.05, ** < 0.01, *** < 0.001.

by exogenous peroxide treatment (Fig. 2-3E-G). These results suggest that some cellular processes might already be maximally affected by the oxidative stress that is caused by the absence of PRDX-2.

2.4.3 Quantitative redox proteomics identifies redox-sensitive *C. elegans* proteins

Peroxide stress conditions affect physiological processes, presumably through the oxidative modification of specific cellular targets. We therefore decided to use OxICAT to reveal particularly stress-sensitive proteins whose redox-regulated function might be responsible for some of the observed behavioral and physiological effects of peroxide stress. The OxICAT technology is based on the differential trapping of reduced and oxidized cysteines with two versions of the isotope coded affinity tag (ICAT): an isotopically light ^{12}C-form (*i.e.,* light ICAT) and a 9 Da heavier, isotopically heavy ^{13}C-form (*i.e.,* heavy ICAT) (Leichert *et al.*, 2008) (for details, see Fig. 2-4). All *in vivo* reduced cysteines are alkylated with the light ICAT reagent, whereas all *in vivo* oxidized cysteines are, upon their reduction, labeled with the heavy ICAT reagent. After tryptic digest and enrichment using affinity chromatography, the ICAT-labeled peptides are separated by liquid chromatography (LC) and identified by mass spectrometry (MS). Because light- and heavy-labeled peptides are chemically identical, the relative ion intensities of the two peaks represents the relative abundance of reduced and oxidized protein species in cells, making this method independent of absolute protein amounts. This makes the OxICAT technique uniquely suited to quantitatively describe changes in the thiol status of hundreds of individual proteins in a single experiment.

To investigate which *C. elegans* proteins are sensitive to oxidative modification, we exposed a synchronized population of ~100,000 young adult wild-type *C. elegans* N2 or *prdx-2* deletion mutants to our previously established oxidative stress regimen and quantified the thiol oxidation status of proteins before and after the stress treatment. We found a considerable number of ICAT-labeled peptides whose masses changed by 9 or 18 Da, indicating that they contain either one or two cysteine residues whose redox status changed upon peroxide treatment. We only considered *C. elegans* peptides to be redox-sensitive if their stress-induced changes in thiol oxidation status were reproducibly greater than 1.5-fold and the oxidized population exceeded 20%, the thresholds we previously used to identify

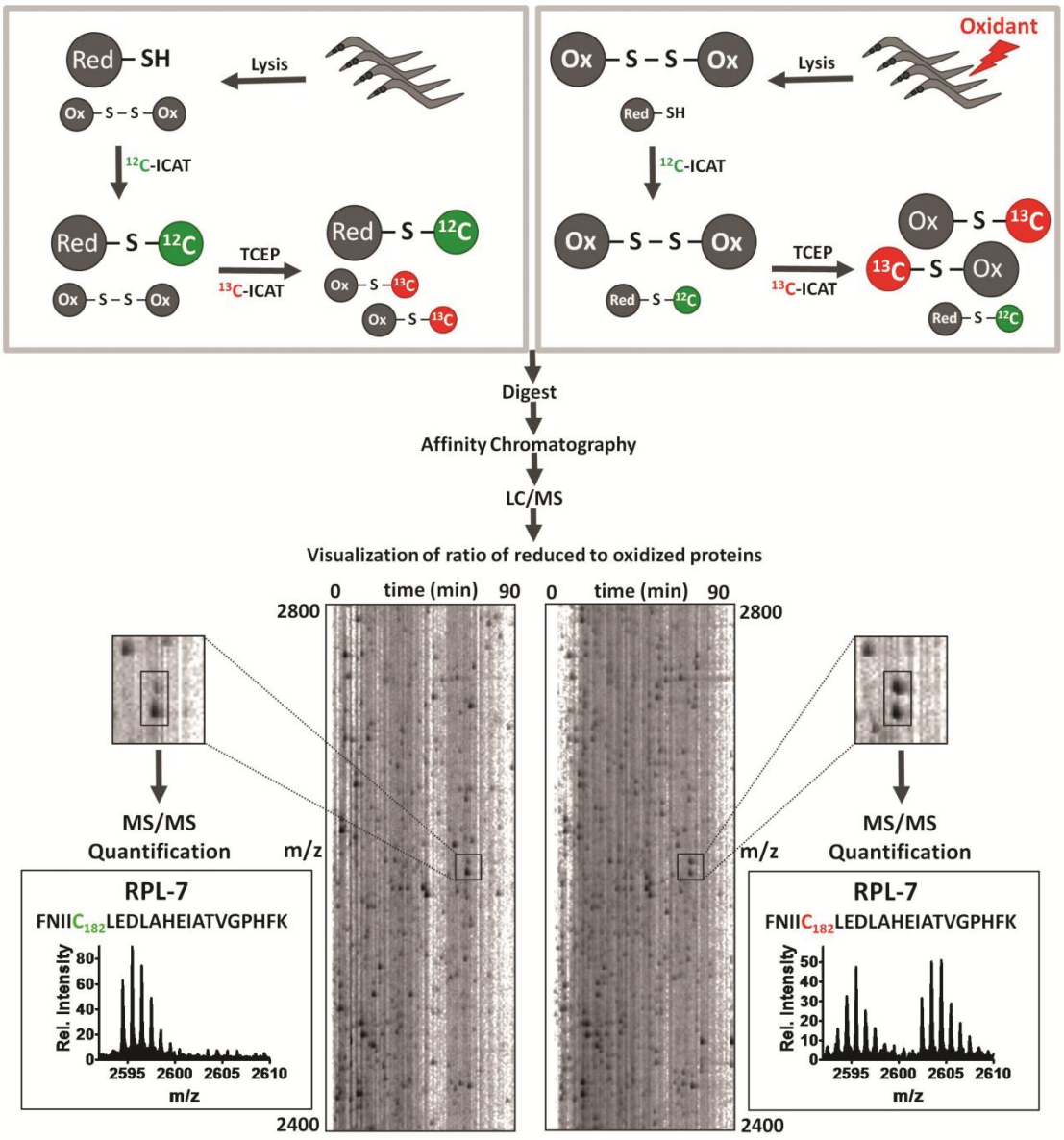

Figure 2-4 Identification of redox-sensitive *C. elegans* proteins using OxICAT

For the OxICAT analysis, a population of ~100,000 worms (day 0 of adulthood) was either left untreated (left panel) or treated with 10 mM H_2O_2 for 30 min (right panel). The worms were washed and lysed. Proteins were incubated with isotopically light ^{12}C-ICAT reagent (green) under denaturing conditions to irreversibly label all reduced cysteines. Then, all reversibly oxidized cysteines were reduced with TCEP [Tris(2-carboxyethyl)phosphine] and subsequently irreversibly labeled with the 9 Da heavier ^{13}C-ICAT reagent (red). The proteins were digested, and ICAT-labeled peptides were purified by affinity chromatography and analyzed using LC/MS. MSInspect was used to illustrate the LC/MS run (for details, see(Leichert *et al.*, 2008)). The mass spectra of a typical ICAT pair harboring one oxidative stress-sensitive cysteine are shown. The mass signal with the m/z value at 2594.5 Da has incorporated one light ICAT molecule and represents the reduced form of the peptide. The mass signal with the higher m/z value of 2603.5 Da (spectra on the right) has incorporated one heavy ICAT molecule and represents the oxidized form of the peptide. MS/MS analysis revealed the identity of the protein (*i.e.,* RPL-7) and of the redox-sensitive cysteine (*i.e.,* Cys182). Analysis of the peak intensity revealed that oxidative stress treatment increased the oxidation status of this cysteine from 6% to 51%.

redox-sensitive proteins in *E. coli* (Leichert *et al.*, 2008). Both the extent of oxidation as well as the total number of identified oxidation-sensitive proteins could be underestimates because only about 60% of the treated worms showed behavioral changes upon stress treatment (Fig. 2-1B). The remaining 40% of worms revealed no obvious defects, suggesting that their redox proteome might not be affected. We then used MS/MS analysis to identify the peptides and the oxidation-sensitive cysteines. We found a total of 40 different proteins whose thiol oxidation status changed at least 1.5-fold and up to 9-fold upon peroxide stress treatment in wild-type and/or *prdx-2* mutant strains (Table 2- 1). Of those, 22 proteins were found to be oxidation-sensitive in both strain backgrounds, confirming their general oxidation sensitivity. Noteworthy, many of these proteins showed very similar absolute oxidation levels, both before and after stress treatment. We identified only two proteins whose cysteines were found to be approximately three-fold more oxidized in non-stress-treated *prdx-2* worms compared to wild-type worms: the highly conserved Cys307 of the Hsp70 homologue HSP-1 and Cys204 of the small subunit ISW-1 of the chromatin remodeling factor (Table 2-1). This increase in thiol oxidation might reflect sub-cellular, localized changes in the peroxide levels of *prdx-2* mutant worms.

All other redox-sensitive peptides that are listed in Table 2-1 were detected either only in wild type or *prdx-2* deletion strains. That we did not detect these peptides in both strain backgrounds might be due to differences in protein expression levels or due to limitations of the LC/MS analysis. The fact, however, that we confirmed so many of the peptides to be sensitive to peroxide stress in both strain backgrounds makes us confident that the listed proteins are indeed peroxide-sensitive.

2.4.4 Protein translation is a major target of oxidative modifications

Proteins involved in translation appear to be among those most heavily targeted by H_2O_2 stress (Table 2-1), a result that agrees well with previous observations that protein translation is a peroxide-sensitive process *in vivo* (Shenton *et al.*, 2006). We identified peroxide-sensitive cysteines in six small (S3A, S14, S17, S19, S21, S28) and three large (L4, L7, L22) ribosomal subunits, in the polyadenylate binding protein PAB-1, and in two elongation factors, EFT-2 and EF-1α (EFT-4). One of the most peroxide-sensitive cysteines that we identified is the lone Cys182 of the large ribosomal subunit protein L7; the oxidation status of this cysteine changed from 6% to over 50% upon peroxide treatment (Fig. 2-4, inset). Although this cysteine is highly conserved in eukaryotes, no studies have addressed its role in L7 function. It is conceivable that formation of sulfenic acid or of an intermolecular

Table 2-1 Thiol oxidation status of *C. elegans* proteins before and after peroxide treatment

	Peptide Annotation		Cysteine Oxidation Status [%]			
ACC Number	Peptide Sequence	Protein	N2	N2 + H_2O_2	*prdx-2*	*prdx-2* + H_2O_2
Protein Translation						
CE00664	TC_{199}SKLYPLQEVYIR	40S ribosomal protein S3a (RPS-1)	14	39	15	25
CE00821	IGRIEDVTPIPSDC$_{140}$TR	40S ribosomal protein S14 (RPS-14)	14	28	17[1]	34
CE26948	VC_{35}DEVAIIGSKPLR	40S ribosomal protein S17 (RPS-17)	11	30	11	37
CE13265	GVAPNHFQTSAGNC$_{99}$LR/K*	40S ribosomal protein S19 (RPS-19)	9/13[2]	34/27[2]	23	34/34[2]
CE30779	YAIC$_{57}$GAIR/R*	40S ribosomal protein S21 (RPS-21)	14/22[2]	39/42[2]	20	47
CE21842	TGSQGQC$_{22}$TQVRVEFINDQNNR	40S ribosomal protein S28 9RPS-28)	18	36	-[3]	-[3]
CE07669	QK/LGPVVIYGQDAEC$_{216}$AR*	Ribosomal protein RL4L4 (RPL-4)	6/12[2]	29/34[2]	12[1]/18[1]	25/34[2]
CE11024	FNIIC$_{182}$LEDLAHEIATVGPHFK	60S ribosomal protein L7 (RPL-7)	6	51	-[3]	-[3]
CE04102	FNVEC$_{27}$KNPVEDGILR	60S ribosomal protein L22 (RPL-22)	10	31	16[1]	37
CE15900	LLEPVYLVEIQC$_{745}$PEAAVGGIYGVLNR/R*	Elongation factor 2 (EFT-2)	7/9[2]	31/27[2]	13	35
CE01270	SGDAGIVELIPTKPLC$_{377}$VESFTDYAPLGR	Elongation factor EF-1 alpha (EFT-4)	-[3]	-[3]	15	36
CE20412	SIYDTFSLFGNILSC$_{149}$K	Polyadenylate-binding protein (PAB-1)	17	34	-[3]	-[3]
Protein Homeostasis						
CE09682	FEELC$_{307}$ADLFR	Heat shock 70 kDa protein A (HSP-1)	7	27	24	42
CE02262	SIHDALC$_{410}$VIR	TCP-1, delta subunit (CCT-4)	13[1]	41	16[1]	36
CE01234	LADHITEC$_{171}$VVDAVLAIR	TCP-1, zeta subunit (CCT-6)	17	33	-[3]	-v
CE27244	LIQDVANKANEEAGDGTTC$_{106}$ATVLAR	Cpn60 (HSP-60)	10	38	11	48
CE05402	AAAPC$_{577}$VLFFDELDSIAK	AAA+-type ATPase (CDC-48.2)	10	22	14[1]	30
CE14954	FLEFVKPFC$_{13}$GFVPEVSKPER	Sec61, alpha-subunit (SEC-61)	-[3]	-[3]	11	30
CE03482	IYHPNINSNGSIC$_{85}$LDILR	Ubiquitin-protein ligase (UBC-2)	12	36	13	29
Motility						
CE06253	C_{280}YHIFYQIYSDFRPELK	Myosin class II heavy chain (LET-75)	8	33	-[3]	-[3]
CE09349	LASC$_{702}$DIEHYLLEK	Myosin class II heavy chain (UNC-54)	-[3]	-[3]	10	26
CE31619	ASGVIDAGLVLNQLTC$_{708}$NGVLEGIR	Myosin-2 (MYO-2)	-[3]	-[3]	20	31
CE04994	NFLAAVC$_{219}$R	Troponin T (MUP-2)	18	25	17	30
CE31204	C_{704}LSHDIDILR	Intermediate filament protein (IFC-2)	-	-	14	29
CE27706	KPQILQQTSAGGEPAIC$_{550}$FDIGYSAR	Immunoglobin-like protein (DIM-1)	6	46	-	-
ATP Homeostasis						
CE22210	LAANNPLLC$_{218}$GQR	Vac. H^+-ATPase V1, subunit A (VHA-13)	18	25	13	35
CE04424	LIYQTVC$_{33}$GVNGPLVILNDVKFPQFSEIVK	Vac. H^+-ATPase V1, subunit B (VHA-12)	7	26	-[3]	-[3]
CE09650	GDFC$_{109}$IQTGR	Nucleoside diphosphate kinase (F25H2.5)	24	41	-[3]	-[3]
CE09650	NIC$_{117}$HGSDAVDSANR	Nucleoside diphosphate kinase (F25H2.5)	9	34	-[3]	-[3]
CE37112	SIC$_{341}$DGLKLQIR	Creatine kinase (F46H5.3)	-[3]	-[3]	13	30
Metabolism and Others						
CE01225	C_{153}VLNIGTHTPSHLGMLENANVLAR	Fructose-biphosphate aldolase (ALDO-2)	21	45	26	47
CE12728	GIFIC$_{76}$DGSQHEADELIDKLIER	PEP-carboxykinase (R11A5.4)	-[3]	-[3]	8	39
CE01130	NTC$_{391}$PGDVSALRPGGIR	Gly/Ser hydroxymethyltransferase (MEL-32)	30	46	32[1]	53
CE25005	TAVPSTIHC$_{123}$DHLIEAQKGGAQDLAR	Aconitase (ACO-2)	-[3]	-[3]	10	43
CE29792	WC$_{204}$PSINAVVLIGDEAAR	Chromatin remodeling complex (ISW-1)	13	22	34	50
CE17691	GPDAGYIATSGC$_{374}$VLSAALTLIR	Uncharacterized membrane protein (F22F7.1)	20	43	23	28
CE17154	HFELLPNDAIVC$_{299}$NVGHFDC$_{306}$EIDVK[4]	S-adenosylhomocysteine hydrolase (AHCY-1)	27	42	23[1]	43
CE23530	LISDIEDEC$_{666}$GGVHIRFPSEK	Vigilin (C08H9.2)	26	36	13	29
CE00913	TAVC$_{354}$DIPPR	Tubulin beta-2 chain (TBB-1)	11	25	-[3]	-[3]
CE01431	GLGTDEAVLIEILC$_{112}$SR	Annexin (NEX-1)	8	23	11	27
E41898	TGLGLC$_{919}$IR	Similarity to human attractin (TAG-53)	-	-	20	36

[1] peptide was identified once only; [2] two peptides differing in their cleavage site were identified; average oxidation status in the respective peptides is shown; [3]peptide was either not identified or the spectra quality was too poor to determine precise oxidation status; [4] both cysteines in this peptide were found to be oxidized.

disulfide with either the small tripeptide glutathione (*i.e.,* S-glutathionylation) or another protein leads to conformational and functional changes in this important component of the eukaryotic translation machinery.

The small subunit S21 (RPS-21) is another ribosomal protein that we found to contain a highly peroxide-sensitive cysteine (*i.e.,* Cys57) in both wild-type and *prdx-2* mutant strains (Fig. 2-5A). Its activity is required for embryonic and germline development and for the overall health of the animal (http://www.wormbase.org, release WS204, 29 Jul 2009). We identified two Cys57-containing RPS-21 peptides in wild-type worms that only differ in their respective cleavage site. Cys57 was oxidized to either 39% or 42% depending on the respective peptide (Table 2-1, Fig. 2-5A), a result that nicely illustrates the accuracy of our

OxICAT technique. Similarly, we identified two Cys745-containing peptides of the elongation factor EFT-2 whose oxidation status changed from either 7% to 31% or from 6% to 27% upon peroxide treatment (Fig. 2-5A). This result strongly suggests that this cysteine, which is highly conserved and located in one of the three highly mobile tRNA mimicking C-terminal domains of EFT-2, is peroxide-sensitive. This notion is consistent with previous studies, which revealed that EFT-2 in Jurkat cells contains peroxide stress-sensitive cysteine(s) (Baty *et al.*, 2005) and that EFT-2 in macrophages and smooth muscle cells undergoes S-nitrosylation reactions (Greco *et al.*, 2006). While the peroxide-sensitive cysteine(s) in EFT-2 have not yet been located, Cys567 has been identified as a target of S-nitrosylation (Greco *et al.*, 2006). We found that a significant proportion of EFT-2 is reproducibly and significantly oxidized at the equally conserved Cys745. Additional studies are necessary to determine if this oxidative cysteine modifications plays indeed a regulatory role in EFT-2 function. Finally, we identified Cys149, one of three conserved cysteines in the polyadenylate binding protein PAB-1, to be sensitive to peroxide-mediated oxidation. Expression of PAB-1 has very recently been shown to suppress peroxide-induced cell death in NIH/3T3 cells, suggesting that it has an oxidative-stress protective function *in vivo* (Nagano-Ito *et al.*, 2009).

2.4.5 Peroxide treatment targets proteins involved in protein homeostasis

Oxidative modification and inactivation of proteins involved in protein translation is considered to be an effective strategy to rapidly down-regulate new protein synthesis under stress conditions that cause harm to newly synthesized and existing proteins. In contrast, molecular chaperones, such as bacterial Hsp33 (Jakob *et al.*, 1999) or eukaryotic peroxiredoxin (Jang *et al.*, 2004), which are involved in maintaining protein homeostasis, use oxidative thiol modifications as a mechanism to rapidly activate their chaperone function. This effectively prevents the aggregation of stress-unfolded proteins and increases oxidative stress resistance (Kumsta & Jakob, 2009). Here, we identified several additional chaperones whose function might be redox-regulated. One of these chaperones is the Hsp70 homologue HSP-1, a highly conserved family of ATP-dependent chaperones whose members play important roles in de novo protein folding, stress-induced unfolding, protein transport, and protein degradation (reviewed in (Liberek *et al.*, 2008)). We found that Cys307, one of the three highly conserved cysteines in eukaryotic Hsp70s, becomes significantly oxidized in both wild-type and prdx-2 deletion strains (Table 2-1, Fig. 2-5B). S-glutathionylation of at least one Hsp70 homologue has been previously shown to increase its *in vitro* chaperone

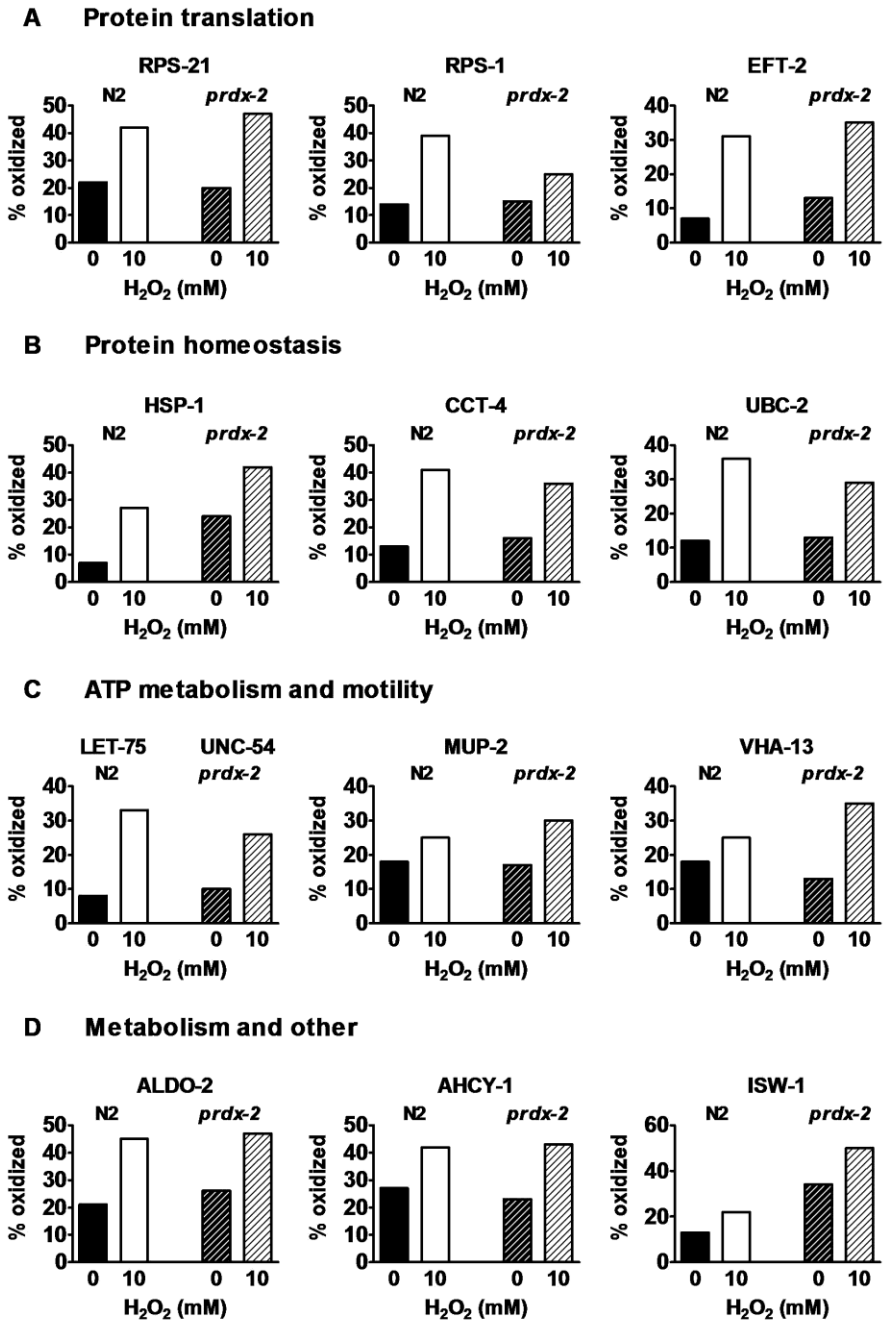

Figure 2-5 Oxidation status of select redox-sensitive *C. elegans* proteins
The oxidation state of cysteines in select redox-sensitive proteins involved in (**A**) protein translation, (**B**) protein homeostasis, (**C**) ATP metabolism and motility and (**D**) metabolism and other functions is shown.

function, suggesting that oxidative cysteine modification might serve as post-translational regulation of Hsp70's chaperone activity (Hoppe *et al.*, 2004). It remains now to be determined whether oxidation of the highly conserved Cys307 is involved in this regulation.

In addition to HSP-1, we also identified one conserved cysteine in the delta subunit of the TCP/TriC chaperonin complex (i.e., CCT-4) to be highly sensitive to peroxide-mediated oxidation (Fig. 2-5B). The TCP/TriC complex supports de novo folding of actin and myosin, as

well as numerous other beta-sheet rich multidomain proteins (Yam *et al.*, 2008). The oxidation-sensitive cysteine that we identified is part of a highly conserved Cys-X3-Cys motif, which is common for redox-sensitive and/or metal binding proteins (Koehler, 2004). We also identified a peroxide-sensitive cysteine in the zeta subunit CCT-6 of the TCP/TriC chaperonin complex, suggesting that several members of this complex might be redox-sensitive.

In addition to identifying these potentially redox-sensitive chaperones, we also noted that peroxide stress targets a set of cysteine-containing proteins involved in protein targeting and degradation. One of these proteins is the class I ubiquitin-conjugating enzyme UBC-2, whose active site cysteine was found to become significantly oxidized upon peroxide stress treatment (Table 2-1). The *C. elegans* orthologue UBC-2, which is encoded by the essential let-70 gene, has been implicated in the ubiquitin-mediated degradation of many short-lived proteins (Zhen *et al.*, 1993). UBC-2 belongs to the highly conserved class of E2-conjugating enzymes. All members of this class share the presence of one active site cysteine (e.g., Cys85 in UBC-2), which catalyzes the transfer of small peptidic modifiers, such as ubiquitin (UB) or SUMO, from specific E1-activating enzymes to protein substrates via the engagement of distinct E3 ligases. These post-translational modifications modify and affect protein-protein interactions, localization, activity, and/or stability of hundreds of different proteins in eukaryotic cells (for recent review, see (Ye & Rape, 2009)). Our study clearly demonstrates that the redox state of the active site cysteine of UBC-2 changes from a predominantly reduced state before oxidative stress treatment to a more than 30% oxidized state upon treatment (Fig. 2-5B). This result is in excellent agreement with previous reports on the redox-regulated activity of both ubiquitin- and SUMO-conjugating enzymes E2 (Jahngen-Hodge *et al.*, 1997; Bossis & Melchior, 2006). Because oxidation of the active site cysteine is known to cause the inactivation of the conjugating enzyme, and by extension, the complete pathway, these results suggest significant changes in the proteostasis network during oxidative stress conditions in *C. elegans*.

In addition to UBC-2, our study revealed at least one more redox-sensitive protein that plays a role in ubiquitin-mediated protein degradation: the highly conserved AAA-protein CDC-48 (i.e., p99, VCP). CDC-48 is an ATP-dependent molecular chaperone whose primary function appears to be the chaperoning of retro-translocated, ubiquitylated ER proteins to the proteasome (reviewed in (Dreveny *et al.*, 2004)). CDC-48 harbors several cysteine residues, of which only three are conserved between yeast CDC-48 and human VCP. Interestingly, one of these conserved cysteines is the highly oxidation-sensitive Cys105 that we identified in our study (Table 2-1). So far, it is unclear how oxidation of Cys105, which

resides in the N-terminal substrate-binding domain of CDC-48, affects the functionality of the chaperone. The C-terminal ATPase activity of mammalian CDC-48 has been shown to be redox-regulated (Noguchi *et al.*, 2005), suggesting that CDC-48 is an intrinsically redox-sensitive protein. The last protein that we identified in this group of redox-sensitive proteins involved in proteostasis is the ER translocation channel protein SEC-61. It has been suggested that SEC-61 mediates the retro-translocation of ubiquitylated ER proteins into the cytoplasm and thereby the transfer to CDC-48 (Jarosch *et al.*, 2002). These results suggest that peroxide stress conditions lead to the reversible down-regulation of ubiquitin-mediated protein degradation. It remains to be tested whether this mechanism prevents the degradation of oxidatively modified proteins during sublethal oxidative stress conditions, which would eliminate the possibility of quickly regenerating their protein activity once reducing conditions have been restored.

2.4.6 Muscle contraction and growth rate are major targets of peroxide stress in *C. elegans*

Another large group of *C. elegans* proteins that is targeted by peroxide stress include muscle-specific proteins and enzymes involved in ATP homeostasis. This result agrees well with our earlier observations that peroxide-treated worms show a massive decline in motility (Fig. 2-1). We found increased cysteine oxidation in three different paralogues of the myosin class II heavy chain: Cys280 of the pharynx-specific LET-75, Cys702 of UNC-54, and the equivalent Cys708 of MYO-2 (Fig. 2-5C). The fact that we independently identified the same cysteine to be redox-sensitive in two different myosin-isoforms (UNC-54, MYO-2) illustrates the general oxidation sensitivity of this specific cysteine residue. This is particularly significant because this cysteine is highly conserved from yeast to human myosin and is located adjacent to a second conserved cysteine, which has been proposed to be redox-sensitive and involved in the ATPase activity of myosin (Konno *et al.*, 2000). Oxidative inactivation of UNC-54, the major *C. elegans* myosin heavy chain required for locomotion and egg-laying, and MYO-2, which is exclusively expressed in the pharynx, might contribute to the observed peroxide-mediated defects in motility, pharyngeal pumping, and egg-laying. In addition to the three myosin class 2 paralogues, we also found MUP-2, a homologue of the invertebrate troponin T, the muscle-organizing protein DIM-1, and the intermediate filament IFC-2 (*i.e.,* lamin) to contain at least one significantly peroxide-sensitive cysteine (Table 2-1, Fig. 2-5C). Like myosin, troponin T is involved in muscle contraction and normal growth rate, whereas IFC-2 is required for movement, growth rate, body size, and body shape (http://www.wormbase.org, release WS204, 29 Jul 2009). It is therefore very likely

that oxidative modification of one or more of these proteins contributes to the severe defects in movement, pharyngeal pumping, and/or growth rate observed in oxidatively stressed animals.

2.4.7 Identification of peroxide sensitive thiols in ATPases and enzymes catalyzing transphosphorylation reactions

Like the defects in *C. elegans* motility, which became immediately obvious in oxidatively stressed animals, we measured a dramatic loss in intracellular ATP levels within 30 min of peroxide treatment in wild-type worms (Fig. 2-1G) and found decreased steady-state ATP levels in *prdx-2* deficient worms (Fig. 2-3G). A similar decrease in cellular ATP levels was previously observed in peroxide-stress treated bacteria and yeast and has, at least in part, been attributed to the oxidative inactivation of GAPDH and F-type ATPases (Hyslop *et al.*, 1988). Although we could not detect the cysteine-containing active site peptides of *C. elegans* GAPDH or F-type ATPase in our mass spectra, we found redox-sensitive cysteines in the A and B subunits of the V-type ATPase and in proteins involved in transphosphorylation reactions [*e.g.,* NDPK, creatine kinase] (Table 2-1, Fig. 2-5C). V-type ATPases deplete cellular ATP levels by hydrolyzing ATP to acidify lysosomal and endosomal organelles, whereas NDPK transfers phosphoryl groups from ATP to other nucleoside diphosphates. Creatine kinase, on the other hand, generates ATP by transferring phosphoryl groups from the phosphocreatine pool of the muscle cells to ADP. Importantly, redox sensitivity has been previously reported for all three proteins, which agrees well with our observed results. It has been shown, for instance, that mammalian and plant V-type ATPases undergo reversible disulfide bond formation in response to H_2O_2 treatment, which leads to the inactivation of the proton pump (Feng & Forgac, 1994; Tavakoli *et al.*, 2001). Whereas some of the redox-sensitive cysteines in subunit A have already been identified (*i.e.,* Cys 254, Cys532) (Feng & Forgac, 1994), we have now also discovered a highly conserved Cys33 in subunit B to be oxidation-sensitive. Inactivation of *C. elegans* V-type ATPase has been recently shown to exert neuroprotective effects against necrosis (Syntichaki *et al.*, 2005), suggesting that oxidation-mediated inactivation of V-type ATPases might not only save already scarce ATP resources during oxidative stress, but may be a strategy to protect against necrosis.

We confirmed previous reports that the active site Cys109 of NDPK is highly susceptible to oxidative modification (Table 2-1) and that the multiple activities of the mammalian NDPK homologue Nm23 in endocytosis and tumor suppression are redox-regulated (Lee *et al.*, 2009). In addition, we detected the nearby Cys117 to be highly oxidation-sensitive as well (Table 2-1), suggesting that peroxide stress leads to

intramolecular disulfide bond formation in NDPK. In the case of creatine kinase, we were unable to identify the peptide containing the active site Cys283, which has also previously been reported to be redox-sensitive (Reddy *et al.*, 2000). Instead, we detected a nearby second cysteine to be highly oxidation-sensitive, implying again the possibility of an intramolecular disulfide bond. In either case, oxidative thiol modification has been demonstrated to cause the inactivation of both kinases, which might contribute to the observed changes in *C. elegans'* ATP homeostasis and/or serve as a protective measure to prevent further ATP depletion. Unfortunately, we did not detect the corresponding active site cysteine-containing peptides in the mass spectra of our *prdx-2* deficient worms, making it impossible for us to confirm whether oxidative modification of any of these proteins is responsible for the significantly decreased steady state ATP levels observed in *prdx-2* deficient worms.

In addition to the redox-sensitive proteins that we identified to be involved in protein translation, protein homeostasis, muscle function, and ATP homeostasis, we also found redox-sensitive proteins involved in a variety of other functions, including metabolism (*e.g.,* aldolase, aconitase), signal transduction (*e.g.,* annexin), chromatin remodeling (*e.g.* ISW-1 complex), and heterochromatin formation (*e.g.,* vigilin) (Table 2-1, Fig. 2-5D). Again, some of these proteins have previously been shown to be redox-sensitive (*e.g.,* annexin) (Caplan *et al.*, 2004), whereas many others have not, to our knowledge, been reported to undergo reversible oxidative modifications (*e.g.,* DIM-1, vigilin, tubulin). However, the fact that we confirmed the oxidation-sensitive cysteines in many of the known redox-sensitive proteins makes us very confident that the newly identified proteins are redox-sensitive as well. Potential functional or structural changes that occur upon the oxidative modification of these proteins will likely contribute to the behavioral and physiological changes that accompany oxidative stress in *C. elegans* and possibly higher eukaryotes.

2.5 Discussion

The accumulation of oxidative damage to biomolecules has been implicated in the pathogenesis of a variety of different diseases and is thought to be one potential cause of aging (Kovacic & Jacintho, 2001; Aliev *et al.*, 2002). The major drawback in analyzing the role of oxidative stress in aging and disease, however, is the inability to define if, when, and which oxidants become physiologically relevant. To start to address some of these questions, we decided to expose synchronized young *C. elegans* to a sublethal short-term treatment of peroxide stress, monitor the physiological effects, and determine potential

eukaryotic target proteins. When we studied the behavioral changes in peroxide-treated worms, we made the surprising observation that the majority of worms suffer from severe, yet fully reversible behavioral changes that are highly reminiscent of well-known age-related changes, such as declines in body movement, pharyngeal pumping, and reproduction, as well as morphological changes and reduced metabolic activity (Collins *et al.*, 2008). In contrast to old worms, however, the peroxide-treated young worms fully recovered from this damage.

We identified the highly conserved enzyme peroxiredoxin (PRDX-2) as a repair system that appears to be involved in the recovery from exogenous peroxide stress. Together with catalases, peroxiredoxins are known to keep intracellular peroxide concentrations low. Lack of either *prdx-2* or the cytosolic catalase *ctl-2* has been shown, both here and elsewhere, to cause a number of so-called progeric (age-related) phenotypes (Petriv & Rachubinski, 2004; Olahova *et al.*, 2008), which are very similar to the changes that we observed in peroxide-treated animals, strongly suggesting that these mutant animals suffer from chronic peroxide stress. Deletion of either one of the two genes significantly shortens the lifespan of *C. elegans*, providing evidence that peroxide-mediated damage contributes to lifespan. These results are in stark contrast to observations made in strains lacking one or more paralogues of superoxide dismutase (SOD-1 through SOD-5), which detoxify the second major physiological oxidant, superoxide. Whereas individual *sod* deletion mutants suffer from increased oxidative damage as assessed by protein carbonylation, the worms did not exhibit progeric phenotypes or shortened lifespan (Yang *et al.*, 2007). These results raise the intriguing possibility that hydrogen peroxide and its reaction products play more prominent roles in aging and lifespan determination than superoxide, which might allow for the development of more targeted antioxidant strategies.

As previously noted, the analysis of protein carbonylation is a widely used method for assessing cellular oxidative damage. One major disadvantage of measuring protein carbonylation is that this oxidative side chain modification is irreversible, which makes its quantification very challenging (Soskic *et al.*, 2008). It is difficult, for instance, to distinguish whether one protein molecule is carbonylated at 100 different sites or whether 100 protein molecules are carbonylated at one site, the two scenarios having very different implications to overall protein function. Thus, conclusions about the extent of oxidative damage are often problematic. These limitations might have contributed to some conflicting findings. For example, mutants defective in superoxide dismutase do not reveal any lifespan defect despite increased levels of protein carbonylation (Yang *et al.*, 2007). In this study, we

therefore decided to use the quantitative thiol trapping method OxICAT to determine (i) which proteins undergo oxidative thiol modification, (ii) what specific cysteine residues are involved, and (iii) how much of a protein population is affected (Leichert *et al.*, 2008). In a single set of experiments, we confirmed or discovered the oxidation sensitivity of many known and unknown redox-sensitive proteins and identified cysteine residues targeted by peroxide stress. We found that most of the identified redox-sensitive cysteines are highly conserved, implying that they likely play structural and/or functional roles in the respective proteins and that their modification reversibly affects the activity of the protein.

The processes that we found to be targeted by peroxide stress involve protein translation, protein homeostasis, and metabolism (Table 2-1). Interestingly, all these cellular processes have previously been implied to be peroxide-sensitive. We find that many individual players in a single process are simultaneously targeted and that the targeting occurs to similar extents. These results suggest that the oxidative modification of these proteins might not simply be a passive, non-specific reaction to oxidants but an active regulatory mechanism, potentially involved in combating oxidative stress. Oxidative inactivation of protein translation, for instance, will not only save scarce energy resources needed to fight oxidative damage but will actively prevent production of nascent polypeptides under potentially error-prone conditions. This response is used to actively fight oxidative stress and has been shown to extend lifespan in a variety of different organisms (Kennedy & Kaeberlein, 2009). Oxidative inactivation of proteins involved in targeted degradation, such as UBC-2, SEC-61, and CDC-48, might prevent proteolysis of proteins whose oxidative modifications are reversible once reducing conditions have been restored. Oxidative modification of critical cysteines in chaperones such as the Hsp70 homologue HSP-1, on the other hand, might be an effective strategy to increase chaperone function under conditions in which protein unfolding and aggregation is likely to occur (Hoppe *et al.*, 2004). This strategy finds precedent in bacteria, where peroxide-mediated activation of the redox-sensitive chaperone Hsp33 is used to combat protein unfolding and aggregation during severe oxidative stress (Winter *et al.*, 2008). Oxidative inactivation of enzymes involved in glycolysis (*e.g.,* aldolase, ALDO-2) will redirect glucose to the pentose phosphate pathway, which is an effective mechanism to increase NADPH levels, necessary to restore redox homeostasis (Godon *et al.*, 1998). Finally, transient oxidative inactivation of ATP-depleting enzymes, such as the muscle-related proteins myosin and troponin, or the vacuolar V-type ATPase and NDPK, would avoid energy expenditure for processes that are not immediately essential for survival. Based on these considerations, it is now tempting to

speculate that peroxide stress, although eventually toxic, might initially be used to actively down-regulate non-essential functions, thereby conserving energy, combating oxidative stress, and, by these means, extending an otherwise even shorter lifespan. This hypothesis would still uphold Harman's free radical theory of aging, which states that the progressive decline observed in aging organisms is due to increased oxidative damage. However, it would also include the potentially beneficial aspects of reactive oxygen species as modulatory second messengers that affect stress resistance and longevity early in life. These conclusions are supported by recent observations by Ristow and coworkers, who reported that lifespan extending regimens in *C. elegans*, such as glucose restriction, involve transient ROS accumulation, causing increased oxidative stress resistance and hormetic life extension (Schulz *et al.*, 2007).

2.6 References

Aliev G, Smith MA, Seyidov D, Neal ML, Lamb BT, Nunomura A, Gasimov EK, Vinters HV, Perry G, LaManna JC & Friedland RP (2002) The role of oxidative stress in the pathophysiology of cerebrovascular lesions in Alzheimer's disease. *Brain Pathol* **12**, 21-35.

Apel K & Hirt H (2004) Reactive oxygen species: metabolism, oxidative stress, and signal transduction. *Annu Rev Plant Biol* **55**, 373-399.

Baty JW, Hampton MB & Winterbourn CC (2005) Proteomic detection of hydrogen peroxide-sensitive thiol proteins in Jurkat cells. *Biochem J* **389**, 785-795.

Bossis G & Melchior F (2006) Regulation of SUMOylation by reversible oxidation of SUMO conjugating enzymes. *Mol Cell* **21**, 349-357.

Brandes N, Schmitt S & Jakob U (2009) Thiol-based redox switches in eukaryotic proteins. *Antioxid Redox Signal* **11**, 997-1014.

Caplan JF, Filipenko NR, Fitzpatrick SL & Waisman DM (2004) Regulation of annexin A2 by reversible glutathionylation. *J Biol Chem* **279**, 7740-7750.

Collins JJ, Huang C, Hughes S & Kornfeld K (2008) The measurement and analysis of age-related changes in *Caenorhabditis elegans*. *WormBook*, 1-21.

Deneke SM (2000) Thiol-based antioxidants. *Curr Top Cell Regul* **36**, 151-180.

Dreveny I, Pye VE, Beuron F, Briggs LC, Isaacson RL, Matthews SJ, McKeown C, Yuan X, Zhang X & Freemont PS (2004) p97 and close encounters of every kind: a brief review. *Biochem Soc Trans* **32**, 715-720.

Feng Y & Forgac M (1994) Inhibition of vacuolar H(+)-ATPase by disulfide bond formation between cysteine 254 and cysteine 532 in subunit A. *J Biol Chem* **269**, 13224-13230.

Finkel T & Holbrook NJ (2000) Oxidants, oxidative stress and the biology of ageing. *Nature* **408**, 239-247.

Godon C, Lagniel G, Lee J, Buhler JM, Kieffer S, Perrot M, Boucherie H, Toledano MB & Labarre J (1998) The H2O2 stimulon in Saccharomyces cerevisiae. *J Biol Chem* **273**, 22480-22489.

Greco TM, Hodara R, Parastatidis I, Heijnen HF, Dennehy MK, Liebler DC & Ischiropoulos H (2006) Identification of S-nitrosylation motifs by site-specific mapping of the S-nitrosocysteine proteome in human vascular smooth muscle cells. *Proc Natl Acad Sci U S A* **103**, 7420-7425.

Hoppe G, Chai YC, Crabb JW & Sears J (2004) Protein s-glutathionylation in retinal pigment epithelium converts heat shock protein 70 to an active chaperone. *Exp Eye Res* **78**, 1085-1092.

Huang C, Xiong C & Kornfeld K (2004) Measurements of age-related changes of physiological processes that predict lifespan of *Caenorhabditis elegans*. *Proc Natl Acad Sci U S A* **101**, 8084-8089.

Hyslop PA, Hinshaw DB, Halsey WA, Jr., Schraufstatter IU, Sauerheber RD, Spragg RG, Jackson JH & Cochrane CG (1988) Mechanisms of oxidant-mediated cell injury. The glycolytic and

mitochondrial pathways of ADP phosphorylation are major intracellular targets inactivated by hydrogen peroxide. *J Biol Chem* **263**, 1665-1675.

Imlay JA (2003) Pathways of oxidative damage. *Annu Rev Microbiol* **57**, 395-418.

Isermann K, Liebau E, Roeder T & Bruchhaus I (2004) A peroxiredoxin specifically expressed in two types of pharyngeal neurons is required for normal growth and egg production in *Caenorhabditis elegans*. *J Mol Biol* **338**, 745-755.

Jahngen-Hodge J, Obin MS, Gong X, Shang F, Nowell TR, Jr., Gong J, Abasi H, Blumberg J & Taylor A (1997) Regulation of ubiquitin-conjugating enzymes by glutathione following oxidative stress. *J Biol Chem* **272**, 28218-28226.

Jakob U, Muse W, Eser M & Bardwell JC (1999) Chaperone activity with a redox switch. *Cell* **96**, 341-352.

Jang HH, Lee KO, Chi YH, Jung BG, Park SK, Park JH, Lee JR, Lee SS, Moon JC, Yun JW, Choi YO, Kim WY, Kang JS, Cheong GW, Yun DJ, Rhee SG, Cho MJ & Lee SY (2004) Two enzymes in one; two yeast peroxiredoxins display oxidative stress-dependent switching from a peroxidase to a molecular chaperone function. *Cell* **117**, 625-635.

Jarosch E, Geiss-Friedlander R, Meusser B, Walter J & Sommer T (2002) Protein dislocation from the endoplasmic reticulum--pulling out the suspect. *Traffic* **3**, 530-536.

Kennedy BK & Kaeberlein M (2009) Hot topics in aging research: protein translation, 2009. *Aging Cell* **8**, 617-623.

Koehler CM (2004) The small Tim proteins and the twin Cx3C motif. *Trends Biochem Sci* **29**, 1-4.

Konno K, Ue K, Khoroshev M, Martinez H, Ray B & Morales MF (2000) Consequences of placing an intramolecular crosslink in myosin S1. *Proc Natl Acad Sci U S A* **97**, 1461-1466.

Kovacic P & Jacintho JD (2001) Mechanisms of carcinogenesis: focus on oxidative stress and electron transfer. *Curr Med Chem* **8**, 773-796.

Kumsta C & Jakob U (2009) Redox-regulated chaperones. *Biochemistry* **48**, 4666-4676.

Larsen PL (1993) Aging and resistance to oxidative damage in *Caenorhabditis elegans*. *Proc Natl Acad Sci U S A* **90**, 8905-8909.

Lee E, Jeong J, Kim SE, Song EJ, Kang SW & Lee KJ (2009) Multiple functions of Nm23-H1 are regulated by oxido-reduction system. *PLoS One* **4**, e7949.

Leichert LI, Gehrke F, Gudiseva HV, Blackwell T, Ilbert M, Walker AK, Strahler JR, Andrews PC & Jakob U (2008) Quantifying changes in the thiol redox proteome upon oxidative stress *in vivo*. *Proc Natl Acad Sci U S A*.

Liberek K, Lewandowska A & Zietkiewicz S (2008) Chaperones in control of protein disaggregation. *EMBO J* **27**, 328-335.

Nagano-Ito M, Banba A & Ichikawa S (2009) Functional cloning of genes that suppress oxidative stress-induced cell death: TCTP prevents hydrogen peroxide-induced cell death. *FEBS Lett* **583**, 1363-1367.

Noguchi M, Takata T, Kimura Y, Manno A, Murakami K, Koike M, Ohizumi H, Hori S & Kakizuka A (2005) ATPase activity of p97/valosin-containing protein is regulated by oxidative modification of the evolutionally conserved cysteine 522 residue in Walker A motif. *J Biol Chem* **280**, 41332-41341.

Olahova M, Taylor SR, Khazaipoul S, Wang J, Morgan BA, Matsumoto K, Blackwell TK & Veal EA (2008) A redox-sensitive peroxiredoxin that is important for longevity has tissue- and stress-specific roles in stress resistance. *Proc Natl Acad Sci U S A* **105**, 19839-19844.

Paulsen CE & Carroll KS Orchestrating redox signaling networks through regulatory cysteine switches. *ACS Chem Biol* **5**, 47-62.

Petriv OI & Rachubinski RA (2004) Lack of peroxisomal catalase causes a progeric phenotype in *Caenorhabditis elegans*. *J Biol Chem* **279**, 19996-20001.

Reddy S, Jones AD, Cross CE, Wong PS & Van Der Vliet A (2000) Inactivation of creatine kinase by S-glutathionylation of the active-site cysteine residue. *Biochem J* **347 Pt 3**, 821-827.

Schulz TJ, Zarse K, Voigt A, Urban N, Birringer M & Ristow M (2007) Glucose restriction extends *Caenorhabditis elegans* life span by inducing mitochondrial respiration and increasing oxidative stress. *Cell Metab* **6**, 280-293.

Shenton D, Smirnova JB, Selley JN, Carroll K, Hubbard SJ, Pavitt GD, Ashe MP & Grant CM (2006) Global translational responses to oxidative stress impact upon multiple levels of protein synthesis. *J Biol Chem* **281**, 29011-29021.

Sohal RS (2002) Role of oxidative stress and protein oxidation in the aging process. *Free Radic Biol Med* **33**, 37-44.

Soskic V, Groebe K & Schrattenholz A (2008) Nonenzymatic posttranslational protein modifications in ageing. *Exp Gerontol* **43**, 247-257.

Stadtman ER (2001) Protein oxidation in aging and age-related diseases. *Ann N Y Acad Sci* **928**, 22-38.

Syntichaki P, Samara C & Tavernarakis N (2005) The vacuolar H+ -ATPase mediates intracellular acidification required for neurodegeneration in *C. elegans*. *Curr Biol* **15**, 1249-1254.

Tavakoli N, Kluge C, Golldack D, Mimura T & Dietz KJ (2001) Reversible redox control of plant vacuolar H+-ATPase activity is related to disulfide bridge formation in subunit E as well as subunit A. *Plant J* **28**, 51-59.

Winter J, Ilbert M, Graf PC, Ozcelik D & Jakob U (2008) Bleach activates a redox-regulated chaperone by oxidative protein unfolding. *Cell* **135**, 691-701.

Yam AY, Xia Y, Lin HT, Burlingame A, Gerstein M & Frydman J (2008) Defining the TRiC/CCT interactome links chaperonin function to stabilization of newly made proteins with complex topologies. *Nat Struct Mol Biol* **15**, 1255-1262.

Yang W, Li J & Hekimi S (2007) A Measurable increase in oxidative damage due to reduction in superoxide detoxification fails to shorten the life span of long-lived mitochondrial mutants of *Caenorhabditis elegans*. *Genetics* **177**, 2063-2074.

Ye Y & Rape M (2009) Building ubiquitin chains: E2 enzymes at work. *Nat Rev Mol Cell Biol* **10**, 755-764.

Zhen M, Heinlein R, Jones D, Jentsch S & Candido EP (1993) The ubc-2 gene of *Caenorhabditis elegans* encodes a ubiquitin-conjugating enzyme involved in selective protein degradation. *Mol Cell Biol* **13**, 1371-1377.

2.7 Supplemental Material and Methods

2.7.1 Large-scale *C. elegans* cultivation and synchronization

For large-scale *C. elegans* cultivation standard egg plates were used (McGhee, 1999). Synchronization was accomplished by isolating eggs by hypochlorite treatment of gravid adults cultivated on these egg plates (McGhee, 1999). Eggs were allowed to hatch by overnight incubation in M9 medium during gentle shaking. Newly hatched L1 larvae were cultured on nematode growth medium (NGM) agar plates with OP50.

2.7.2 Lifespan, movement and brood size analysis

Synchronized L4 larvae (day 0 of adulthood) of wild type N2 and *prdx-2* worms were singled and transferred onto fresh NGM plates with OP50 every other day until egg production ceased. After this period, animals were transferred every 4-7 days. Animals were scored as dead when they failed to respond to repeated tapping with a platinum wire pick. Animals that desiccated at the edge of the plate, escaped or died due to internal hatching were excluded from the lifespan analysis. At least 50 worms were tested in each experiment. Animals were scored for their movement behavior as described in (Huang *et al.*, 2004). Animals that were affected in their movement due to internal hatching or protruding gonads were excluded from the analysis. Animals were scored as self-fertile when progeny was present on the plate on the day of transfer. For brood size evaluation, the number of eggs and larvae was counted. Animals that suffered from internal hatching were excluded from fertility and brood size measurements.

2.7.3 Statistical Analysis of Lifespan and Behavior

All statistical analyses were performed using GraphPad Prism4 software. The mean lifespan (MLS) and Standard Error (SE) were calculated using the following equations (Wu *et al.*, 2006):

with d_j: number of worms that died in time interval x_j+x_{j+1}

x_j+x_{j+1}: time interval

N: total number of worms

$$SE = \sqrt{\frac{1}{N(N-1)}\sum_j \left(\frac{x_j + x_{j+1}}{2} - MLS\right)^2 \cdot d_j}$$

The same equations were used to calculate the mean fast movement span except that d_j represented the number of worms that no longer showed fast movement behavior. To compare lifespan and behavior of two or more populations, the Mann-Whitney test or the Kruskal-Wallis test and Dunn's post hoc test were performed, respectively. To compare survival after oxidative stress treatment the non-parametric log-rank test was used (Glantz, 2005).

2.7.4 OXICAT data analysis

The OxICAT data were analyzed using a modified version of the open source program *msinspect*, which is described in great detail in (Leichert *et al.*, 2008). In short, ICAT pairs were defined as mass signals that differ by multiples of 9 Da and elute in the same fraction of the HPLC. The oxidation state of these ICAT pairs was calculated by the *msinspect* software. To be considered redox-sensitive, cysteines had to be on average at least 1.5 fold more oxidized under the chosen experimental conditions as compared to control conditions and the largest mass peak had to be at least 4-fold above background under all conditions. All redox sensitive peptides were individually confirmed using the visualization tools in msInspect. Calculations were performed in Excel and at least two and up to eight independent replicates were performed per sample. Values that were two standard deviations above or below the mean were omitted.

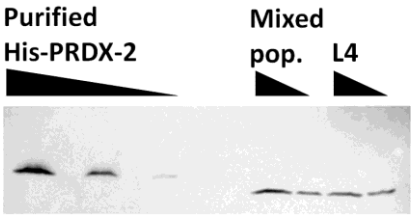

Suppl. Figure 2-1 PRDX-2 is a high-abundance protein
Lysates from either a mixed population of *C. elegans* or synchronized L4 larvae were prepared and two different concentrations (10 μg and 5 μg) of total protein were applied onto reducing SDS-PAGE. A standard curve with defined concentrations of purified His-tagged *C. elegans* PRDX-2 (50 ng, 25 ng, 5 ng) was used to determine the amount of PRDX-2 in *C. elegans* lystaes. The westernblot using antibodies against *C. elegans* PRDX-2 is shown.

3 IS OVEROXIDATION OF PEROXIREDOXIN PHYSIOLOGICALLY SIGNIFICANT?

Maike Thamsen[1], Caroline Kumsta[1], Fei Li[1], Ursula Jakob[1,2]

Antioxid Redox Signal., 2011 14(4):725-30

[1]Department of Molecular, Cellular, and Developmental Biology and [2]Program in Cellular and Molecular Biology, University of Michigan, Ann Arbor, MI, USA

3.1 Abstract

Eukaryotic peroxiredoxins are highly susceptible to sulfinic acid formation. This overoxidation, which is thought to convert peroxiredoxins into chaperones, can be reversed by sulfiredoxins. Several organisms, including *Caenorhabditis elegans*, lack sulfiredoxins but encode sestrins, proteins proposed to be functionally equivalent. We induced peroxiredoxin overoxidation in *C. elegans* with a short peroxide pulse. We found that reduction of overoxidized peroxiredoxin 2 (PRDX-2) was extremely slow and sestrin-independent, strongly implying that worms lack an efficient repair system. Analysis of PRDX-2's overoxidation status during *C. elegans* lifespan revealed no accumulation of overoxidized PRDX-2 at any point, questioning whether PRDX-2 overoxidation in worms is physiologically relevant.

3.2 Introduction

Reactive oxygen species (ROS), such as hydrogen peroxide (H_2O_2), superoxide anions ($O_2^{\bullet-}$), and hydroxyl radicals ($OH^{\bullet}$) are constantly produced by NADPH oxidases and mitochondria during oxidative phosphorylation (Halliwell & Gutteridge, 2007). At low concentrations, they play important roles as signaling molecules, regulating a multitude of different processes that range from gene regulation and metabolism to protein translation and degradation (Forman *et al.*, 2010). At high concentrations, however, ROS can cause damage to virtually every cellular macromolecule and, if not detoxified, will lead to apoptosis and cell death (Gardner, 1989; Evans *et al.*, 2004; Davies, 2005). Not surprisingly, cells harbor a machinery of antioxidant proteins to combat oxidative stress conditions and redox-balancing systems to sustain the reducing environment of the cell (Mathers *et al.*, 2004). One large family of antioxidant proteins are peroxiredoxins, which use an active site cysteine to attack the O-O bond of ROOH substrates thus converting harmful peroxides to harmless water (Ellis & Poole, 1997). Some of their members play important physiological roles as illustrated for instance in *C. elegans*, where lack of the cytosolic peroxiredoxin homologue PRDX-2 causes progeric phenotypes and a shortened lifespan (Olahova *et al.*, 2008; Kumsta *et al.*, 2010), or in mice,

where absence of Prdx1 leads to hemolytic anemia and increased tumor frequency, which contributes to shortened lifespan as well (Neumann *et al.*, 2003).

One of the unique features of eukaryotic typical 2-Cys peroxiredoxins is their high susceptibility to cysteine overoxidation (Yang *et al.*, 2002). In the presence of elevated concentrations of peroxide, the active site cysteine of peroxiredoxins, which forms a sulfenic acid (-SOH) intermediate during the regular detoxification cycle, is further oxidized to sulfinic acid ($-SO_2H$), which leads to the inactivation of the peroxidase function (Woo *et al.*, 2003). This finding led to the "floodgate model", which proposes that peroxide-mediated inactivation of peroxiredoxin allows localized peroxide-signaling events to occur, potentially necessary to combat oxidative stress (Wood *et al.*, 2003). This model was supported by the discovery of sulfiredoxins, which appear to specifically reduce the overoxidized 2-Cys peroxiredoxins (Biteau *et al.*, 2003). Furthermore, *in vitro* studies with yeast and human peroxiredoxin suggested that overoxidation might cause a functional switch in peroxiredoxin, turning the peroxidase into a chaperone-active oligomer (Jang *et al.*, 2004; Moon *et al.*, 2005). Limited *in vivo* evidence exists to support this conclusion, including recent studies in peroxide-treated *C. elegans*, which suggested a correlation between accumulation of overoxidized PRDX-2 and increased heat resistance of the worms. This observation led the authors to the conclusion that the potential chaperone activity of overoxidized PRDX-2 might be involved in the heat shock tolerance of peroxide-treated worms (Olahova *et al.*, 2008).

These results suggested that eukaryotic peroxiredoxins are posttranslationally regulated by the oxidation status of their active site cysteine. It came thus as a surprise when genomic studies revealed that certain organisms, including *C. elegans*, lack sulfiredoxin homologues (Lowther & Haynes, 2010). One possible explanation was that these organisms might use sestrins, a family of antioxidant proteins, to regenerate overoxidized peroxiredoxins (Budanov *et al.*, 2004; Essler *et al.*, 2009). This alternative scenario was, however, recently challenged by a study demonstrating that sestrins are unable to reduce overoxidized peroxiredoxins *in vitro* or *in vivo* (Woo *et al.*, 2009). To shed light into the question how organisms, such as *C. elegans* deal with peroxiredoxin overoxidation, we therefore decided to expose *C. elegans* to a short peroxide treatment, monitor overoxidation of the highly abundant peroxiredoxin homologue PRDX-2 and follow its regeneration. Our results strongly suggest that *C. elegans* lack an enzymatic system that clears overoxidized PRDX-2 and raise the general question whether overoxidation of PRDX-2 is a physiological event in worms.

3.3 Materials and Methods

3.3.1 Strains and culture conditions

The Bristol strain N2 (wild type) was provided by the *Caenorhabditis* Genetics Center and the *sesn-1* knockout strain by the Mitani Laboratory at the Tokyo Women's Medical University School of Medicine. The *sesn-1* knockout strain was back-crossed three times to the wild type strain N2. Worms were cultured using standard protocols.

3.3.2 Oxidative stress treatment

Oxidative stress treatment was performed as previously described (Kumsta *et al.*, 2010). In short, a synchronized L4 population of *C. elegans* N2 or *sesn-1* was treated with 10 mM H_2O_2 for 30 min while shaking continuously. Worms were washed twice with M9 and either plated on NGM plates seeded with OP50 for recovery or shock frozen in liquid nitrogen and stored at -80°C. Worms were lysed in 10% trichloroacetic acid using a Fisher Scientific Power Gen 125 homogenizer.

3.3.3 2D gel electrophoresis, western blot analysis and protein quantification

Samples for 2D gel electrophoresis were prepared as described (Leichert & Jakob, 2004) with the exception that protein thiols were reduced with dithiothreitol and subsequently labeled with iodoacetamide. 2D-gel electrophoresis was performed using the Ettan IPGphor II and DALT II system by Amersham Biosciences as described previously (Leichert & Jakob, 2004). Western Blot analysis was performed using standard protocols using polyclonal antibodies raised against *C. elegans* PRDX-2 (Alpha Diagnostics International), or antibodies against a peptide derived from overoxidized human Prx-SO_2H (Abcam Inc). Protein quantification was performed using ImageJ or Delta 2D (Decodon) software.

3.3.4 PRDX-2 purification, reduction and overoxidation

The plasmid pJC45 containing the His-tagged variant of *C. elegans* PRDX-2 was kindly provided by Dr. Bruchhaus (Isermann *et al.*, 2004) and transformed into *E. coli* BL21 (DE3)(pAPlacIQ). After IPTG induction and overexpression of PRDX-2, the protein was purified with a Ni-NTA column using standard procedures. *In vitro* reduction of purified PRDX-2 was achieved by incubating PRDX-2 with 5 mM DTT for 15 min at room temperature. To overoxidize PRDX-2, 100 µM purified PRDX-2 was incubated with 2.5 µM *E. coli* thioredoxin (Trx), 0.08 µM *E. coli* thioredoxin reductase (TrxR) and 10 mM H_2O_2 for 1h at RT (Chang *et al.*, 2004).

3.3.5 Chaperone Assay

Influence of PRDX-2 on the thermal aggregation of bovine citrate synthase (CS) (Sigma) was analyzed at 43°C. 100 µM $PRDX_{red}$, PRDX-SO_2H or lysozyme was diluted 1:10 into 40 mM Hepes, pH 7.5 at 43°C. Then, CS (final concentration 0.5 µM) was added and the samples were incubated for 20 min at 43°C. After the incubation, the samples were centrifuged (5,000 rpm, for 30 in at 4°C) and the soluble supernatant was loaded onto a 14% SDS-PAGE.

3.4 Results

3.4.1 Exogenous peroxide treatment causes overoxidation and inactivation of *C. elegans* PRDX-2

Previous analysis of the physiological consequences of an acute 30 min peroxide stress treatment in *C. elegans* revealed a multitude of defects, including a decrease in motility, brood size, and pharyngeal pumping, which were highly reminiscent of alterations observed in aging animals (Kumsta *et al.*, 2010). In contrast to aging organisms, however, which eventually succumb and die, we found that young wild-type *C. elegans* recover from these transient oxidative stress conditions within 24-48 hours. We identified the protein that appeared to play an essential role in this recovery process to be the cytosolic peroxiredoxin homologue PRDX-2 (Kumsta *et al.*, 2010). In the absence of PRDX-2, animals were unable to fully recover from the short exposure to peroxide stress, and showed persistent peroxide-mediated defects in mobility and egg laying (Kumsta *et al.*, 2010). Analysis of the *in vivo* oxidation status of PRDX-2 in wild type worms using 2D gels revealed that 50% of the total *C. elegans* PRDX-2 protein was shifted to an acidic pI within 30 min of H_2O_2 exposure, suggestive of PRDX-2 overoxidation (Fig. 3-1A, upper panel). Western blot analysis using antibodies against a conserved sulfinic acid peptide derived from human PRDX-2 reacted with the shifted PRDX-2 species from *C. elegans*, confirming that this shift is indeed due to sulfinic acid formation (Fig. 3-1A lower panel). These results suggested that PRDX-2 is involved in the initial detoxification of exogenous peroxide, and, during this process, undergoes peroxide-mediated overoxidation and potentially inactivation. That overoxidation of PRDX-2's active site cysteine abolishes its protective peroxidase function was furthermore suggested by our finding that the steady-state concentration of one of the best known substrate proteins of peroxiredoxins, glutamine synthetase (GLN-3) (Netto *et al.*, 1996), decreased dramatically upon peroxide treatment (Fig. 3-1B). The peroxidase function of peroxiredoxins has previously been shown to protect glutamine synthetase from H_2O_2-mediated inactivation and oxidative degradation in cell lysates, and was in fact the activity that led to the original purification of peroxiredoxins (Netto *et al.*, 1996). Our observation that GLN-3 is rapidly

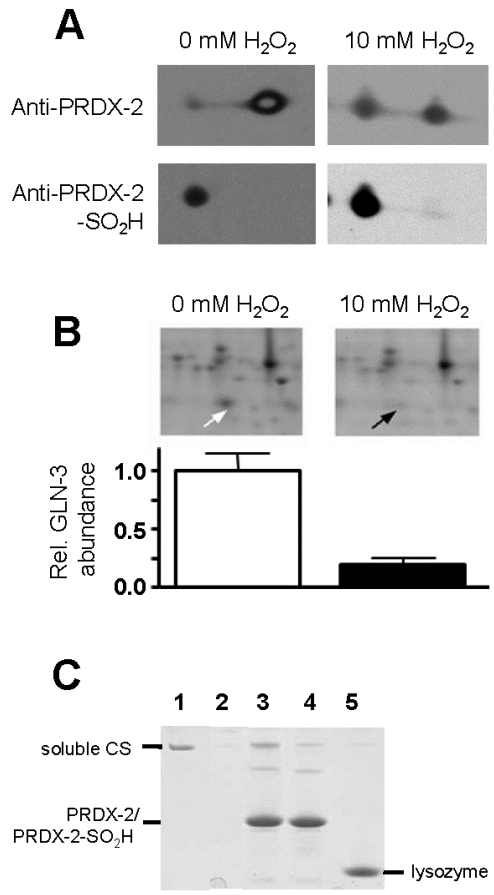

Figure 3-1 Overoxidation of PRDX-2 upon exogenous oxidative stress

A) Analysis of the overoxidation status of PRDX-2 upon exogenous oxidative stress *in vivo*. Synchronized L4 larvae were treated with 10 mM H_2O_2 for 30 min. Worms were lysed and *C. elegans* proteins were separated on 2D gels. Western blot analysis using antibodies against *C. elegans* PRDX-2 (upper panel) or against overoxidized PRDX-2-SO_2H (lower panel) was performed.

B) Glutamate synthetase GLN-3 is rapidly degraded upon oxidative stress treatment of *C. elegans*. Details of the Coomassie stained 2D gels are shown. The arrows indicate the position of GLN-3, which was identified by mass spectrometry.

C) Chaperone activity of reduced and overoxidized PRDX-2 was analyzed by testing its influence on the thermal aggregation pattern of citrate synthase (CS) at 43°C. 0.5 µM CS was incubated in the absence (lane 2) of chaperones or in the presence of 10 µM PRDX-2_{red} (lane 3), 10 µM overoxidized PRDX-2-SO_2H (lane 4) or 10 µM lysozyme (lane 5) in 40 mM Hepes, pH 7.5 for 20 min at 43°C. Then, samples were centrifuged and the soluble supernatant was loaded onto a 14% SDS-PAGE. The amount of soluble CS in the native protein sample is shown as control in lane 1.

oxidatively degraded agrees with our overoxidation results, suggesting that a large proportion of PRDX-2 becomes inactivated upon exogenous peroxide stress.

To test whether *C. elegans* PRDX-2, like the typical 2-Cys peroxiredoxins from yeast and humans, functions as a peroxidase under low H_2O_2 conditions and as a chaperone under high H_2O_2 stress, we overexpressed and purified the His-tagged version of *C. elegans* PRDX-2 from *Escherichia coli* cells. We generated overoxidized PRDX-2 using cycles of thioredoxin-mediated reduction and H_2O_2–mediated oxidation and confirmed that overoxidation leads to a loss in peroxidase activity (data not shown) (Yang *et al.*, 2002). Next we tested the influence of reduced and overoxidized PRDX-2 on the *in vitro* aggregation of thermally denatured citrate synthase (CS) by analyzing the amount of soluble CS after 20 min of thermal inactivation in the absence or presence of PRDX-2 (Buchner *et al.*, 1998). As shown in Fig. 3-1C, we found that PRDX-2's chaperone function was increased upon overoxidation of PRDX-2. Presence of a 20:1 ratio of overoxidized PRDX-2 monomers to CS monomers almost completely prevented the thermal aggregation of CS and maintained CS in a soluble form while the same concentration of reduced PRDX-2 monomers showed only minor influence on the aggregation behavior of CS. In contrast to human and yeast peroxiredoxins (Jang *et al.*, 2004; Moon *et al.*, 2005), however, significantly higher concentrations of PRDX-2 were required

to prevent the aggregation of CS, suggesting that *C. elegans* PRDX-2 might be less efficient as a chaperone. Nevertheless, however, these results indicated that overoxidation of *C. elegans* PRDX-2 causes the inactivation of its peroxidase activity and an increase in chaperone activity.

3.4.2 Overoxidation of *C. elegans* PRDX-2 appears to be an irreversible process *in vivo*

To investigate the fate of overoxidized PRDX-2 in nematodes, we decided to elucidate whether this process is reversible *in vivo*. We exposed synchronized wild-type *C. elegans* to our 30 min short-term peroxide stress treatment, washed the worms and analyzed the time course over which overoxidized PRDX-2 disappeared from the worms. As before, we lysed ~ 100,000 synchronized worms before and after oxidative stress treatment, separated the proteins by 2D gels and performed western blot analysis to quantify the amount of shifted (*i.e.,* overoxidized) PRDX-2 *in vivo*. We found that it required more than 22 hours to fully clear the worms from overoxidized PRDX-2. Noteworthy, this time frame was similar to the time it took peroxide-treated animals to recover from the stress treatment (24-48 h), suggesting that reactivation of PRDX-2's peroxidase function might contribute to the recovery process of the animals (Kumsta *et al.*, 2010). Our observation that the disappearance of overoxidized PRDX-2 is very slow strongly argued against an efficient endogenous repair system that reduces sulfinic acid and restores the peroxidase activity of PRDX-2. Instead it suggested that *C. elegans* depends on the degradation of overoxidized PRDX-2 and new synthesis of PRDX-2 to maintain their pool of peroxidase-active PRDX-2.

Consistent with the very long lifetime of overoxidized *C. elegans* PRDX-2 was the finding that *C. elegans*, like many other organisms such as *Xenopus laevis*, *Gallus gallus* and *Neurospora crassa*, do not encode any sulfiredoxin homologues, enzymes previously shown to reduce overoxidized peroxiredoxins (Lowther & Haynes, 2010). Further analysis of the *C. elegans* genome revealed, however, that *C. elegans* encodes the sestrin homologue Y74C9A.5. Sestrins have also been implied in the reduction of overoxidized peroxiredoxins (Budanov *et al.*, 2004; Essler *et al.*, 2009), although recent reports challenged these results by demonstrating that overexpression of Sesn 2 in HeLa or A549 cells did not reduce overoxidized Prxs, and that deletion of the *sesn2* gene in mouse embryonic fibroblasts had no effect on the recovery of overoxidized peroxiredoxin (Woo *et al.*, 2009). We decided that our ability to monitor PRDX-2's overoxidation *in vivo* and the fact that *C. elegans* encodes only one member of the sestrin family, which is non-essential for growth (data not shown), put us into an excellent position to evaluate the role of sestrins in the regeneration of overoxidized PRDX-2 in organisms that lack sulfiredoxin.

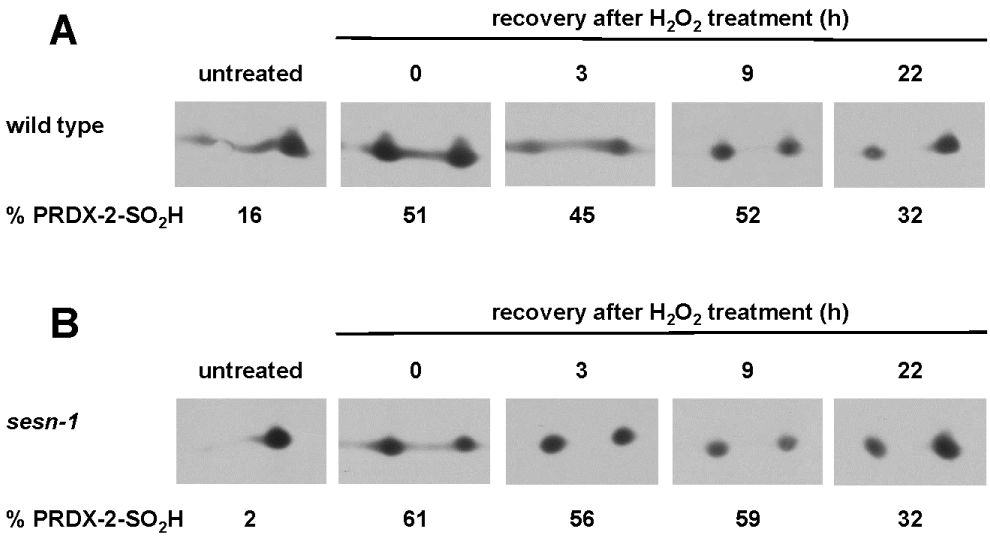

Figure 3-2 PRDX-2 recovery after exogenous oxidative stress treatment of *C. elegans*
A synchronized L4 population of wild type (A) or *sesn-1* deletion mutants (B) was treated with 10 mM H_2O_2 for 30 min, washed and seeded on fresh plates. Aliquots of the worms were taken before and at defined time points after the stress treatment and lysed. *C. elegans* proteins were separated on 2D gels and subsequent western blot analysis with antibodies against PRDX-2 was performed. Three independent experiments were performed and a representative result is shown. ImageJ software was used to quantify the % overoxidized PRDX-2 in the worms.

We obtained and back-crossed the Y74C9A.5 knockout strain, and, based on the homology of Y74C9A.5 to human sestrin, decided to rename the *C. elegans* gene *sesn-1* and the protein SESN-1. We exposed *sesn-1* mutant worms to our previously established peroxide stress regiment and compared the overoxidation status of PRDX-2 between wild type and *sesn-1* mutant strains before and after the 30 min peroxide stress treatment. As shown in Fig. 3-2B, we did not observe any significant difference in the steady-state levels of overoxidized PRDX-2 in wild type and mutant strains, either before or at any time point after the oxidative stress treatment. As before, we found that the overoxidized form of PRDX-2 was only very slowly cleared and the time line agreed again well with the recovery of the *sesn-1* mutant animals from peroxide stress (data not shown). These results strongly implied that SESN-1 is not involved in the regeneration of PRDX-2.

3.4.3 Overoxidation of PRDX-2 appears insignificant during the lifespan of *C. elegans*

The slow regeneration of PRDX-2 under conditions where exogenous peroxide has long been removed, suggested that worms lack an enzymatic system that regenerates overoxidized PRDX-2 and rely on the slow and selective degradation of overoxidized PRDX-2 and the new synthesis of unmodified PRDX-2 to maintain their pool of peroxidase-active PRDX-2. These results left us wonder

whether organisms that lack sulfiredoxins are less likely to encounter peroxide stress conditions that are sufficiently high to cause overoxidation of peroxiredoxins in the first place. Alternatively, overoxidation of peroxiredoxins might provide a strategy for these organisms to generate a pool of chaperones, necessary to combat protein-unfolding conditions at distinct stages in their life. To test to what extent PRDX-2 overoxidation actually takes place during the life span of *C. elegans*, we synchronized worms, cultivated them at 15°C and monitored the overoxidation status of PRDX-2 between the larval stage L4 and day 20 of adulthood. At day 20 under these cultivation conditions, most worms show motility defects and other age-related changes (Croll *et al.*, 1977) (data not shown). As before, we lysed aliquots of the synchronized worms at defined time points, separated the proteins on 2D gels and performed western blot analysis with antibodies against PRDX-2. As shown in Fig. 3-3A, we were unable to see any increase in the overoxidation status of PRDX-2 even in aged worms. Given the slow kinetic with which overoxidized PRDX-2 is cleared from the cells, these results suggest that *C. elegans* PRDX-2, at least under our growth conditions, has a very low tendency for overoxidation *in vivo*. We obtained very similar results when we analyzed the overoxidation status of PRDX-2 in sesn-1 deletion worms (Fig. 3-3B), which serves as further indication that sestrin does not affect the overoxidation status of PRDX-2 in *C. elegans*.

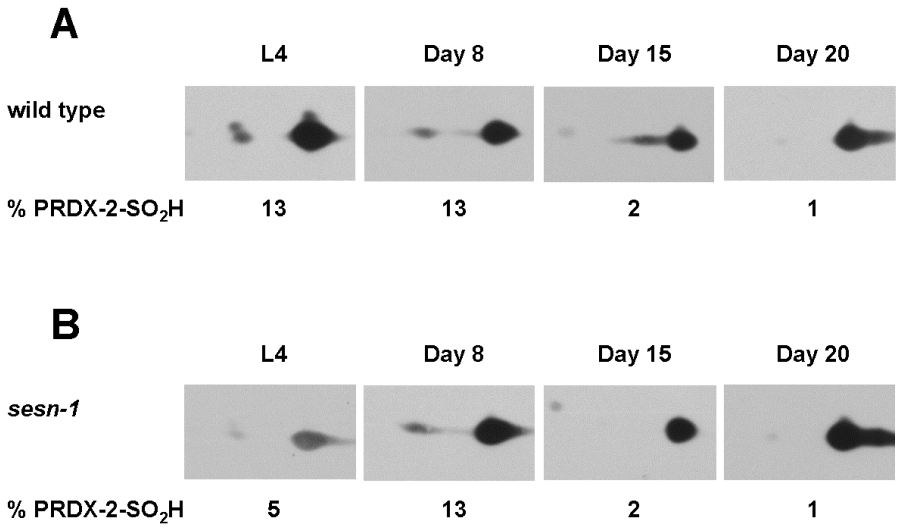

Figure 3-3 Analysis of PRDX-2 overoxidation during the lifespan of *C. elegans*
Synchronized populations of wild type N2 (A) and sesn-1 deletion worms (B) were cultivated at 15°C. Aliquots of worms were taken at L4, day 8, day 15 and day 20 of adulthood and lysed. *C. elegans* proteins were separated on 2D gels and western blot analysis was performed using antibodies against PRDX-2. Four independent experiments were performed and a representative result is shown. ImageJ software was used to quantify the % overoxidized PRDX-2 in the worms.

3.5 Concluding remarks

Eukaryotic type-2 peroxiredoxins are characterized by their high susceptibility to overoxidation. This initial finding, combined with the discovery of sulfiredoxins, enzymes specialized to reduce sulfinic acid and regenerate peroxiredoxins, led to an attractive model, in which the rapid inactivation of peroxiredoxin would permit transient, potentially compartmentalized peroxide-mediated signaling events, critical to combat oxidative stress (Jonsson & Lowther, 2007). This model left unexplained, however, the fact that many organisms lack sulfiredoxin, and raised the question how these organisms deal with overoxidation and inactivation of peroxiredoxins (Lowther & Haynes, 2010). One possible explanation was that sestrins, highly conserved Nrf2-dependent antioxidant proteins, take over the function of sulfiredoxins in those organisms. We tested this hypothesis in *C. elegans*, which lacks sulfiredoxin, encodes only one member of the sestrin family and accumulates overoxidized PRDX-2 when treated exogenously with peroxide. Our studies showed that *C. elegans* clears overoxidized PRDX-2 only very slowly, in a process that seemed unaffected by the lack of sestrin. These results are in excellent agreement with very recent studies, which demonstrated that sestrins do not play a major role in the regeneration of overoxidized human PRDX-2 (Woo *et al.*, 2009). One possible explanation for the finding that *C. elegans*, and potentially other organisms lack the need for sulfiredoxin might be that they do not encounter endogenous peroxide concentrations during their normal lifespan that lead to significant accumulation of overoxidized PRDX-2, which would require enzymatic removal. We analyzed the overoxidation status of worms until day 20 of their lifespan, where worms have been shown to suffer from oxidative stress conditions and new protein synthesis is thought to decrease. However, we were unable to detect any significant amount of overoxidized PRDX-2 even at this advanced stage in their life span. Although we cannot exclude that increased proteolysis of overoxidized PRDX-2 factors into these low steady state levels, we found no significant change in the overall levels of PRDX-2. Thus, very rapid proteolysis of overoxidized PRDX-2 combined with rapid new PRDX-2 synthesis would be required to maintain these high levels of unmodified PRDX-2, an unlikely event given their advanced age. Our results suggest however, that during the lifespan of *C. elegans*, peroxide conditions do not reach levels that are high enough to cause the overoxidation of PRDX-2, and thus to switch PRDX-2 into a molecular chaperone. While we cannot exclude the possibility that *C. elegans* will encounter stress conditions that might cause PRDX-2 overoxidation, we propose that overoxidation and its concurrent switch to molecular chaperone function does not play a significant physiologically role during the normal lifespan of *C. elegans*, and potentially other organisms that lack the sulfiredoxin system.

3.6 References

Biteau B, Labarre J & Toledano MB (2003) ATP-dependent reduction of cysteine-sulphinic acid by S. cerevisiae sulphiredoxin. *Nature* **425**, 980-984.

Buchner J, Grallert H & Jakob U (1998) Analysis of chaperone function using citrate synthase as nonnative substrate protein. *Methods Enzymol* **290**, 323-338.

Budanov AV, Sablina AA, Feinstein E, Koonin EV & Chumakov PM (2004) Regeneration of peroxiredoxins by p53-regulated sestrins, homologs of bacterial AhpD. *Science* **304**, 596-600.

Chang TS, Jeong W, Woo HA, Lee SM, Park S & Rhee SG (2004) Characterization of mammalian sulfiredoxin and its reactivation of hyperoxidized peroxiredoxin through reduction of cysteine sulfinic acid in the active site to cysteine. *J Biol Chem* **279**, 50994-51001.

Croll NA, Smith JM & Zuckerman BM (1977) The aging process of the nematode *Caenorhabditis elegans* in bacterial and axenic culture. *Exp Aging Res* **3**, 175-189.

Davies MJ (2005) The oxidative environment and protein damage. *Biochim Biophys Acta* **1703**, 93-109.

Ellis HR & Poole LB (1997) Novel application of 7-chloro-4-nitrobenzo-2-oxa-1,3-diazole to identify cysteine sulfenic acid in the AhpC component of alkyl hydroperoxide reductase. *Biochemistry* **36**, 15013-15018.

Essler S, Dehne N & Brune B (2009) Role of sestrin2 in peroxide signaling in macrophages. *FEBS Lett* **583**, 3531-3535.

Evans MD, Dizdaroglu M & Cooke MS (2004) Oxidative DNA damage and disease: induction, repair and significance. *Mutat Res* **567**, 1-61.

Forman HJ, Maiorino M & Ursini F (2010) Signaling functions of reactive oxygen species. *Biochemistry* **49**, 835-842.

Gardner HW (1989) Oxygen radical chemistry of polyunsaturated fatty acids. *Free Radic Biol Med* **7**, 65-86.

Halliwell B & Gutteridge JMC (2007) *Free radicals in biology and medicine*, 4th ed. Oxford ; New York: Oxford University Press.

Isermann K, Liebau E, Roeder T & Bruchhaus I (2004) A peroxiredoxin specifically expressed in two types of pharyngeal neurons is required for normal growth and egg production in *Caenorhabditis elegans*. *J Mol Biol* **338**, 745-755.

Jang HH, Lee KO, Chi YH, Jung BG, Park SK, Park JH, Lee JR, Lee SS, Moon JC, Yun JW, Choi YO, Kim WY, Kang JS, Cheong GW, Yun DJ, Rhee SG, Cho MJ & Lee SY (2004) Two enzymes in one; two yeast peroxiredoxins display oxidative stress-dependent switching from a peroxidase to a molecular chaperone function. *Cell* **117**, 625-635.

Jonsson TJ & Lowther WT (2007) The peroxiredoxin repair proteins. *Subcell Biochem* **44**, 115-141.

Kumsta C, Thamsen M & Jakob U (2010) Effects of Oxidative Stress on Behavior, Physiology, and the Redox Thiol Proteome of *Caenorhabditis elegans*. *Antioxid Redox Signal*.

Leichert LI & Jakob U (2004) Protein thiol modifications visualized *in vivo*. *PLoS Biol* **2**, e333.

Lowther WT & Haynes AC (2010) Reduction of Cysteine Sulfinic Acid in Eukaryotic, Typical 2-Cys Peroxiredoxins by Sulfiredoxin. *Antioxid Redox Signal*.

Mathers J, Fraser JA, McMahon M, Saunders RD, Hayes JD & McLellan LI (2004) Antioxidant and cytoprotective responses to redox stress. *Biochem Soc Symp*, 157-176.

Moon JC, Hah YS, Kim WY, Jung BG, Jang HH, Lee JR, Kim SY, Lee YM, Jeon MG, Kim CW, Cho MJ & Lee SY (2005) Oxidative stress-dependent structural and functional switching of a human 2-Cys peroxiredoxin isotype II that enhances HeLa cell resistance to H2O2-induced cell death. *J Biol Chem* **280**, 28775-28784.

Netto LES, Chae HZ, Kang SW, Rhee SG & Stadtman ER (1996) Removal of hydrogen peroxide by thiol-specific antioxidant enzyme (TSA) is involved with its antioxidant properties. TSA possesses thiol peroxidase activity. *J Biol Chem* **271**, 15315-15321.

Neumann CA, Krause DS, Carman CV, Das S, Dubey DP, Abraham JL, Bronson RT, Fujiwara Y, Orkin SH & Van Etten RA (2003) Essential role for the peroxiredoxin Prdx1 in erythrocyte antioxidant defence and tumour suppression. *Nature* **424**, 561-565.

Olahova M, Taylor SR, Khazaipoul S, Wang J, Morgan BA, Matsumoto K, Blackwell TK & Veal EA (2008) A redox-sensitive peroxiredoxin that is important for longevity has tissue- and stress-specific roles in stress resistance. *Proc Natl Acad Sci U S A* **105**, 19839-19844.

Woo HA, Bae SH, Park S & Rhee SG (2009) Sestrin 2 is not a reductase for cysteine sulfinic acid of peroxiredoxins. *Antioxid Redox Signal* **11**, 739-745.

Woo HA, Chae HZ, Hwang SC, Yang KS, Kang SW, Kim K & Rhee SG (2003) Reversing the inactivation of peroxiredoxins caused by cysteine sulfinic acid formation. *Science* **300**, 653-656.

Wood ZA, Poole LB & Karplus PA (2003) Peroxiredoxin evolution and the regulation of hydrogen peroxide signaling. *Science* **300**, 650-653.

Yang KS, Kang SW, Woo HA, Hwang SC, Chae HZ, Kim K & Rhee SG (2002) Inactivation of human peroxiredoxin I during catalysis as the result of the oxidation of the catalytic site cysteine to cysteine-sulfinic acid. *J Biol Chem* **277**, 38029-38036.

4 QUANTITATIVE *IN VIVO* REDOX SENSORS UNCOVER OXIDATIVE STRESS AS AN EARLY EVENT IN LIFE

Daniela Knoefler[1†], Maike Thamsen[1†], Martin Koniczek[2,3], Ann-Kristin Diederich[1], Ursula Jakob[1]

Submitted to PNAS

[†]authors contributed equally to this work

[1]Department of Molecular, Cellular, and Developmental Biology, University of Michigan, Ann Arbor, MI, USA, [2]Department of Radiation Oncology, University of Michigan, Ann Arbor, Michigan, USA, [3]Department of Experimental Radiation Oncology, University Medical Center Mannheim, Heidelberg University, Mannheim, Germany

4.1 Abstract

A major obstacle in analyzing the role of oxidative stress in aging multicellular organisms is the inability to precisely localize, track, and quantify the oxidants, to identify proteins and pathways that might be affected, and ultimately, to correlate changes in oxidant levels with the lifespan of the organism. We have established highly quantitative tools that allow us to address these fundamental questions in the nematode *Caenorhabditis elegans,* a popular model organism for eukaryotic aging studies. We employed the quantitative redox proteomic technique OxICAT to monitor the oxidation status of redox-sensitive proteins as read-out for onset, localization, and protein targets of oxidative stress at distinct stages during the lifespan of *C. elegans*. In parallel, we made use of an integrated peroxide-specific fluorescent biosensor called HyPer, which allows *in vivo* quantification of endogenous peroxide levels in live animals in real time. By using these two independent redox-sensing methods, we made the surprising observation that *C. elegans* is exposed to high peroxide levels during development, presumably as a result of increased metabolism and/or reactive oxygen species (ROS) signaling. Peroxide levels drop rapidly as animals mature, and reducing redox conditions prevail throughout the reproductive age, after which age-induced peroxide-mediated protein oxidation sets in. We found that long-lived *daf-2* mutants transition faster to reducing conditions, whereas short-lived *daf-16* mutants retain higher peroxide levels throughout their mature life. These results suggest that changes in the cellular redox homeostasis, encountered at a very early stage in life, determine subsequent redox levels and potentially the lifespan of organisms.

4.2 Introduction

The oxidative stress theory of aging postulates that oxidative damage to cellular macromolecules, caused by the progressive accumulation of reactive oxygen species (ROS), contributes and possibly even leads to the decline in physiological functions observed in aging organisms (Harman, 1956; Finkel & Holbrook, 2000). Since its inception, extensive correlative evidence has been collected that corroborates this popular theory. For instance, it has been shown that oxidative damage to proteins, lipids, and DNA increases with age (Finkel & Holbrook, 2000), that oxidative stress is involved in the pathogenesis of many age-related diseases, such as Alzheimer's disease (Gella & Durany, 2009), and that interventions that delay aging (e.g., reduced caloric intake) decrease the extent of oxidative damage and mediate the rapid removal of damaged macromolecules through proteolysis and autophagy (Cavallini *et al.*, 2008). Moreover, one of the unifying features that distinguish many long-lived mutant invertebrates and rodents from their wild-type cohorts appears to be a significant increase in oxidative stress resistance (Salmon *et al.*, 2005). However, the validity of the free radical theory of aging recently came under dispute when a series of genetic studies, particularly those in mice, failed to generate conclusive results about the role of ROS in aging (Gems & Doonan, 2009; Perez *et al.*, 2009). These findings suggested a more complex aging mechanism, potentially driven by more subtle changes in ROS levels or the cellular redox state and involving a number of complimentary and compensatory systems.

One aspect of redox biology that has long been overlooked when testing the free radical theory of aging is the fact that ROS, like peroxide, not only damage cellular macromolecules but also play important regulatory roles as intracellular signaling molecules (Groeger *et al.*, 2009). While high levels of peroxide are thought to be toxic, low levels of peroxide, which are continuously produced during mitochondrial respiration, by NADH oxidases and during the oxidative folding process in the endoplasmic reticulum, set the pace of numerous metabolic and signaling pathways in the cell (Santos *et al.*, 2009). Proteins that are regulated by peroxide and potentially other reactive oxygen and nitrogen species commonly contain highly oxidation-sensitive cysteine residues whose thiol oxidation status controls the protein's activity, and by extension, the activity of the pathway that the protein is part of. Over the past few years, an increasing number of redox-sensitive proteins have been identified, including many phosphatases (e.g., PTEN), kinases (e.g., JNK), antioxidant transcription factors (e.g., Nrf2, Yap1p), and molecular chaperones (e.g., Hsp33), whose activity is fine-tuned by the cellular redox environment (Kim *et al.*, 2008; Kumsta & Jakob, 2009; Li & Kong, 2009). Given the many processes that are directly or indirectly affected by ROS levels, it is thus very likely that depletion of pro-oxidants by either dietary antioxidants or genetic manipulation

profoundly impacts development, differentiation, and stress responses and, when applied at the wrong stage in life, potentially outweighs the beneficial effects.

We decided to take a different approach in evaluating the role that reactive oxygen species play in lifespan. We used recently developed, highly quantitative probes to precisely determine when oxidative stress occurs, which proteins and pathways are affected, and whether a correlation exists between the onset and extent of endogenous oxidative stress and the lifespan of the organism. We chose *C. elegans* as our model system because it is a well-established eukaryotic aging model (Johnson, 2008) and is well-suited for redox proteomic analyses and the application of fluorescent biosensors (Kumsta *et al.*, 2010). To monitor the temporal changes in endogenous ROS levels, we applied the highly quantitative redox proteomic technique OxICAT at distinct time points in *C. elegans* lifespan and simultaneously monitored the precise thiol redox status of almost 150 different proteins. Several of the identified proteins are known to be redox-sensitive; their diverse tissue and subcellular distribution also provided us with a spatial read-out for changing redox conditions. In parallel, we employed the chromosomally encoded hydrogen peroxide (H_2O_2) sensor protein HyPer (Belousov *et al.*, 2006), which is constitutively expressed in the body wall muscle cells of *C. elegans,* as read-out for changes in endogenous peroxide levels. Using these highly quantitative redox sensors, we discovered that *C. elegans* suffers from increased oxidative stress at two distinct stages in life: during development and aging. Comparative analysis with long- and short-lived mutants of the insulin/IGF-1 signaling pathway revealed that long-lived mutant worms recovered faster from the oxidative stress encountered during development and reached lower steady-state redox levels during their reproductive life than short-lived worms, which failed to completely restore redox homeostasis. Our studies provide evidence for the exciting possibility that oxidative stress encountered as early as during development might have profound impacts on the lifespan of *C. elegans* and potentially other organisms.

4.3 Material and Methods

4.3.1 Strains, Culture Conditions, and Lifespan Analysis

The *C. elegans* Bristol strain N2 (wild-type) and GR1307 (*daf-16(mgDf50)I*) were provided by the *Caenorhabditis* Genetics Center. The strain CF1041 [(*daf-2(e1370)]* was kindly provided by Dr. Ao-Lin Hsu. Strains were cultured under standard conditions on NGM plates using 10^{10} cells/ml OP50 as food source. For large scale cultivation of synchronized worms, see Kumsta et al. (Kumsta *et al.*, 2010). To prevent hatching of progeny, fertile adults were cultured on plates containing 20 mg/l FUdR (Sigma). Unless otherwise indicated, all experiments were carried out at 15°C. The L4 molt stage was considered day 0 (t=0). Survival was assessed every other day. Animals were considered

dead when they did not move or respond to prodding. Animals that crawled off the plate were censored at the time of the event.

Note: We conducted all our experiments at 15°C to exclude potential temperature-dependent influences on oxidative stress levels. Although we used the temperature sensitive strain *daf-2(e1370)*, we verified that it is long-lived at 15°C, which is in compliance with another study by Gems et al. (Gems *et al.*, 1998).

4.3.2 Generation of Transgenic Animals

The *HyPer* gene (Belousov *et al.*, 2006) was cloned into the plasmid pPD30.38 (Addgene plasmid 1443) using restriction sites *NheI* and *NcoI* to construct the plasmid pPD30.38::HyPer [*unc-54::HyPer*]. Transgenic *C. elegans* were generated by gonad microinjection (Mello *et al.*, 1991). Plasmid pPD30.38::HyPer [*unc-54::HyPer*] was coinjected with the plasmid pPD118.33 [*myo-2::gfp*] (Addgene plasmid 1596) into N2 wild-type animals at a concentration of 100 ng/µl for each plasmid. Fluorescent animals were selected and maintained using a fluorescent microscope (Olympus SZX16, GFP filter: EX460-480HQ; EM495-540HQ). Animals carrying extrachromosomal arrays were irradiated with 3000 rad of a Cs137 source to generate a chromosomal integrated line. The homozygous transgenic strain N2 [*unc-54::HyPer; myo-2::gfp*] was out-crossed three times with our laboratory wild-type strain N2 to minimize the mutations in the wild-type background, and is referred to as N2 [*unc-54::HyPer*]. To generate mutant strains that express the HyPer transgene, N2 [*unc-54::HyPer*; *myo-2::gfp*] males (Sulston, 1988) were crossed to GR1307 [*daf-16(mgDf50)I*] or CF1041 [*daf-2(e1370)*] hermaphrodites. The mutant genotype was verified by PCR (*daf-16*) or by sequencing (*daf-2*).

4.3.3 Sample Preparation for OxICAT

A synchronized population of wild-type or mutant worms was cultivated at 15°C and aliquots of worms were taken at the indicated time points. Samples for OxICAT were prepared as previously described (Kumsta *et al.*, 2010). In short, worms were lysed in 10% TCA, and proteins were dissolved in denaturing buffer (6 M urea, 0.5% (wt/vol) SDS, 10 mM EDTA, 200 mM Tris·HCl, pH 8.5) and transferred into an anaerobic chamber for the first alkylation reaction with the light ICAT reagent. All subsequent steps, including reduction, alkylation with the heavy ICAT reagent, trypsin digest, purification of labeled peptides, mass spectrometry, and data analysis were performed according to the published protocol by Leichert et al. (Leichert *et al.*, 2008).

4.3.4 Worm Image Acquisition

Animals of a synchronized worm population were taken for image acquisition at different time points during larval development and adult life. Worms were mounted on a 2% agarose pad and immobilized using 2 mM levamisole hydrochloride. 20 to 40 animals were imaged per day and group. A Leica SP5 confocal imaging system on a DM 6000B upright microscope body (Wetzlar, Germany) was used for image acquisition. The fluorescent sensor protein HyPer was excited sequentially with 405 nm diode and 488 nm argon laser, and the emission was measured at 505–530 nm using the same photomultiplier tube set to zero offset and adequate gain. The RSP 500 dichroic beam splitter in conjunction with a 20× objective (NA 0.7 HC PL APO CS) was used. The resulting "405 image" and "488 image" have 1024×1024 pixels at 16-bit resolution. Additionally, a differential interference contrast image was acquired to assist the image quantification. The laser and microscope settings were kept constant throughout each experiment. To account for fluctuations in laser power, a fluorescent objective slide was imaged before and after each group.

4.3.5 Image Quantification

A MATLAB (The MathWorks) script was used in conjunction with ImageJ (Rasband, 1997-2009) to perform mostly automated image quantification and HyPer ratio calculation. A detailed description of the image quantification process can be found in Protocol S1.

Statistical Analysis - GraphPad Prism 5 Version 5.01 for Windows (GraphPad Software, San Diego, California, www.graphpad.com) was used for statistical analysis. Lifespan data were analyzed using the log-rank test (Mantel Cox) or the Gehan-Breslow-Wilcoxon test. P values ≤ 0.05 were considered significant. The HyPer ratio values were log-transformed for the statistical analysis. The transformed values were analyzed with One-way ANOVA, followed by Tukey multiple comparison test. Comparison of the HyPer ratio of two groups was done with the Student's t-test on log-transformed data.

4.4 Results

4.4.1 The *C. elegans* Redoxome: Establishing the Redox Baseline

The *in vivo* thiol oxidation status of redox-sensitive proteins serves as a sensitive and specific read-out for the presence of even small quantities of ROS in cellular and sub-cellular compartments (Leichert *et al.*, 2008). Even subtle changes in the cellular redox potential can be detected, as every 30 mV change in redox potential causes a 10-fold shift in the thiol/disulfide or thiol/sulfenic acid equilibrium of proteins (Gilbert, 1990). We pioneered a highly quantitative redox proteomic

technique, termed OxICAT, which allows us to monitor the exact *in vivo* oxidation status of hundreds of different protein thiols in a single experiment (Leichert *et al.*, 2008; Kumsta *et al.*, 2010). Identification of the affected proteins and their redox-sensitive cysteines by mass spectrometry provides information about the cellular processes and pathways that might be affected by the prevailing redox conditions, and allows a temporal and spatial assessment of redox-mediated changes.

In OxICAT, we use the quantitative properties of the thiol-reactive isotope-coded affinity tag (ICAT), which comes in an isotopically light ^{12}C-ICAT and in a 9 Da heavier ^{13}C-ICAT version (Leichert *et al.*, 2008). A differential thiol trapping approach allows us to label all *in vivo* reduced protein thiols with light ICAT and all *in vivo* oxidized cysteines (after their *ex vivo* reduction) with heavy ICAT. This differential thiol trapping technique generates chemically identical proteins whose specific mass difference reflects their *in vivo* redox state. After digestion of the proteins and affinity purification of all ICAT-labeled peptides, high-performance liquid chromatography is conducted to separate the peptides. Mass spectrometry (MS) and tandem MS/MS is used for the identification and quantification of the *in vivo* oxidation status of the peptides. Peptides of a partially oxidized protein will co-elute as ICAT pairs from the high-performance liquid chromatography column and will behave identically in the mass spectrometer. The relative peak intensity of the light- and heavy-labeled mass peaks allows calculation of the *in vivo* oxidation status. Since the ratio of light- to heavy-labeled peptide peak is independent of the relative protein amount, OxICAT is ideally suited to monitor changes in protein oxidation over time.

We applied OxICAT to analyze the redox status of proteins in synchronized wild-type *C. elegans* on day 2 of their adulthood. This analysis in young adults was intended to serve as the basis for all subsequent studies so that changes in the redox status of the proteins could be determined at different points during *C. elegans* lifespan. As shown in Supplemental Table 4-1, we reproducibly determined the redox status of 170 thiol-containing peptides, representing 138 different *C. elegans* proteins. Database analysis revealed that we identified the redox status of numerous ubiquitously expressed proteins (e.g*.,* HSP-1, ribosomal proteins) as well as proteins selectively expressed in body wall muscle cells (e.g*.,* ANC-1, DIM-1, myosin-3), intestine (e.g*.,* vitellogenin-3, vitellogenin-6, neprilysin), nervous system (e.g*.,* degenerin), and pharynx (e.g*.,* myosin-2, myosin-4, annexin); these data may thus provide cell type-specific read-outs of changing ROS levels (Suppl. Table 4-1A). Of the identified protein thiols, 65% exhibited oxidation states of less than 20%, with most of these being less than 10% oxidized. These protein thiols, which we consider reduced, were found predominantly in cytosolic and mitochondrial proteins (Fig. 4-1). Only about 10% of protein thiols were oxidized to more than 80%, providing quantitative proof for earlier redox proteomic studies, which suggested

Table 4-1A Select protein thiols whose oxidation increases with age

Proteins affected	Acc No (CE) [a]	Oxidation State [%] at day L2	0	2	8	15	Tissue[c]	H_2O_2 sens.
ATP synthase (β-sub.) (Cys119)	29950	14	19	25	31	32	U	
Hsp70 (Cys587)	08631	12	9	12	17	28	I, M	
TIF-5A (Cys111)	37787	17	18	27	33	47	G	Yes[d]
Myosin-3 (Cys707)	34936	18	21	26	39	37	BW	Yes[e]
RNA helicase CGH-1 (Cys336)	00839	n.i.	n.i.	22	28	45	G	
Methylase C28H8.7 (Cys224)	01829	2	2	12	23	26		

Table 4-1B Select protein thiols with biphasic oxidation pattern

Proteins affected	Acc No (CE) [a]	Oxidation State [%] at day L2	0	2	8	15	Fold ox. D2→D15[b]	Tissue[c]	H_2O_2 sens.
RPS-12 (Cys114)	26896	20	30	13	24	34	2.6	U	
RPS21 (Cys57)	30779	38	35	27	44	43	1.6	U	Yes[d]
RPS-23 (Cys90)	05747	17	27	22	32	39	1.8	U	
RPS-28 (Cys22)	21842	10	20	6	16	29	4.8	U	Yes[d]
Protein K07C5.4 (Cys390)	06114	12	15	9	8	28	3.1		
EF-2 (Cys598)	15900	14	22	11	15	21	1.9	U	Yes[d]
Actin-2 (Cys258)	13150	19	24	16	24	30	1.9	BW, N	
DIM-1 (Cys234)	04038	11	18	8	18	33	4.1	BW	Yes[f]
NDPK (Cys109)	09650	36	35	28	36	47	1.7	U	Yes[d]
NDPK (Cys117)	09650	37	36	30	45	54	1.8	U	Yes[d]
T-complex zeta (Cys517)	01234	26	30	12	9	26	2.2	U	Yes[f]
Neprilysin (Cys170)	43217	66	n.i.	22	n.i.	62	2.8	I	
S-adenosylhomocysteine hydrolase (Cys280)	17154	14	17	5	14	20	4	P, I	
Methylcrotonoyl-CoA carboxylase (Cys212)	00136	15	26	10	18	22	2.2	P	
Isocitrate lyase/malate synthase (Cys271)	32565	15	26	14	14	26	1.9		
COPII, SAR-1 (Cys174)	07622	23	23	10	27	25	2.5		
Protein K04G2.6 (Cys234)	06100	17	13	5	6	20	4		
MEL-32 (Cys391)	01130	63	34	31	60	44	1.4	I, H	
EF1-alpha (Cys152)	01270	10	15	10	9	16	1.6	BW, P, I	
PEP-carboxykinase (Cys9)	36359	n.i.	18	10	19	21	2.1	I, R	

[a]Accession number (composite element).
[b]Change in oxidation status from day 2 to day 15.
[c]Tissue localization according to WormBase (www.wormbase.org); U, ubiquitous; BW, body wall muscle; M, muscle; N, neuron; I, intestine, P, pharynx; H, hypodermis; G, gonads; R, reproductive system.
[d]Cysteine identified to be peroxide-sensitive; [e]corresponding cysteine in *C. elegans* homologue identified to be peroxide-sensitive, or [f]protein contains redox-sensitive cysteines (Kumsta *et al.*, 2010).
n.i. = not identified.

that the majority of protein thiols are reduced *in vivo* (Leichert & Jakob, 2004). Most of these oxidized proteins turned out to be secreted proteins, which are often known to form disulfide bonds for increased stability (Fig. 4-1 and Suppl. Table 4-1). Among the group of oxidized proteins that we identified were two transthyretin homologues, TTR-2 and TTR-6, for which we identified the corresponding cysteine-containing peptides. We found that each of these peptides harbored two

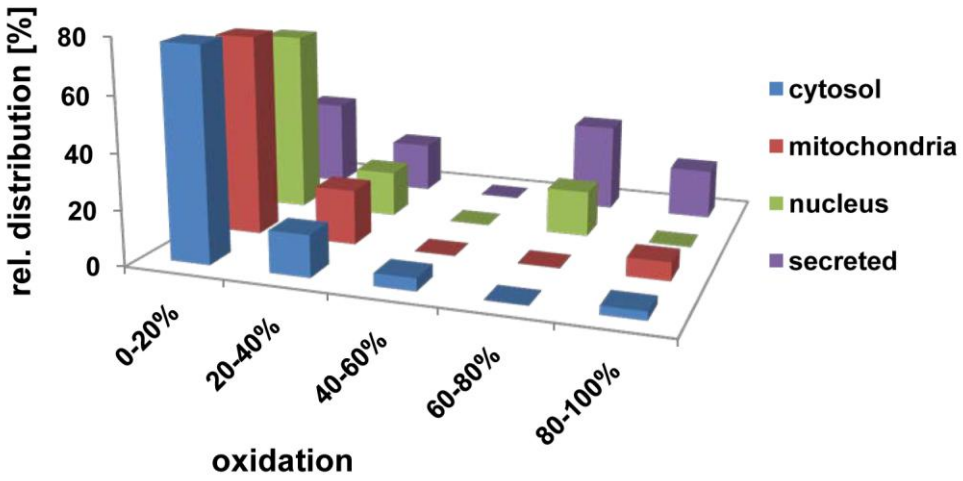

Figure 4-1 *In vivo* thiol oxidation status of *C. elegans* proteins.
Wild-type N2 worms were synchronized and cultivated at 15°C. At day 2 of adulthood, worms were lysed and the protein thiol oxidation status was determined by using the differential thiol trapping technique OxICAT. Proteins are categorized by their oxidation status and sub-cellular localization, according to WormBase (http://www.wormbase.org/). The complete list of proteins and their respective oxidation states with standard deviations can be found in Supplemental Table 4-1.

cysteine residues that were oxidized to 93% (TTR-2) and 97% (TTR-6), respectively—just one example illustrating the high reproducibility of the OxICAT method (Suppl. Table 4-1). Two other peptides that were mostly oxidized contained a C-X-C motif, typical for metal-coordinating proteins or proteins with redox-active cysteines. They were identified to be peptides of attractin (TAG-53: Cys263/Cys265) and degenerin (ASIC-1: Cys659/Cys669). The fact that the two cysteines in each of these peptides were almost fully oxidized strongly suggests that they form intramolecular disulfide bonds in these proteins. In addition to the peptides containing either mostly reduced or mostly oxidized cysteine thiols, we found about 15% of peptides containing cysteines with oxidation levels between 20% and 40% (Fig. 4-1). These peptides might belong to proteins that occur in several isoforms, distributed in sub-cellular locations that differ in their redox environment. Alternatively, they might belong to redox-sensitive proteins, which are partially oxidized in response to either local or global increases in ROS levels *in vivo*.

In summary, we identified a substantial number of cysteine thiols that cover a wide range of thiol oxidation states and belong to proteins that are localized to specific tissues and sub-cellular locations. We thus generated an unbiased redox proteomic framework that should provide us with a quantitative read-out for the presence of ROS in multicellular organisms like *C. elegans*.

4.4.2 Monitoring Changes in Protein Thiol Redox State during the Lifespan of *C. elegans*

To investigate onset and extent of oxidative stress during the lifespan of *C. elegans*, we synchronized wild-type N2 worms, cultivated them at 15°C, and took aliquots of ~100,000 worms during early (i.e., L2) and late (i.e. L4) development and at days 2, 8, and 15 of adulthood for subsequent OxICAT analysis. Adult worms were cultivated on FUdR-supplemented plates to prevent the hatching of eggs. At day 15, when the last worm aliquot was taken, the survival was still about 80%, but mobility defects were observed in the majority of worms. We separated the live worms from eggs and any dead worms by sucrose flotation, lysed the worms in TCA to maintain the *in vivo* redox status of the protein thiols, and conducted our differential OxICAT thiol trapping. We performed four independent replicates for each sample and were able to reproducibly determine the redox status of the majority of our previously identified peptides at each time point, with the exception of proteins that are either not expressed during larval stages (e.g., vitellogenin) or whose expression decreases as the worms age (e.g., lysozyme) (Suppl. Table 4-2).

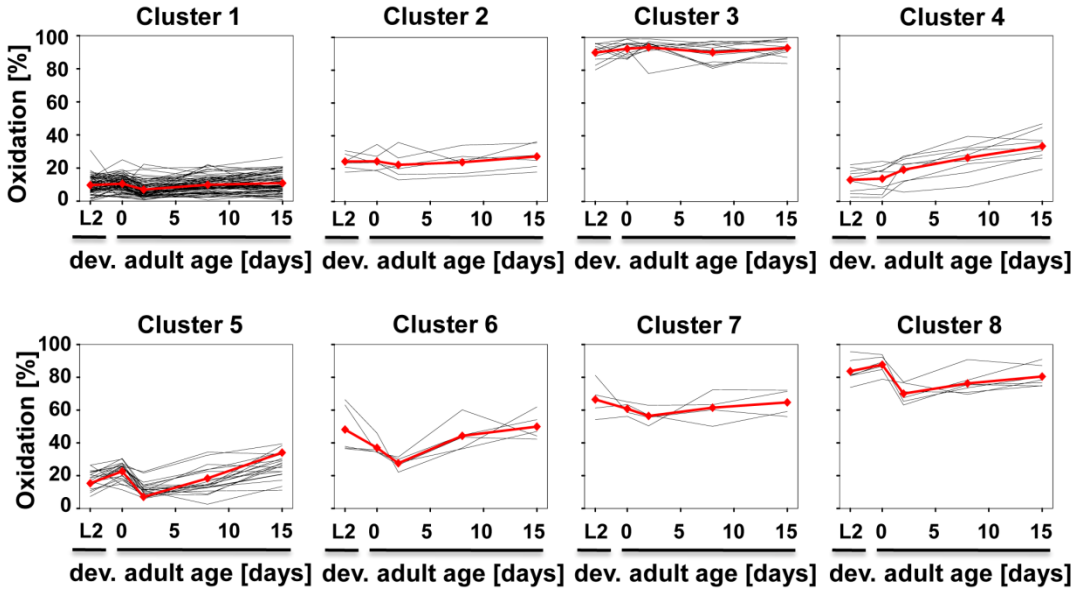

Figure 4-2 Monitoring thiol oxidation during the lifespan of *C. elegans*.
The thiol oxidation status of proteins in a synchronized population of wild-type N2 worms cultivated at 15°C was determined at the larval stage L2 and at days 0 (i.e., L4), 2, 8, and 15 of adulthood. The identified protein thiols were clustered into 8 groups according to their oxidation pattern; the individual oxidation pattern of each protein thiol is shown as black traces and the calculated average for each time point is shown in red. Data from 2 to 4 independent experiments were used. Missing values were calculated using the CTWC algorithm (http://ctwc.weizmann.ac.il/). The complete list of proteins in each cluster and their respective oxidation states can be found in Supplemental Table 4-2.

We performed a cluster analysis using the oxidation state of all identified protein thiols at the five time points as input. We found that the oxidation state of the majority of protein thiols did not significantly change and either stayed reduced (Fig. 4-2, cluster 1), partially oxidized (Fig. 4-2, cluster 2) or fully oxidized (Fig. 4-2, cluster 3) throughout development and adulthood. We detected only a small sub-population of identified peptide thiols that was reduced in young worms and became increasingly oxidized as the worms aged (Fig. 4-2, cluster 4 and Table 4-1A), thus following a trend that would be predicted by the free radical theory of aging (Petropoulos & Friguet, 2006). To our surprise, however, we observed that almost 30% of our identified protein thiols followed a biphasic oxidation pattern (Fig. 4-2, clusters 5–8). The thiol oxidation state of these peptides was significantly higher during development than at day 2 of adulthood, where the oxidation state of these protein thiols appears to reach a minimum. The thiol oxidation state of these peptides then slowly increased with increasing age of the animals, reaching oxidation states at day 15 that were between 1.5- and 5-fold higher than in 2-day old adults (Table 4-1B). Although the extent of oxidation was generally lower in developing worms and pre-fertile adults compared to 15 day-old worms, the results were highly reproducible, suggesting that animals are exposed to considerable amounts of oxidants early in life, either as part of extensive ROS signaling, increased metabolic activity, or a combination thereof. That the observed thiol oxidation, both during development as well as in aging worms is likely caused by increasing levels of peroxide and/or byproducts of peroxide became evident when we compared the list of our oxidized protein thiols with our earlier OxICAT studies in peroxide treated *C. elegans* (Kumsta *et al.*, 2010) and other eukaryotic organisms (Tables 4-1 and 4-2). Many of the proteins that we identified to change their oxidation states early and late in life contain cysteines previously shown to be peroxide-sensitive. These results strongly suggest that a surge of peroxide production occurs during development, which leads to the considerable oxidation of numerous *C. elegans* proteins. The proteins that we identified to be most affected by endogenous peroxide stress are proteins involved in protein translation (e.g., ribosomal proteins), mobility (e.g., actin, Dim-1), and metabolism (e.g., MEL-32), cellular processes known to be affected by oxidative stress conditions (Brandes *et al.*, 2009).

Note that comparison with previous studies also revealed several *C. elegans* proteins that were highly sensitive to exogenous peroxide treatment but did not alter their oxidation status during the worm's lifespan. These results suggest that the endogenous peroxide accumulation that we observed during development and aging might either be more

Table 4-2 Oxidation status of select *C. elegans* proteins of wild-type (N2), *daf-2* and *daf-16* mutants

Proteins affected	Acc No (CE) [a]	Oxidation State [%] at L4			H_2O_2 sens.
		daf-2	WT	*daf-16*	
UNC-87 (Cys472)	36924	54	68	65	
40S ribosomal protein S21 (Cys57)	30779	29	34	49	Yes[b]
CDC-48.2 (Cys697)	05402	27	35	48	Yes[b]
40S ribosomal protein S23 (Cys90)	05747	26	27	38	
NDPK (Cys109)	09650	29	35	38	Yes[b]
Vacuolar ATP synthase (a sub.) (Cys218)	22210	13	28	34	Yes[b]
ATP synthase (b sub.) (Cys119)	29950	18	19	33	
Protein F37C4.5 (Cys53)	33640	17	18	33	
Myosin-4 (Cys700)	06253	13	18	23	Yes[b]
Glutamyl-tRNA synthetase (Cys377)	06580	16	26	29	
40S ribosomal protein S14 (Cys140)	00821	13	13	25	Yes[b]
DNA repair protein RAD-50 (Cys1174)	21149	9	14	25	
Vacuolar ATP synthase (a sub.) (Cys521)	22210	11	14	24	Yes[c]
MUA-3 (Cys2258)	37256	14	14	24	
T-complex, subunit zeta (Cys517)	01234	12	30	24	Yes[c]
Helicase (C28H8.3) (Cys669)	29195	11	15	23	
Pyruvate carboxylase (Cys637)	09072	8	9	22	
Dynamin GTPase (Cys430)	07832	5	5	22	Yes[d]
40S ribosomal protein SA (Cys107)	00854	4	8	20	Yes[e]
Heat shock protein 70 (Cys243)	09682	7	5	18	Yes[c]
60S ribosomal protein L12 (Cys141)	17986	1	3	16	

[a] Accession number (composite element).
[b] Cysteine identified to be peroxide-sensitive (Kumsta *et al.*, 2010).
[c] Protein contains redox-sensitive cysteines (Kumsta *et al.*, 2010).
[d] Protein contains NO-sensitive cysteine.
[e] Protein shown to be S-glutathionylated.

localized and tissue-specific than exogenous peroxide treatment, or that exogenous treatment with 10 mM H_2O_2 reaches higher endogenous peroxide levels than would accumulate under physiological conditions. The latter is less likely, as we identified several proteins, such as the small ribosomal protein S21, whose extent of age-induced cysteine oxidation was found to be very similar to the oxidation observed in worms treated with 10 mM peroxide for 20 min (43% versus 41%) (Table 4-1B) (Kumsta *et al.*, 2010).

To assess whether ROS accumulation is indeed a more localized, cell type-specific event, we then studied the localization of the proteins that showed the most significant oxidation (Table 4-1A and 4-1B). WormBase (www.wormbase.org) indicates that most of these proteins are ubiquitously distributed throughout the whole organism. The observation that at a maximum only 30% to 50% of the cysteine thiols are oxidized suggests at least two possibilities: (1) oxidation is a system-wide process that affects only a sub-population of each protein, or (2) oxidation affects the complete protein population in some tissues and

not in others. We did observe that four of the proteins that get substantially oxidized in developing and aging worms are either exclusively localized to the intestine (neprilysin, vitellogenin-3) or localized in intestine and one other cell type (MEL-32, PEP-carboxykinase) (Table 4-1A and 4-1B and Suppl. Table 4-1). Moreover, actin and DIM-1 are localized exclusively to the body wall muscle cells. While these results do not exclude a tissue-wide phenomenon, they at least suggest increased ROS production in body wall muscle cells and the intestine, cell types known for their high metabolic activity and involvement in aging (Libina *et al.*, 2003).

4.4.3 Insulin-like Signaling (ILS) Pathway Mutants Are Affected in Oxidative Stress Recovery

To assess whether the onset, extent, and pattern of oxidative stress is altered in mutant strains that show either shortened or prolonged lifespan, we decided to conduct our OxICAT experiments in worms defective in ILS pathway. The ILS pathway is evolutionarily conserved, and genetic manipulation of the signaling cascade has been shown to affect the lifespan of *C. elegans* as early as in young adults (Dillin *et al.*, 2002a). DAF-2, the insulin/IGF-1-like receptor, negatively regulates the forkhead transcription factor DAF-16, which controls expression of numerous antioxidant genes, including catalase 1 and 2, metallothionein 1, and superoxide dismutase 3 (Murphy *et al.*, 2003). Reduced DAF-2 function abrogates this negative regulation, promotes DAF-16-mediated gene expression, and increases lifespan. Conversely, deletion of *daf-16* significantly reduces lifespan (Kenyon *et al.*, 1993).

As before, we synchronized the worms and took worm aliquots at the same time points as in the previous experiments. The majority of peptides that we identified in wild-type N2 were also identified at the individual time points in *daf-2* and *daf-16* worms, making a direct comparison of their oxidation status possible. As shown in Figure 4-3, we did not observe any significant difference in the overall oxidation status of proteins isolated from *daf-2* or *daf-16* worms at the larval stage L2, suggesting that disruption of the ILS pathway during early development does not globally change the extent of ROS signaling (Fig. 4-3). However, differences between the strains were clear and reproducible by the time *C. elegans* reached the last larval stage. In the long-lived *daf-2* mutants, protein oxidation was only slightly shifted towards higher oxidation levels, whereas in wild-type worms, close to 50% of identified proteins showed oxidation levels of more than 15%. The effect was even more pronounced in the short-lived *daf-16* deletion strain, which showed more than 60% of their proteins to be oxidized at the last larval stage. Direct comparison of the oxidation

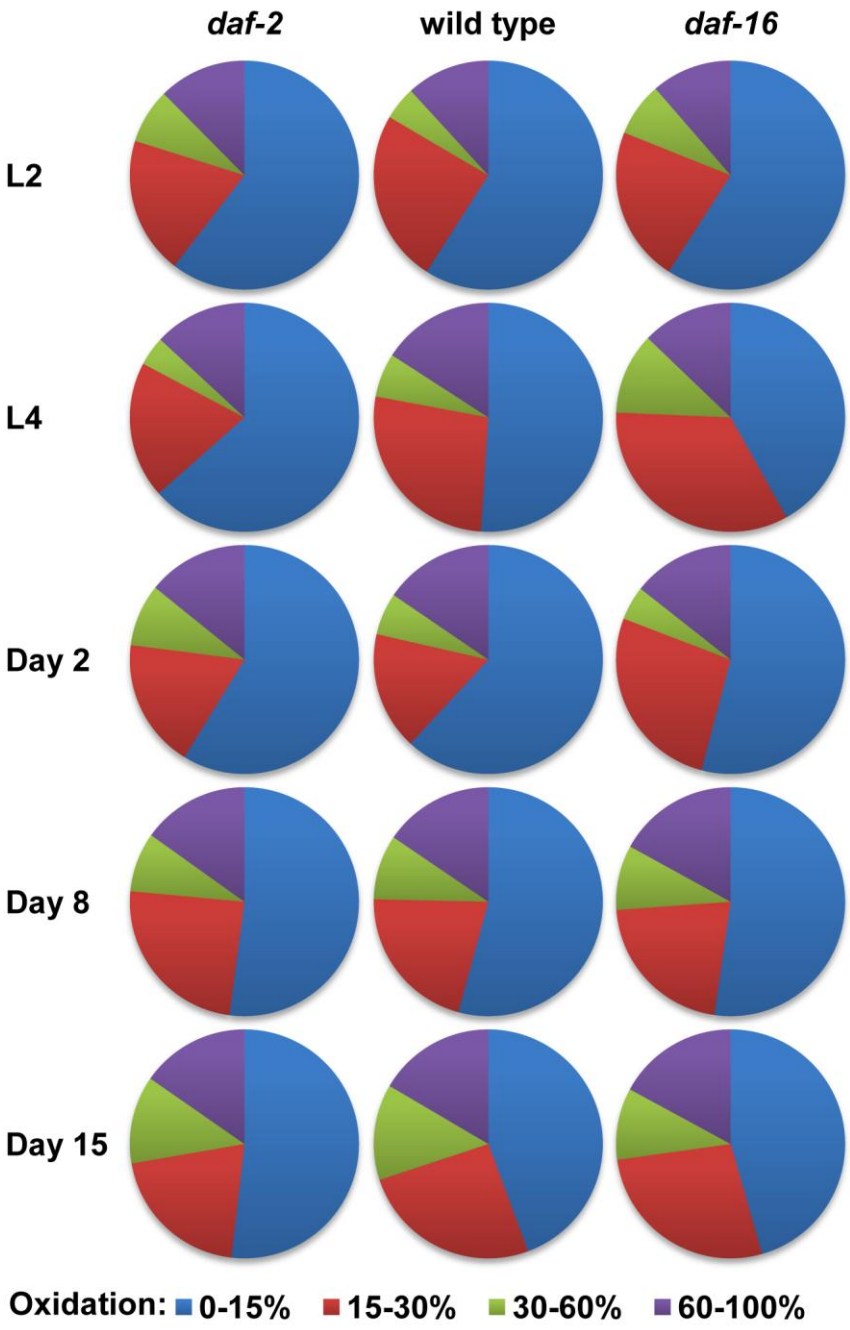

Figure 4-3 Protein oxidation during the lifespan of WT, *daf-2,* and *daf-16* worms.
Displayed is the relative distribution of protein thiol oxidation in synchronized populations of wild-type N2 and *daf-2* and *daf-16* mutant strains at the larval stages L2 and L4 and at days 2, 8, and 15 of adulthood. Protein oxidation was determined using OxICAT. Worms were grown at 15°C. Data of 2 to 4 independent experiments were used.

states of individual proteins confirmed these results (Table 4-2). As observed before, reducing redox conditions appeared largely restored by day 2 in both wild-type and *daf-2* mutant strains, whereas the overall protein oxidation levels was still reproducibly higher in strains lacking DAF-16. This difference in steady-state oxidation levels remained throughout the whole fertile lifespan of the worms. *daf-2* mutant worms maintained low oxidation

levels at least until day 15 of their lifespan, whereas the oxidation levels of *daf-16* deletion worms increased steadily as the worms aged. These results suggest that recovery from oxidative stress encountered during late development and early adulthood might play an important role in the lifespan of *C. elegans*. Protein oxidation levels in early stages of life might thus provide an early read-out for the life expectancy of worms.

4.4.4 Using HyPer to Determine Endogenous Peroxide Levels in *C. elegans*

Our OxICAT results revealed an increase in the oxidation status of a number of protein thiols in late development and early adulthood. Based on the observation that many of the oxidative thiol modifications that we found appear to be mediated by peroxide, we decided to make use of HyPer, a recently developed peroxide-specific sensor protein, which has been previously used in *Escherichia coli*, HeLa cells, and zebrafish to specifically monitor peroxide levels *in vivo* (Belousov *et al.*, 2006; Niethammer *et al.*, 2009). We reasoned that expressing HyPer in *C. elegans* would allow us to monitor and track oxidative stress levels in individual worms, and to determine whether the extent of oxidative stress (H_2O_2 levels) at a particular point in life affects or possibly correlates with the lifespan of the animals.

The peroxide-sensor HyPer consists of a circularly permuted yellow fluorescent protein fused to the H_2O_2 sensing domain of *E. coli* OxyR (Belousov *et al.*, 2006). The sensor protein possesses two excitation maxima at ~420 nm and ~500 nm, and a single emission maximum at 516 nm. Upon exposure of HyPer to peroxide, one intramolecular disulfide bond forms within the OxyR domain causing conformational changes that result in a ratiometric shift. The emission upon excitation at 500 nm increases, whereas the emission upon excitation at 420 nm decreases proportionally, leading to an overall increase in the 500 nm/420 nm ratio (i.e., HyPer ratio) with rising peroxide levels and making the sensor, at least in principle, independent of protein expression. Our measurements were conducted with a confocal microscope using excitation wavelengths of 488 nm and 405 nm, which are close to the reported optima.

To use the HyPer protein as an endogenous peroxide sensor in *C. elegans*, we cloned the HyPer gene under the control of the *C. elegans* UNC-54 promoter, which targets HyPer expression to the body wall muscle cells (www.wormbase.org). We chose the muscle-specific expression of HyPer because detection of the reporter protein requires high expression levels, which are achieved by using the strong UNC-54 promoter, and we knew from our OxICAT studies that significant oxidation occurs in the body wall muscle cells (Table 4-1B). We generated a stable transgenic line of wild-type N2 worms expressing the peroxide

sensor and confirmed the expression of HyPer in the body wall muscle cells (Suppl. Fig. 4-1). We then backcrossed the strain several times and conducted lifespan assays, verifying that the expression of HyPer did not affect the median life span of the worms (Suppl. Fig. 4-2). As changes in protein expression levels occur during development and aging, we also decided to test to what expression level the HyPer ratio was independent of the amount of HyPer protein expressed. We synchronized HyPer expressing wild-type worms, and sorted L2/L3 larvae according to their fluorescence emission intensity upon excitation at 488 nm into groups with strong, weak, and very weak emission intensities (i.e., HyPer expression levels) (Suppl. Fig. 4-3A). We then determined the 488 nm/405 nm ratio (i.e., HyPer ratio) for each animal using confocal microscopy to assess the relative level of endogenous peroxide (Suppl. Fig. 4-3B). We found a similar HyPer ratio in all animals, independent of their HyPer fluorescence intensity and thus HyPer expression level, making HyPer well-suited to monitor endogenous peroxide levels in individual worms over their lifespan.

4.4.5 Monitoring Endogenous Peroxide Levels in Real Time

To determine whether the increase in protein thiol oxidation that we observed with OxICAT was indeed due to increased amounts of peroxide, we synchronized HyPer expressing wild-type worms and cultivated them at 15°C. We then took aliquots of about 30 worms in either development (larval stages L2, L3 and L4) or at defined days during adulthood (days 2, 8, 15, 20, and 23) and imaged the animals to determine the HyPer ratio for each individual animal. As shown in Figure 4-4, our results are in excellent agreement

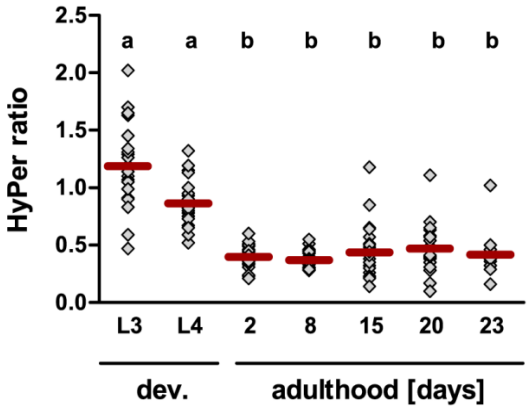

Figure 4-4 Monitoring endogenous peroxide levels during the lifespan of *C. elegans*. The H_2O_2 sensor HyPer was used to determine hydrogen peroxide levels during the lifespan of wild-type N2 [*unc-54::HyPer*] cultivated at 15ºC at the indicated time points. Every symbol represents the HyPer ratio of an individual animal; the bar illustrates the average HyPer ratio per day (n = 14-31, except for L2 larvae with n = 5). A One-way ANOVA followed by Tukey multiple comparison test was performed on the log-transformed ratio. Means that are not significantly different from each other ($p > 0.05$) share the same letter. Experiments were performed a minimum of three times and a representative graph is shown here.

with the results of our OxICAT experiments. We observed high levels of endogenous peroxide accumulation during larval development, which rapidly decreased as the worms reached their reproductive phase. The peroxide levels remained low during the fertile phase and seemed to increase slightly again as the population reached its mean survival (average 19 days for N2 [*unc-54::HyPer*] at 15°C), although this increase was not significant. The observation that the endogenous peroxide levels did not reach the high levels that we found during development stages is most likely due to the fact that the HyPer expression level in very old-looking worms was often too low to be quantified. Thus, at advanced stages, healthier animals had a selective advantage in our HyPer measurements.

To exclude that the high peroxide levels observed in the late larval stages was due to the synchronization procedure, which is conducted by treating gravid adults with a bleach solution that causes the release of the eggs, we also analyzed the HyPer ratio in animals that were manually synchronized (Suppl. Fig. 4-4). Again, we found a significantly higher HyPer ratio in developing animals as compared to fertile, mature adults, making it unlikely that the high peroxide levels were caused by the synchronization procedure. These results suggested that we now have a powerful probe that allows us to directly monitor endogenous oxidative stress levels in multicellular organisms. The observation that *C. elegans* experiences very high levels of endogenous peroxide during late development followed by a rapid recovery as it reaches fertility is in excellent agreement with our OxICAT results, providing independent confirmation that *C. elegans* indeed suffers from two bursts of oxidative stress, early and late in life.

4.4.6 Correlation between Early Oxidative Stress Recovery and Lifespan

The results of our OxICAT analysis revealed not only the accumulation of ROS during late development but suggested that differences exist in the extent to which animals defective in the ILS pathway are able to recover from this oxidative stress. To address this aspect in more detail and to determine whether the differences are indeed significant, we decided to generate HyPer-expressing *daf-2* and *daf-16* strains and use the HyPer ratio as a quantitative read-out for endogenous peroxide levels. We mated *daf-2* or *daf-16* mutants with wild-type N2 [*unc-54::HyPer*] and confirmed that these strains express the H_2O_2 sensor in their body wall muscle cells. As before, we synchronized the worms and directly compared the HyPer ratios in all three strain backgrounds during development and adulthood. In full agreement with our OxICAT analysis, we did not detect any significant

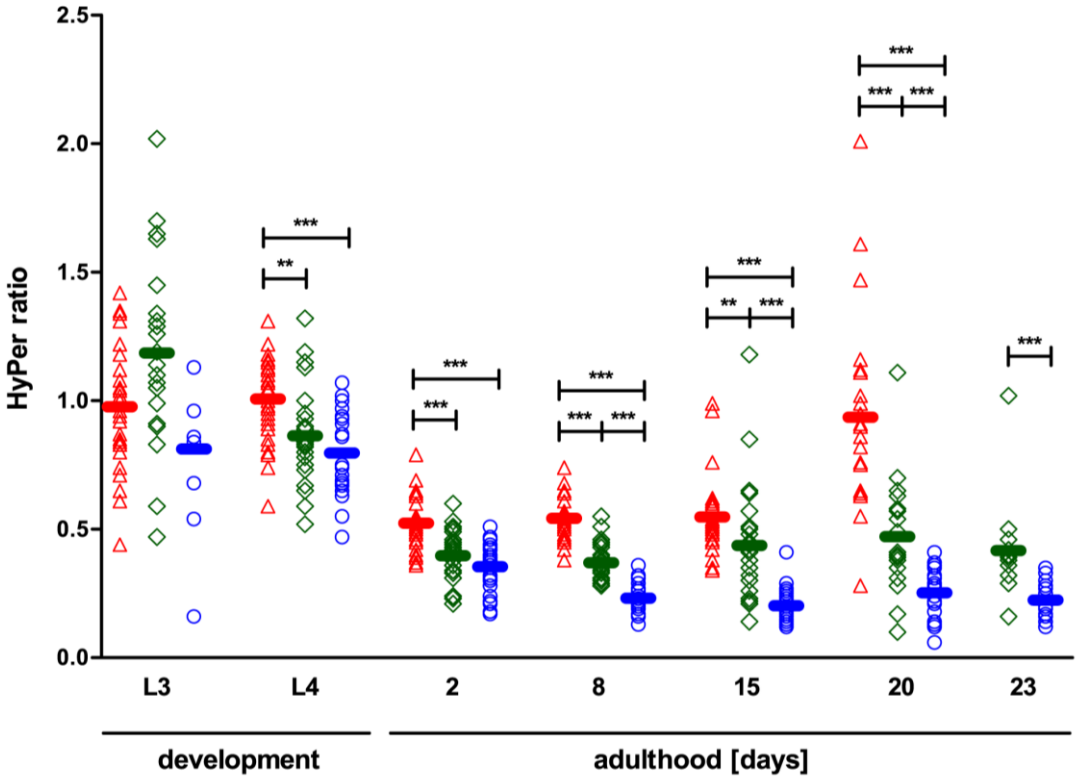

Figure 4-5 Hydrogen peroxide levels in wild-type N2, short-lived *daf-16,* and long-lived *daf-2* mutants during development and adulthood.
The H_2O_2 sensor HyPer was used to determine hydrogen peroxide levels during the lifespan of wild-type and mutant worms. Every symbol represents the HyPer ratio of an individual animal; *daf-16* [*unc-54::HyPer*] is shown in red, N2 [*unc-54::HyPer*] in green, and *daf-2* [*unc-54::HyPer*] in blue. The bar depicts the average HyPer ratio per strain and day (n = 11 – 31, except for N2 [*unc54::HyPer*] L2 stage with n = 5). The HyPer expression levels of *daf-2* [*unc-54::HyPer*] L2 larvae and of *daf-16* [*unc-54::HyPer*] at day 23 were too low to allow accurate determination of the HyPer ratio. A One-way ANOVA followed by Tukey multiple comparison test was performed on the log-transformed ratio to compare the means between genotypes within a day. *P* values from 0.001 to 0.01 are indicated with **, *P* values 〈 0.001 are indicated with ***. For the comparison of N2 [*unc-54::HyPer*] and *daf-2* [*unc-54::HyPer*] on day 23, a two-tailed, unpaired t-test was used: $p < 0.0001$ (n = 14–19). Experiments were performed a minimum of three times and a representative graph is shown here.

differences between the HyPer ratios in wild- type N2 [*unc-54::HyPer*], *daf-16* [*unc-54::HyPer*], and *daf-2* [*unc-54::HyPer*] mutant animals at the L2 larval stage (Fig. 4-5). All animals appeared to be exposed to a significant bolus of hydrogen peroxide in their body wall muscle cells (Fig. 4-5), implying that at this stage, functional signaling through the ILS pathway neither is involved in ROS generation nor in ROS detoxification. However, as with our OxICAT experiments, a clear correlation between the time of recovery from oxidative stress and the strain background was detected. By day 2, *daf-2* mutant animals had reached significantly lower steady-state levels of peroxide than the short-lived *daf-16* mutants, and they maintained these low peroxide levels at least until day 23 of their lifespan. Worms

lacking DAF-16, however, never fully recovered from the oxidative stress levels encountered during late development, and peroxide levels remained significantly higher throughout their entire adult lifespan. Peroxide levels increased dramatically with age, eventually reaching the same levels as observed during development (Fig. 4-5). These results suggest that the ability to deal with and recover from oxidative stress encountered at very early stages in life affects redox homeostasis during adulthood and ultimately might correlate with the lifespan of *C. elegans*.

4.5 Discussion

In this study, we used an innovative set of quantitative tools to determine at what point in life and to what extent multicellular organisms like *C. elegans* are exposed to elevated levels of ROS and to explore the potential physiological consequences of these changes. We first used the redox proteomics technique OxICAT, which provides a quantitative read-out of the thiol oxidation status of a wide range of redox-sensitive proteins. We discovered that many cytosolic proteins contained significantly oxidized cysteine thiols during the late stages of *C. elegans* development; these thiols were found to be reduced by the time the animals entered their reproductive stage and were slowly re-oxidized as the animals aged. Many of the identified proteins were previously shown to be peroxide-sensitive, leading us to believe that the protein oxidation is mediated by the accumulation of endogenous peroxide (Kumsta *et al.*, 2010). In full agreement with these results, using the peroxide-specific sensor protein HyPer to monitor peroxide levels *in vivo*, we found that animals were indeed exposed to high peroxide levels during development from which they recovered during early adulthood. Importantly, we found that thiol oxidation status and peroxide levels differed significantly in the ILS pathway mutants *daf-2* and *daf-16*, a difference that first became evident in the young adult stage and persisted throughout adulthood. These results support the exciting possibility that animals with improved ability to recover from early oxidative stress might have significant advantages later in life.

Our observations concur with previous studies in *C. elegans* and rodents, which led the authors to conclude that events early in life might dictate lifespan (Dillin *et al.*, 2002b; Ben-Zvi *et al.*, 2009; Sun *et al.*, 2009). Morimoto and coworkers, for instance, reported recently that the capacity to maintain a functional proteome (i.e*.,* proteostasis) decreases with age and that the onset of the proteostasis collapse, which is particularly obvious in muscle cells and neurons, becomes apparent as early as day 2 or 3 of adulthood (Ben-Zvi *et*

al., 2009). Overexpression of stress transcription factors such as heat shock factor HSF-1 or DAF-16 delayed the collapse and in turn increased lifespan, whereas deletion of either of these factors accelerated the collapse and decreased lifespan. It is well known that proteins are one of the main cellular targets of reactive oxygen species and once oxidized, tend to form high molecular weight aggregates that require removal by the proteasome (Bader & Grune, 2006). Protein aggregates that are resistant to proteolytic degradation can accumulate in the cell, interfere with basic cellular functions, and ultimately lead to cell death (Davies, 2001). Based on our results that oxidative stress precedes the proteostasis collapse, it is now tempting to speculate that the observed lack of recovery from developmental oxidative stress in *daf-16* deletion mutants might contribute to the accelerated collapse of proteostasis and shorter lifespan. Conversely, rapidly restoring the redox conditions and keeping ROS levels low as observed in *daf-2* mutants will inevitably reduce the load of oxidatively stressed proteins and might delay the collapse of proteostasis.

That early oxidative stress levels might also affect lifespan in mammals was suggested by recent studies with mice in which caloric restriction (CR), when applied during the first three weeks of pre-weaning only, was found to extend lifespan by a significant 18% (Sun *et al.*, 2009). Although the molecular mechanism by which CR extends lifespan is not understood in detail, a correlation between CR and increased oxidative stress resistance has been documented for numerous CR models, implying that increased capacity to deal with and recover from oxidative stress is involved in the lifespan extending effects of CR (Sohal & Weindruch, 1996).

Many processes have the potential to increase the level of peroxide during development. One process that might contribute to increased ROS levels specifically in *C. elegans* is larval molting, as it has been demonstrated that the dual oxidase Duox, a H_2O_2 generating enzyme, is required for correct cuticle formation (Edens *et al.*, 2001). Since the cuticle is located above the hypodermis, high amounts of unreacted H_2O_2 would need to diffuse through the hypodermis to cause the significant amount of oxidation that we observed in muscle-specific proteins, intestinal proteins, and proteins expressed selectively in neurons. A more likely explanation is that higher metabolic rates encountered during development are responsible for the increased ROS production (Wadsworth & Riddle, 1989). In C. *elegans*, it is known that upon consumption of stored lipid resources during embryogenesis, metabolism shifts from the glyoxylate cycle towards the TCA cycle, which increases the respiratory rate and thus potentially ROS production. This increased metabolism is reflected in a peak in ATP generation between the L2 and L4 larval stage,

which has been shown to decline when animals enter adulthood (Wadsworth & Riddle, 1989). It is interesting to note at this point that one protein we found to get increasingly oxidized between L2 and L4 larval stages is the bifunctional glyoxylate cycle protein isocitrate lyase/malate synthase (Table 4-1B). It now remains to be tested whether increased oxidative inactivation of this enzyme functions as a feedback mechanism to reduce the flux of acetyl-CoA through the glyoxylate cycle during later stages of development.

Oxidants have been shown to play crucial roles as second messengers in signal transduction (e.g., epidermal growth factor signaling, MAP kinase pathway), in the activation of transcription factors (e.g., NF-κB), and in the control of many metabolic processes (Schreck *et al.*, 1991; Bae *et al.*, 1997; Song & Lee, 2003). Our findings that *C. elegans* generates significant amounts of oxidants during development are in excellent agreement with the recently proposed mitohormesis theory, which suggests that a transient increase in ROS production induces adaptive responses that increase metabolic fitness, oxidative stress resistance and ultimately lifespan (Schulz *et al.*, 2007). Our *in vivo* redox sensors revealed that *C. elegans* has evolved effective mechanisms to recover from this oxidative stress by the time reproductive age is reached. At least one pathway that we identified to be involved in this recovery process is the ILS pathway (Murphy, 2006; Kenyon, 2010), which functions to mediate stress resistance and lifespan in adult *C. elegans* and has been shown to control the timing of reproduction and diapause in late development (Dillin *et al.*, 2002a). The long-lived *daf-2* mutant lacks the negative regulation of the transcription factor DAF-16, which positively controls expression of stress response genes like superoxide dismutase and catalase and thus mediates increased antioxidant capacity. It is interesting to note that we did not observe any significant difference in early developmental ROS levels between mutants lacking *daf-2* and mutants lacking *daf-16*, suggesting that at this stage, DAF-16-mediated expression of antioxidant genes might be down-regulated, thus enabling ROS signaling to occur. We did, however, find a significant difference in the ability of *daf-2* and *daf-16* mutants to recover from oxidative stress and to achieve the low ROS levels that are likely to be necessary for reproduction. While *daf-2* mutants recovered from oxidative stress during early adulthood and maintained low ROS levels throughout much of their mature life, *daf-16* mutants failed to fully recover and showed significantly increased ROS levels throughout their life. These results are in good agreement with ILS timing studies, which showed that the ILS pathway influences lifespan particularly when disrupted in the early days of adulthood (Dillin *et al.*, 2002a).

Our conclusion that increased levels of peroxide contribute to shortened lifespan in *C. elegans* concurs with previous mutant studies in *C. elegans*, which showed that deletion of either one of the two main peroxide-detoxifying enzymes, catalase (CTL-2) or peroxiredoxin (PRDX-2), causes progeric phenotypes that become apparent as early as in young adults and shortens lifespan (Petriv & Rachubinski, 2004; Kumsta *et al.*, 2010). Moreover, treatment of *C. elegans* with a short bolus of exogenous peroxide stress caused behavioral and physiological changes highly reminiscent of aging phenotypes (Kumsta *et al.*, 2010). In contrast, absence of the abundant cytoplasmic Cu/Zn-SOD (*sod-1*) and/or mitochondrial matrix Mn-SOD (*sod-2*) did not cause any progeric phenotypes nor did it shorten the lifespan of *C. elegans* despite an increase in oxidative protein modification as assessed by monitoring protein carbonylation (Yang *et al.*, 2007). These studies strongly point to the possibility that peroxide plays a more prominent role than superoxide in the lifespan of *C. elegans* and possibly other organisms. Both oxidants are often used interchangeably when the influence of ROS is being investigated. This is based on the fact that superoxide dismutase rapidly converts superoxide into H_2O_2, which is detoxified to harmless water. However, many organisms mount separate transcriptional responses to superoxide and peroxide (Lushchak, 2011), not only illustrating the distinct chemistry and reactivity of these oxidants but demonstrating that both oxidants can accumulate independently of each other *in vivo*. These results also raise the question as to whether monitoring protein carbonylation, a commonly used semi-quantitative method to assess protein oxidation *in vivo*, is suited to establish early correlations between oxidative stress and lifespan. With this method, it is usually unclear how much of a protein population is affected, and which, if any, functional or physiological consequences result. With OxICAT, HyPer, and other related redox sensors (Meyer & Dick, 2010), we now have the unique opportunity to precisely track reactive oxygen species *in vivo* and to clearly distinguish between ROS that might or might not be relevant for lifespan.

It has long been observed that the lifespan of individual animals is quite variable, even when isogenic populations like *C. elegans* are considered. These findings led to the suggestion that individual lifespan determination might not simply follow a genetic program, but might be ruled by a complexity of processes that are influenced by environmental, genetic, and stochastic factors (Wu *et al.*, 2006). The stochastic component in particular is thought to significantly contribute to *C. elegans* senescence, displaying heterogeneity in the mobility, aging morphology, and lifespan of individuals (Herndon *et al.*, 2002). A recent study demonstrated that stochastic variances in the expression levels of a stress-inducible

gene in early adulthood might predict life expectancy in an isogenic population, thus serving as biomarkers of aging (Rea *et al.*, 2005). Our observation that *in vivo* peroxide levels vary dramatically within an isogenic wild-type population of the same chronological age (Fig. 4-4 and 4-5) supports the exciting possibility that we have discovered not only another biomarker of aging but possibly one of the main factors contributing to stochastic variances. As transcriptional and epigenetic control mechanisms involve redox-regulated proteins (Cyr & Domann, 2010), early variances in ROS levels might play the important role of individualizing gene expression and ultimately determining lifespan.

4.6 References

Bader N & Grune T (2006) Protein oxidation and proteolysis. *Biol Chem* **387**, 1351-1355.

Bae YS, Kang SW, Seo MS, Baines IC, Tekle E, Chock PB & Rhee SG (1997) Epidermal growth factor (EGF)-induced generation of hydrogen peroxide. Role in EGF receptor-mediated tyrosine phosphorylation. *J Biol Chem* **272**, 217-221.

Belousov VV, Fradkov AF, Lukyanov KA, Staroverov DB, Shakhbazov KS, Terskikh AV & Lukyanov S (2006) Genetically encoded fluorescent indicator for intracellular hydrogen peroxide. *Nat Methods* **3**, 281-286.

Ben-Zvi A, Miller EA & Morimoto RI (2009) Collapse of proteostasis represents an early molecular event in Caenorhabditis elegans aging. *Proc Natl Acad Sci U S A* **106**, 14914-14919.

Brandes N, Schmitt S & Jakob U (2009) Thiol-based redox switches in eukaryotic proteins. *Antioxid Redox Signal* **11**, 997-1014.

Cavallini G, Donati A, Gori Z & Bergamini E (2008) Towards an understanding of the anti-aging mechanism of caloric restriction. *Curr Aging Sci* **1**, 4-9.

Cyr A & Domann F (2010) The Redox Basis of Epigenetic Modifications: From Mechanisms to Functional Consequences. *Antioxid Redox Signal*.

Davies KJ (2001) Degradation of oxidized proteins by the 20S proteasome. *Biochimie* **83**, 301-310.

Dillin A, Crawford DK & Kenyon C (2002a) Timing requirements for insulin/IGF-1 signaling in *C. elegans*. *Science* **298**, 830-834.

Dillin A, Hsu AL, Arantes-Oliveira N, Lehrer-Graiwer J, Hsin H, Fraser AG, Kamath RS, Ahringer J & Kenyon C (2002b) Rates of behavior and aging specified by mitochondrial function during development. *Science* **298**, 2398-2401.

Edens WA, Sharling L, Cheng G, Shapira R, Kinkade JM, Lee T, Edens HA, Tang X, Sullards C, Flaherty DB, Benian GM & Lambeth JD (2001) Tyrosine cross-linking of extracellular matrix is catalyzed by Duox, a multidomain oxidase/peroxidase with homology to the phagocyte oxidase subunit gp91phox. *J Cell Biol* **154**, 879-891.

Finkel T & Holbrook NJ (2000) Oxidants, oxidative stress and the biology of ageing. *Nature* **408**, 239-247.

Gella A & Durany N (2009) Oxidative stress in Alzheimer disease. *Cell Adh Migr* **3**, 88-93.

Gems D & Doonan R (2009) Antioxidant defense and aging in *C. elegans*: is the oxidative damage theory of aging wrong? *Cell Cycle* **8**, 1681-1687.

Gems D, Sutton AJ, Sundermeyer ML, Albert PS, King KV, Edgley ML, Larsen PL & Riddle DL (1998) Two pleiotropic classes of daf-2 mutation affect larval arrest, adult behavior, reproduction and longevity in Caenorhabditis elegans. *Genetics* **150**, 129-155.

Gilbert HF (1990) Molecular and cellular aspects of thiol-disulfide exchange. *Adv Enzymol Relat Areas Mol Biol* **63**, 69-172.

Groeger G, Quiney C & Cotter TG (2009) Hydrogen peroxide as a cell-survival signaling molecule. *Antioxid Redox Signal* **11**, 2655-2671.

Harman D (1956) Aging: a theory based on free radical and radiation chemistry. *J Gerontol* **11**, 298-300.

Herndon LA, Schmeissner PJ, Dudaronek JM, Brown PA, Listner KM, Sakano Y, Paupard MC, Hall DH & Driscoll M (2002) Stochastic and genetic factors influence tissue-specific decline in ageing *C. elegans*. *Nature* **419**, 808-814.

Johnson TE (2008) Caenorhabditis elegans 2007: the premier model for the study of aging. *Exp Gerontol* **43**, 1-4.

Kenyon C (2010) A pathway that links reproductive status to lifespan in Caenorhabditis elegans. *Ann N Y Acad Sci* **1204**, 156-162.

Kenyon C, Chang J, Gensch E, Rudner A & Tabtiang R (1993) A *C. elegans* mutant that lives twice as long as wild type. *Nature* **366**, 461-464.

Kim JH, Na HJ, Kim CK, Kim JY, Ha KS, Lee H, Chung HT, Kwon HJ, Kwon YG & Kim YM (2008) The non-provitamin A carotenoid, lutein, inhibits NF-kappaB-dependent gene expression through redox-based regulation of the phosphatidylinositol 3-kinase/PTEN/Akt and NF-kappaB-inducing kinase pathways: role of H(2)O(2) in NF-kappaB activation. *Free Radic Biol Med* **45**, 885-896.

Kumsta C & Jakob U (2009) Redox-regulated chaperones. *Biochemistry* **48**, 4666-4676.

Kumsta C, Thamsen M & Jakob U (2010) Effects of Oxidative Stress on Behavior, Physiology, and the Redox Thiol Proteome of Caenorhabditis elegans. *Antioxid Redox Signal*.

Leichert LI, Gehrke F, Gudiseva HV, Blackwell T, Ilbert M, Walker AK, Strahler JR, Andrews PC & Jakob U (2008) Quantifying changes in the thiol redox proteome upon oxidative stress *in vivo*. *Proc Natl Acad Sci U S A* **105**, 8197-8202.

Leichert LI & Jakob U (2004) Protein thiol modifications visualized *in vivo*. *PLoS Biol* **2**, e333.

Li W & Kong AN (2009) Molecular mechanisms of Nrf2-mediated antioxidant response. *Mol Carcinog* **48**, 91-104.

Libina N, Berman JR & Kenyon C (2003) Tissue-specific activities of *C. elegans* DAF-16 in the regulation of lifespan. *Cell* **115**, 489-502.

Lushchak VI (2011) Adaptive response to oxidative stress: Bacteria, fungi, plants and animals. *Comp Biochem Physiol C Toxicol Pharmacol* **153**, 175-190.

Mello CC, Kramer JM, Stinchcomb D & Ambros V (1991) Efficient gene transfer in C.elegans: extrachromosomal maintenance and integration of transforming sequences. *EMBO J* **10**, 3959-3970.

Meyer AJ & Dick TP (2010) Fluorescent protein-based redox probes. *Antioxid Redox Signal* **13**, 621-650.

Murphy CT (2006) The search for DAF-16/FOXO transcriptional targets: approaches and discoveries. *Exp Gerontol* **41**, 910-921.

Murphy CT, McCarroll SA, Bargmann CI, Fraser A, Kamath RS, Ahringer J, Li H & Kenyon C (2003) Genes that act downstream of DAF-16 to influence the lifespan of Caenorhabditis elegans. *Nature* **424**, 277-283.

Niethammer P, Grabher C, Look AT & Mitchison TJ (2009) A tissue-scale gradient of hydrogen peroxide mediates rapid wound detection in zebrafish. *Nature* **459**, 996-999.

Perez VI, Bokov A, Van Remmen H, Mele J, Ran Q, Ikeno Y & Richardson A (2009) Is the oxidative stress theory of aging dead? *Biochim Biophys Acta* **1790**, 1005-1014.

Petriv OI & Rachubinski RA (2004) Lack of peroxisomal catalase causes a progeric phenotype in Caenorhabditis elegans. *J Biol Chem* **279**, 19996-20001.

Petropoulos I & Friguet B (2006) Maintenance of proteins and aging: the role of oxidized protein repair. *Free Radic Res* **40**, 1269-1276.

Rasband WS (1997-2009) ImageJ: U. S. National Institutes of Health, Bethesda,
Maryland, USA.

Rea SL, Wu D, Cypser JR, Vaupel JW & Johnson TE (2005) A stress-sensitive reporter predicts longevity in isogenic populations of Caenorhabditis elegans. *Nat Genet* **37**, 894-898.

Salmon AB, Murakami S, Bartke A, Kopchick J, Yasumura K & Miller RA (2005) Fibroblast cell lines from young adult mice of long-lived mutant strains are resistant to multiple forms of stress. *Am J Physiol Endocrinol Metab* **289**, E23-29.

Santos CX, Tanaka LY, Wosniak J & Laurindo FR (2009) Mechanisms and implications of reactive oxygen species generation during the unfolded protein response: roles of endoplasmic reticulum oxidoreductases, mitochondrial electron transport, and NADPH oxidase. *Antioxid Redox Signal* **11**, 2409-2427.

Schreck R, Rieber P & Baeuerle PA (1991) Reactive oxygen intermediates as apparently widely used messengers in the activation of the NF-kappa B transcription factor and HIV-1. *EMBO J* **10**, 2247-2258.

Schulz TJ, Zarse K, Voigt A, Urban N, Birringer M & Ristow M (2007) Glucose restriction extends Caenorhabditis elegans life span by inducing mitochondrial respiration and increasing oxidative stress. *Cell Metab* **6**, 280-293.

Sohal RS & Weindruch R (1996) Oxidative stress, caloric restriction, and aging. *Science* **273**, 59-63.

Song JJ & Lee YJ (2003) Catalase, but not MnSOD, inhibits glucose deprivation-activated ASK1-MEK-MAPK signal transduction pathway and prevents relocalization of Daxx: hydrogen peroxide as a major second messenger of metabolic oxidative stress. *J Cell Biochem* **90**, 304-314.

Sulston J, Hodgkin, J. (1988) *The Nematode C. elegans* Cold Spring Harbor, New York: Cold Spring Harbor Laboratory Press

Sun L, Sadighi Akha AA, Miller RA & Harper JM (2009) Life-span extension in mice by preweaning food restriction and by methionine restriction in middle age. *J Gerontol A Biol Sci Med Sci* **64**, 711-722.

Wadsworth WG & Riddle DL (1989) Developmental regulation of energy metabolism in Caenorhabditis elegans. *Dev Biol* **132**, 167-173.

Wu D, Rea SL, Yashin AI & Johnson TE (2006) Visualizing hidden heterogeneity in isogenic populations of *C. elegans*. *Exp Gerontol* **41**, 261-270.

Yang W, Li J & Hekimi S (2007) A Measurable increase in oxidative damage due to reduction in superoxide detoxification fails to shorten the life span of long-lived mitochondrial mutants of Caenorhabditis elegans. *Genetics* **177**, 2063-2074.

4.7 Supplemental Methods

Image quantification: A MATLAB (The MathWorks) script was used in conjunction with ImageJ (Rasband, 1997-2009) to perform the automated image quantification. The MATLAB script contained the following steps:

1. Defining worm spine and body wall trace - Initially, each worm was identified by tracing its center in the DIC image. This track is referred to as the *worm spine*. In a similar manner, the body wall was traced as the *body wall trace*.

2. Worm region and background region - The automated image analysis then dilated the *worm spine* to define a binary mask, called the *worm region*. The number of dilation iterations was set so that all worms lay completely within this *worm region*, including a decent margin of about 100 pixels. The inverse of that *worm region* is referred to as the *background region*. Regions with very high signal in any channel (e.g., fluorescent particles, pharyngeal co-injection marker) were identified by applying an over-saturation threshold and were excluded from both the *worm region* and the *background region*.

3. Correction for channel backgrounds - The average signal of the *background region* in the 405 image and 488 image (i.e., background or offset) was subtracted from the value of each pixel in the *worm region* of the corresponding image.

4. Defining the Hyper Regions and obtaining the HyPer Ratio - For each set of microscope and laser settings, an appropriate minimum HyPer signal threshold was chosen for the 405 and 488 channel. Contiguous blocks of pixels above that threshold within the *worm region* and in proximity to the *body wall trace* defined *preliminary HyPer regions*. The result of this automated selection is then displayed in ImageJ and a manual check is performed. If necessary, corrections are applied (e.g., exclusion of obviously incorrectly identified *preliminary HyPer regions*). The mean pixel intensities of the *final HyPer selection* in the background-corrected 405 and 488 images are then divided by each other to obtain the final *HyPer ratio*.

5. Reference Ratios for Normalization - In parallel, a fluorescent reference slide was used to calculate a *reference ratio* with backgrounds defined as zero and the whole image treated as HyPer selection. This is acceptable since the fluorescent slide signal is very uniform and more than a magnitude higher than the (almost constant) dark signal of the imaging chain. Whenever comparisons between days were performed, the daily average of these *reference ratios* was used to normalize the actual *HyPer ratios* for each worm of that day (through dividing by the *reference ratio*).

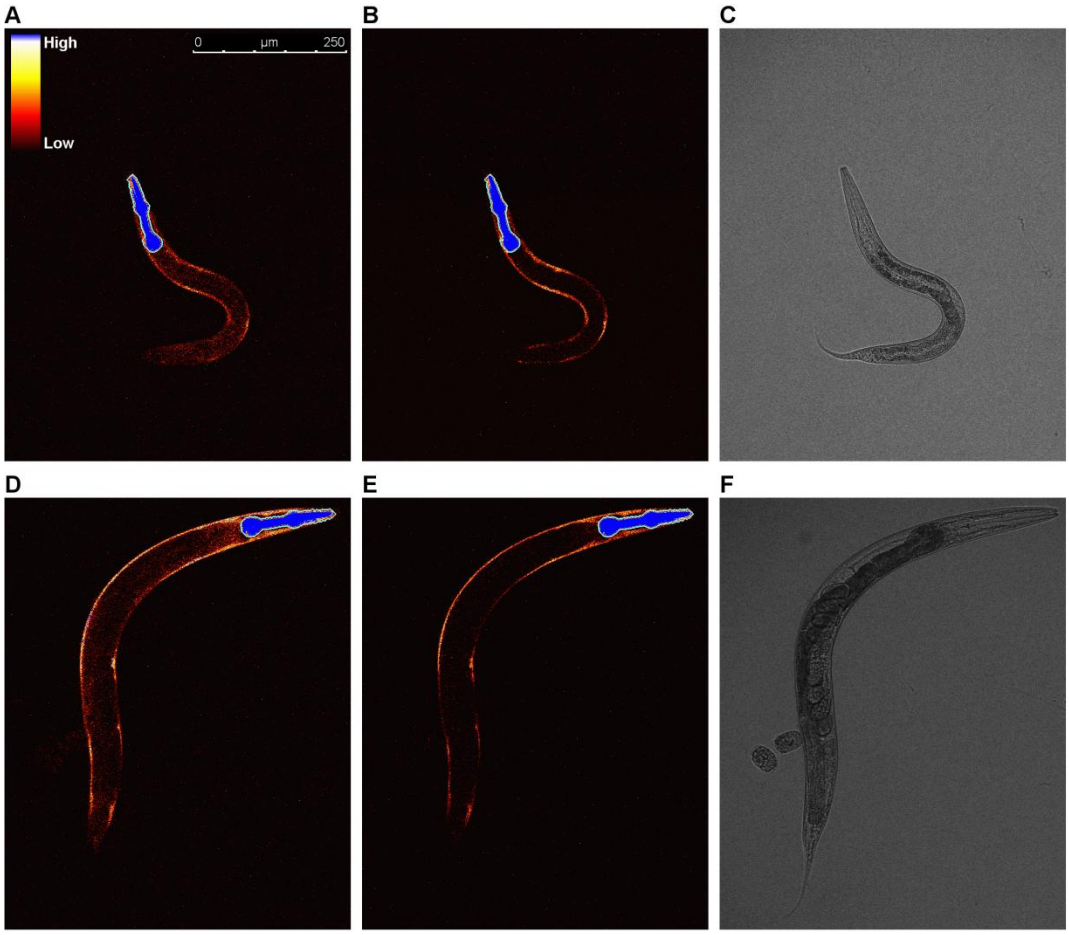

Suppl. Figure 4-1 HyPer fluorescence in the body wall muscle cells of larvae and adult wild type *C. elegans*.
Fluorescence (left and center column) and DIC (right column) images of N2 [*unc-54::HyPer*] larvae (L4, upper row) and young adults (Day 2, bottom row). The fluorescence emissions upon excitation with 405 nm laser (A, D) and with 488 nm laser (B, E) are displayed on a LUT scale. High emission intensities are shown in blue (oversaturated) and white; whereas low intensities are represented in shades of red (see scale in image A). The emission ranges from 505 nm to 530 nm. DIC images are shown in C and F. In L4 larvae, the emission intensity at 488 nm is higher than the emission intensity at 405 nm (A, B), whereas young adults show a higher emission intensity at 405 than at 488 nm (D, E). The same microscope settings were used. The fluorescence in the pharynx (cyan outline) is the co-injection maker *myo2::gfp* and was excluded from the HyPer ratio determination.

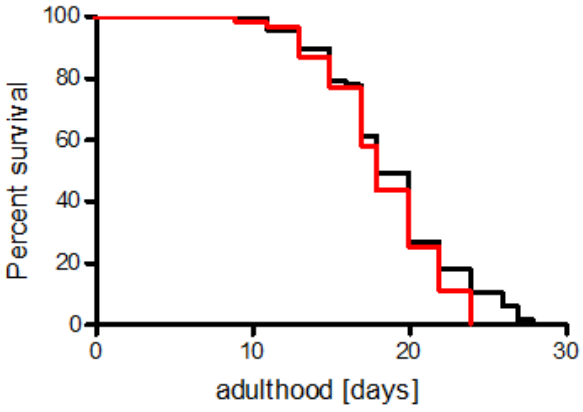

Suppl. Figure 4-2 Median life span of transgenic N2 [*unc-54::HyPer*] and wild type N2 animals at 15°C.
The median survivals of the wild type (n = 69) and the transgenic (n = 65) strain are not significantly different (18 days). Worms that crawled of the plates were censored. A Log-rank (Mantel-Cox) test (p = 0.1956) and a Gehan-Breslow-Wilcoxon test (p = 0.4882) were performed using GraphPad Prism Version 5.01 for Windows.

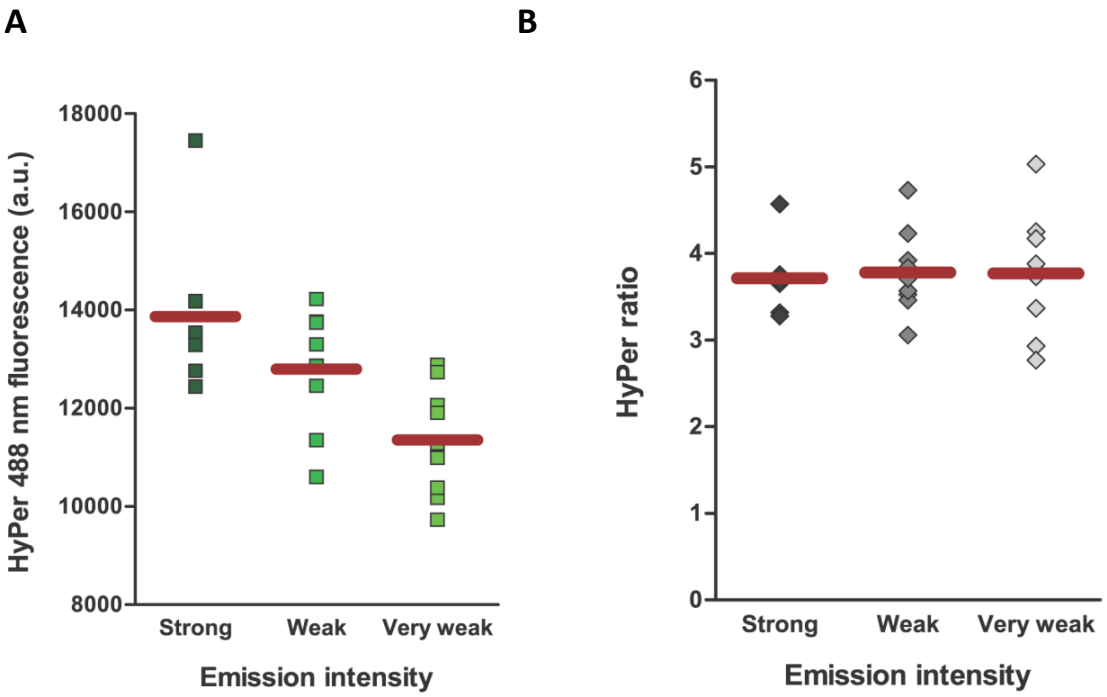

Suppl. Figure 4-3 Grouping of N2 [*unc-54::HyPer*] for HyPer fluorescence using the worm sorter COPAS SELECT.

Synchronized wild type N2 [*unc-54::HyPer*] animals were sorted at L2-L3 stage with a COPAS worm sorter for emission intensities upon excitation with a 510/10 nm band pass filter into three different groups: strong, weak and very weak. The following day the worms were imaged with a confocal microscope and the sorting for HyPer fluorescence (3A) was confirmed using the 488 nm confocal microscope laser. The HyPer ratio determination (3B) showed that the ratio is independent of HyPer fluorescence (e.g., read-out of protein expression).

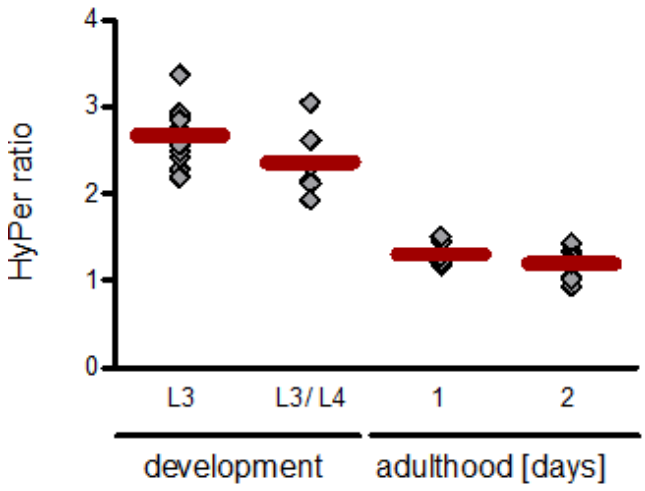

Suppl. Figure 4-4 Endogenous peroxide levels of unbleached N2 [unc-54::HyPer] animals.

A synchronized population of worms was generated by carefully washing worms of a plate with eggs remaining on the plate. The hatched L1 larvae were transferred onto a fresh NGM plate. At different time points, the HyPer ratio of developing *C. elegans* larvae and young adults were determined. Developing animals have elevated HyPer ratio, indicating that the increased peroxide levels observed in larval stages do not result from the synchronization procedure.

Suppl. Table 4-1 Oxidation status of *C. elegans* proteins in young WT worms (Day 2 of adulthood)

Protein	Acc No	Cys	ox. [%]	stdv	cellular localization	tissue localization
2-oxoglutarate dehydrogenase E1	CE28486	947	12	3	mitochondria[1]	ubiquitous
40S ribosomal protein S12	CE26896	114	13	4	ribosome	
40S ribosomal protein S14	CE00821	140	5	2	ribosome	pharynx, intestine, hypodermis
40S ribosomal protein S17	CE26948	35	5	2	ribosome	pharynx, intestine, body wall muscle, excretory cells
40S ribosomal protein S19	CE13265	99	4	1	ribosome	
40S ribosomal protein S21	CE30779	57	26	8	ribosome	ubiquitous
40S ribosomal protein S23	CE05747	90	22	3	ribosome	ubiquitous
40S ribosomal protein S25	CE04691	95	6	3	ribosome	
40S ribosomal protein S28	CE21842	22	6	3	ribosome	
40S ribosomal protein S3	CE01810	99/104	34	5	ribosome	
40S ribosomal protein S3a	CE00664	199	13	2	ribosome	
40S ribosomal protein S5	CE06360	161	3	0	ribosome	
40S ribosomal protein S5	CE06360	178	3	2	ribosome	
40S ribosomal protein S6	CE24592	83	3	1	ribosome	
40S ribosomal protein SA	CE00854	107	2	2	ribosome	ubiquitous
40S ribosomal protein SA	CE00854	163	12	2	ribosome	ubiquitous
60S ribosomal protein L11	CE07033	28/32	18	3	ribosome	ubiquitous
60S ribosomal protein L12	CE17986	141	8	2	ribosome	ubiquitous
60S ribosomal protein L22	CE04102	27	6	2	ribosome	
60S ribosomal protein L4	CE07669	216	7	4	ribosome	
aconitate hydratase	CE32436	29	6	1	mitochondria[1]	soma
aconitate hydratase	CE32436	288	18	1	mitochondria[1]	soma
actin-2	CE13150	258	16	3	cytosol	body wall muscle, neurons
adenylate kinase	CE29198	53	57	6	cytosol, mitochondria	intestine, neurons
alcohol dehydrogenase	CE12212	114	47	1	cytosol	
ANC-1	CE33588	1632	84	6	cytosol, nuclear envelope	body wall muscle
annexin	CE01431	112	5	2	membrane	pharynx
aspartyl-tRNA synthetase	CE00015	233	6	2	nucleus	
ATP synthase (subunit alpha)	CE36263	202	6	2	mitochondria	ubiquitous
ATP synthase (subunit beta)	CE29950	119	25	3	mitochondria	ubiquitous
attractin	CE41899	263/265	94	4		
calponin	CE09767	22	3	1	cytosol	ubiquitous
carbonic anhydrase	CE04755	155	30	6	cytosol	head, intestine
CDC-48.2	CE05402	696	26	6	ER, cytosol, nuclear membrane[1]	body wall muscle, intestine
CDC-48.2	CE05402	577	8	3	ER, cytosol, nuclear membrane[1]	body wall muscle, intestine
chitinase	CE32592	738/747	68	1	secreted[1]	somatic gonad
citrate synthase	CE00513	434	8	3	mitochondria	ubiquitous
clathrin (heavy chain)	CE00480	353	2	1	plasma	oocyte
COPI coatomer (subunit beta)	CE18673	688	8	4	golgi, ER	
COPI coatomer (subunit gamma)	CE06451	806	15	4	golgi, ER	
COPII coatomer (subunit SAR-1)	CE07622	174	10	2	golgi, ER	
cyclin (ZK353.1)	CE34452	92	96	3	cytosol	
degenerin (ASIC-1)	CE40185	659/661	98	2	membrane	

Suppl. Table 4-1 continued

Protein	Acc No	Cys	ox. [%]	stdv	cellular localization	tissue localization
degenerin (DEL-1)	CE05547	180/182	14	3	membrane	nervous system
DHHC-type Zn-finger protein	CE42532	134/137/138/139	8	3	golgi[1]	ubiquitous
DIM-1	CE04038	234	8	3	membrane	bodywall muscles
DNA polymerase (subunit delta)	CE09308	1043	77	7	nucleus	
DNA repair protein RAD-50	CE21149	1174	12	3	nucleus	
dynamin GTPase	CE07832	430	4	2	membrane, golgi[1]	ubiquitous
dynein light chain 1	CE00788	56	26	7	cytosol	pharynx, intestine, nervous system
egg-laying defective protein 27	CE31287	227	1	0	ribosome	pharynx, intestine, body wall muscle
elongation factor 1-alpha	CE01270	152	10	4	ribosome	pharynx, intestine, body wall muscle
elongation factor 1-alpha	CE01270	411	6	3	ribosome	pharynx, intestine, body wall muscle
elongation factor 2	CE15900	598	14	7	ribosome	ubiquitous
elongation factor 2	CE15900	745	5	3	ribosome	ubiquitous
endonuclease III	CE44645	48	5	5	nucleus	
forkhead transcription factor FKH-5	CE02683	265	96	4	nucleus, cytosol	
fructose-bisphosphate aldolase	CE16341	178/198	23	8	cytosol	ubiquitous
glutamyl-tRNA synthetase	CE06580	377	22	2	mitochondria	
glutathione S-transferase (class Pi)	CE00302	52	4	1	cytosol, mitochondria[1]	
glycine decarboxylase	CE06652	232	3	1	cytosol, mitochondria[1]	pharynx, intestine
glycosyl transferase	CE31185	97	20	2	membrane	pharynx, body wall muscle, reproductive system
GTP-binding protein (TAG-210)	CE14708	54	7	6		intestine
heat shock protein 60	CE42184	106	4	3	mitochondria	
heat shock protein 70	CE09682	307	3	1	cytosol	pharynx, body wall muscle, intestine
heat shock protein 70	CE09682	243	4	2	cytosol	pharynx, body wall muscle, intestine
heat shock protein 70	CE08631	587	12	5	mitochondria	intestine, muscles
heat shock protein Hsp-12.2	CE00072	61	9	2		
helicase (C28H8.3)	CE29195	669	10	5	nucleus	
heparan sulfate proteoglycan	CE37074	1245	3	4	membrane	hypodermis
HIS-40	K03A1.1	63	96	1		
integrin (subunit beta)	CE01102	445	94	6	membrane	muscles
intermediate filament B	CE02618	367	5	4	cytosol	nervous system, excretory cells
isocitrate dehydrogenase (subunit alpha)	CE34018	208	8	5	mitochondria, cytosol, peroxisome[1]	ubiquitous
isocitrate dehydrogenase (subunit alpha)	CE34018	343/351	26	4	mitochondria, cytosol, peroxisome[1]	ubiquitous
isocitrate lyase/malate synthase	CE32565	218	9	4	peroxisomes, mitochondria[1]	

Suppl. Table 4-1 continued

Protein	Acc No	Cys	ox. [%]	stdv	cellular localization	tissue localization
isocitrate lyase/malate synthase	CE32565	271	14	6	peroxisomes, mitochondria[1]	
LIN-28	CE24879	168/171/181	9	2	cytosol	pharynx, body wall muscle, reproductive system
lysozyme	CE06003	80	78	6	secreted	
metallothionein 1	CE07379	61	3	0	cytosol	pharynx, intestine
methylcrotonyl-CoA carboxylase	CE00136	212	10	6	mitochondria	pharynx
mitochondrial ADP/ATP carrier protein ANT-1.4	CE12898	146	5	2	mitochondria	intestine, nervous system
MUA-3	CE37256	2258	28	3	secreted	hypodermis
myosin-2	CE31619	970	3	1	cytosol	pharynx
myosin-2	CE31619	708	14	2	cytosol	pharynx
myosin-2	CE31619	1932	7	4	cytosol	pharynx
myosin-3	CE34936	707	26	3	cytosol	body wall muscle
myosin-4	CE06253	259	6	4	cytosol	pharynx
myosin-4	CE06253	700	19	5	cytosol	pharynx
NADH-ubiquinone oxidoreductase	CE10972	124/129	1	1	mitochondria[1]	
neprilysin	CE43217	170	22	6	membrane	intestine
NHP2 like protein	CE02283	93	20	4	nucleus	
nucleoside diphosphate kinase	CE09650	109	28	4		ubiquitous
nucleoside diphosphate kinase	CE09650	117	30	5		ubiquitous
papilin PPN-1	CE17536	477	98	3	secreted	muscles, reproductive system
paramyosin	CE42754	297	56	10	cytosol	muscles, pharynx
phosphatase 2A	CE30997	150	5	4	cytosol, nucleus	pharynx, intestine, body wall muscle
phosphatidylglycerol-phosphate	CE09617	14	95	4	mitochondria	
phosphoenolpyruvate carboxykinase	CE36359	9	10	2	cytosol, mitochondria[1]	intestine, reproductive system
phosphoinositide 3-kinase AGE-1	CE23506	710	50	12	cytosol	intestine, nervous system
polyadenylate-binding protein (pab-	CE36227	86	9	3	cytosol, nucleus[1]	
proliferating cell nuclear antigen	CE14512	197	13	1	nucleus	
proteasome alpha subunit (PAS-3)	CE30307	74	13	1	cytosol, nucleus[1]	
protein B0361.2	CE33549	242	10	2		
protein C08F11.11	CE17388	34	94	2		
protein C08F11.11	CE17388	81	99	0		
protein C44B12.5	CE16921	178/189/192/193	77	1		
protein CE32871	CE32871	374	12	3	membrane	pharynx, intestine, nervous system
protein F37C4.5	CE33640	53	18	5		
protein F46H5.3	CE33098	226	11	4		
protein F46H5.3	CE33098	304	4	1		
protein F46H5.3	CE33098	275	12	7		
protein K04G2.6	CE06100	234	5	3		
protein K07C5.4	CE06114	390	9	5		
protein T13F3.6	CE39775	83	77	4		
protein W07G4.4	CE03794	187	48	5		
protein Y57G11C.15	CE14954	13	3	2		
pyruvate carboxylase	CE09072	637	8	2	mitochondria	

Suppl. Table 4-1 continued

Protein	Acc No	Cys	ox. [%]	stdv	cellular localization	tissue localization
pyruvate carboxylase	CE09072	371	22	2	mitochondria	
RETR-1	CE41402	478	8	1		
ribonucleoprotein ROP-1	CE15613	185	5	3	cytosol	ubiquitous
RNA helicase CGH-1	CE00839	336	22	4	nucleus	gonads
RNA helicase CGH-1	CE00839	49	11	3	nucleus	gonads
RNA helicase GLH-1	CE25121	417	30	2	nucleus	gonads
RNA helicase HEL-1	CE32593	161	11	5	nucleus	pharynx, reproductive
S-adenosylhomocysteine hydrolase	CE17154	280	5	2	cytosol	pharynx, intestine
serine hydroxymethyltransferase MEL-32	CE01130	391	31	4	cytosol, mitochondria[1]	intestine, hypodermis
small molecules methylase	CE01829	224	12	1	secreted	
SMC4	CE03287	740	62	1	nucleus	
SURF family member SFT-4	CE06987	39	6	3	ER	ubiquitous
T-complex protein 1 (subunit beta)	CE16437	445	4	1	cytosol	ubiquitous
T-complex protein 1 (subunit theta)	CE44228	35	3	1	cytosol	
T-complex protein 1 (subunit zeta)	CE01234	517	12	2	cytosol	
T-complex protein 1 (subunit zeta)	CE01234	171	4	1	cytosol	
translation initiation factor 2	CE16227	138	5	2	ribosome	
translation initiation factor 5A	CE37787	111	27	6	ribosome	gonad
transthyretin-like protein TTR-2	CE00475	98/105	93	4	secreted[1]	
transthyretin-like protein TTR-6	CE14325	91/98	97	3	secreted[1]	
troponin T	CE04994	219	3	1	cytosol	
tubulin (alpha-2 chain)	CE09692	314	7	2	cytosol	ubiquitous
tubulin (beta-2 chain)	CE00913	239	5	2	cytosol	pharynx, reproductive system, body wall muscle, excretory cells
tubulin (gamma chain)	CE00224	252	92	8	cytosol	gonad
ubiquitin-conjugating enzyme E2	CE03482	85	9	1	cytosol	ubiquitous
UNC-87	CE36924	472	40	2	cytosol	pharynx, body wall muscle, intestine
UNC-89	CE37702	4588	4	3	cytosol	pharynx, body wall muscle
vacuolar ATP synthase (subunit A)	CE22210	521	10	2	cytosol	intestine, body wall muscle, excretory cells
vacuolar ATP synthase (subunit A)	CE22210	218	10	2	cytosol	intestine, body wall muscle, excretory cells
vacuolar ATP synthase (subunit A)	CE22210	266	36	9	cytosol	intestine, body wall muscle, excretory cells
vacuolar ATP synthase (subunit B)	CE04424	94	5	2	cytosol	pharynx, excretory cells
vacuolar ATP synthase (subunit B)	CE04424	33	1	1	cytosol	pharynx, excretory cells
vacuolar proton pump (subunit G)	CE10604	104	3	3	cytosol	
vigilin	CE23530	1063	7	4		
vigilin	CE23530	666	17	3		
vinculin	CE31398	336	11	7	cytosol	myoepithelial sheath
vitellogenin-2	CE41109	627	10	5	secreted	

Suppl. Table 4-1 continued

Protein	Acc No	Cys	ox. [%]	stdv	cellular localization	tissue localization
vitellogenin-2	CE41109	1489/ 1498	63	10	secreted	
vitellogenin-3	CE20900	626	10	2	secreted	intestine
vitellogenin-4	CE26817	206	63	5	secreted	
vitellogenin-4	CE26817	1474	5	1	secreted	
vitellogenin-6	CE28594	218	71	2	secreted	intestine
vitellogenin-6	CE28594	384	4	2	secreted	intestine
vitellogenin-6	CE28594	468	65	4	secreted	intestine
vitellogenin-6	CE28594	655	13	4	secreted	intestine
vitellogenin-6	CE28594	1364	22	3	secreted	intestine
vitellogenin-6	CE28594	1417	22	8	secreted	intestine
vitellogenin-6	CE28594	1514	27	4	secreted	intestine
vitellogenin-6	CE28594	1569	69	15	secreted	intestine
vitellogenin-6	CE28594	1479/ 1482	90	8	secreted	intestine
vitellogenin-6	CE28594	1645	16	6	secreted	intestine
WDR-23	CE23620	73	3	3		ubiquitous

[1]protein location determined on the basis of protein homologs in other organisms

Suppl. Table 4-2 *C. elegans* wild type proteins listed according to cluster analysis shown in Fig. 2

Cluster 1

Protein	Acc No	Cys	L2	L4	Day 2	Day 8	Day 15
2-oxoglutarate dehydrogenase E1	CE28486	947	17	14	12	21	**18**
40S ribosomal protein S14	CE00821	140	9	15	5	15	15
40S ribosomal protein S17	CE26948	35	7	7	5	9	7
40S ribosomal protein S19	CE13265	99	5	7	4	5	6
40S ribosomal protein S25	CE04691	95	6	10	6	14	14
40S ribosomal protein S3a	CE00664	199	12	13	13	16	15
40S ribosomal protein S5	CE06360	178	5	5	3	5	4
40S ribosomal protein S5	CE06360	161	0	10	3	6	14
40S ribosomal protein S6	CE24592	83	8	5	3	**8**	6
40S ribosomal protein SA	CE00854	107	19	8	2	22	4
40S ribosomal protein SA	CE00854	163	13	17	12	12	19
60S ribosomal protein L4	CE07669	216	10	10	7	8	9
aconitase	CE32436	29	6	12	6	13	14
annexin	CE01431	112	12	7	5	6	5
ATP synthase (subunit alpha)	CE36263	202	10	17	6	12	12
calponin	CE09767	22	2	9	3	2	**7**
CDC-48.2	CE05402	577	11	16	8	10	11
citrate synthase	CE00513	434	14	**13**	8	1	**4**
clathrin (heavy chain)	CE00480	353	4	2	2	4	1
COPI coatomer (subunit beta)	CE18673	688	7	12	8	9	9
COPI coatomer (subunit gamma)	CE06451	806	15	13	15	12	17
degenerin (DEL-1)	CE05547	180/182	13	16	14	11	11
DHHC-type Zn-finger protein	CE42532	134/137/ 138/139	**11**	8	8	4	6
DNA repair protein RAD-50	CE21149	1174	13	14	12	12	21
dynamin GTPase	CE07832	430	2	5	4	**5**	3
egg-laying defective protein 27	CE31287	227	15	2	1	6	1
elongation factor 1-alpha	CE01270	152	10	15	10	9	16
elongation factor 1-alpha	CE01270	411	9	10	6	10	13
elongation factor 2	CE15900	745	7	7	5	7	10
endonuclease III	CE44645	48	4	10	5	10	10
glutathione S-transferase (class Pi)	CE00302	52	8	4	4	5	2
glycine decarboxylase	CE06652	232	0	5	3	10	8
heat shock protein 60	CE42184	106	8	8	4	8	8
heat shock protein 70	CE09682	307	4	3	3	3	3
heat shock protein 70	CE09682	243	31	5	4	10	9
heat shock protein Hsp-12.2	CE00072	61	11	12	9	10	19
helicase (C28H8.3)	CE29195	669	18	15	10	12	18
heparan sulfate proteoglycan	CE37074	1245	6	**9**	3	2	10
intermediate filament B	CE02618	367	5	10	5	8	6
isocitrate dehydrogenase (subunit alpha)	CE34018	208	8	11	8	**9**	6
isocitrate lyase/malate synthase	CE32565	218	15	16	9	14	17
LIN-28	CE24879	168/171/1 81	7	13	9	11	18
mitochondrial ADP/ATP carrier protein ANT-1.4	CE12898	146	8	6	5	13	**13**
myosin-2	CE31619	708	8	15	14	**13**	20
myosin-2	CE31619	1932	15	11	7	**9**	**9**
myosin-4	CE06253	259	9	8	6	8	8
myosin-4	CE06253	700	16	18	19	14	12
NADH-ubiquinone oxidoreductase	CE10972	124/129	4	2	1	**4**	6
NHP2 like protein	CE02283	93	14	25	20	21	26
phosphatase 2A	CE30997	150	7	11	5	7	12
phosphoenolpyruvate carboxykinase	CE36359	9	**13**	18	10	19	21

Suppl. Table 4-2 continued

Cluster 1 continued

Protein	Acc No	Cys	L2	L4	Day 2	Day 8	Day 15
protein B0361.2	CE33549	242	11	14	10	10	5
protein F46H5.3	CE33098	304	14	9	4	5	6
protein Y57G11C.15	CE14954	13	2	4	3	5	2
pyruvate carboxylase	CE09072	637	2	9	8	11	8
RETR-1	CE41402	478	14	16	8	20	14
ribonucleoprotein ROP-1	CE15613	185	8	14	5	9	10
RNA helicase CGH-1	CE00839	49	15	11	11	9	8
RNA helicase HEL-1	CE32593	161	16	12	11	18	20
S-adenosylhomocysteine hydrolase	CE17154	280	9	11	5	9	12
SURF family member SFT-4	CE06987	39	13	8	6	8	15
T-complex protein 1 (subunit beta)	CE16437	445	6	9	4	12	13
T-complex protein 1 (subunit theta)	CE44228	35	13	8	3	8	10
translation initiation factor 2 (subunit beta)	CE16227	138	11	9	5	9	9
troponin T	CE04994	219	13	6	3	10	9
tubulin (beta-2 chain)	CE00913	239	10	13	5	21	**18**
ubiquitin-conjugating enzyme E2	CE03482	85	6	8	9	8	11
UNC-89	CE37702	4588	**9**	12	4	2	3
vacuolar ATP synthase (subunit A)	CE22210	521	7	14	10	15	7
vacuolar ATP synthase (subunit B)	CE04424	94	6	10	5	8	9
vacuolar ATP synthase subunit B	CE04424	33	7	10	1	**7**	12
vacuolar proton pump (subunit G)	CE10604	104	6	12	3	5	12
vitellogenin-2	CE41109	627	**10**	9	10	11	18
vitellogenin-6	CE28594	384	**9**	8	4	5	7
vitellogenin-6	CE28594	1364	**12**	8	22	16	17
vitellogenin-6	CE28594	655	**15**	19	13	18	20
vitellogenin-6	CE28594	1645	**15**	**17**	16	13	10
WDR-23	CE23620	73	**4**	3	3	5	4

Cluster 2

Protein	Acc No	Cys	L2	L4	Day 2	Day 8	Day 15
CDC-48.2	CE05402	696	24	35	26	34	36
glycosyl transferase	CE31185	97	29	23	20	26	28
proliferating cell nuclear antigen	CE14512	197	21	19	13	15	18
vacuolar ATP synthase (subunit A)	CE22210	266	31	**27**	36	24	**36**
vigilin	CE23530	666	23	24	17	**17**	**21**
vitellogenin-6	CE28594	1417	**18**	**19**	22	27	25

Cluster 3

Protein	Acc No	Cys	L2	L4	Day 2	Day 8	Day 15
attractin	CE41899	263/265	90	96	94	98	97
cyclin (ZK353.1)	CE34452	92	89	94	96	**92**	**94**
degenerin (ASIC-1)	CE40185	659/661	**93**	87	98	94	100
forkhead transcription factor FKH-5	CE02683	265	90	97	96	81	92
HIS-40	K03A1.1	63	96	96	96	96	88
integrin (subunit beta)	CE01102	445	80	**90**	94	83	**91**
lysozyme	CE06003	80	83	93	78	**85**	**84**
phosphatidylglycerol-phosphate synthase	CE09617	14	96	99	95	89	93
protein C08F11.11	CE17388	34	**93**	96	94	92	93
protein C08F11.11	CE17388	81	**92**	99	99	96	99
transthyretin-like protein TTR-2	CE00475	98/105	95	88	93	98	94
transthyretin-like protein TTR-6	CE14325	91/98	**87**	87	97	82	93
tubulin (gamma chain)	CE00224	252	96	89	92	96	97

Suppl. Table 4-2 continued

Cluster 4

Protein	Acc No	Cys	L2	L4	Day 2	Day 8	Day 15
60S ribosomal protein L22	CE04102	27	6	8	6	9	19
ATP synthase (subunit beta)	CE29950	119	14	19	25	31	32
fructose-bisphosphate aldolase	CE16341	178/198	5	4	23	**24**	**30**
heat shock protein 70	CE08631	587	12	9	12	17	28
myosin-3	CE34936	707	18	21	26	39	37
protein F37C4.5	CE33640	53	21	18	18	32	**36**
RNA helicase CGH-1	CE00839	336	**22**	**24**	22	28	45
small molecules methylase (C28H8.7)	CE01829	224	2	2	12	23	26
translation initiation factor 5A	CE37787	111	17	18	27	33	47

Cluster 5

Protein	Acc No	Cys	L2	L4	Day 2	Day 8	Day 15
40S ribosomal protein S12	CE26896	114	20	30	13	24	34
40S ribosomal protein S28	CE21842	22	10	20	6	16	29
actin-2	CE13150	258	19	23	16	24	30
aspartyl-tRNA synthetase	CE00015	233	**19**	27	6	13	17
COPII coatomer (subunit SAR-1)	CE07622	174	23	23	10	27	25
DIM-1	CE04038	234	11	18	8	18	33
elongation factor 2	CE15900	598	14	25	14	23	23
isocitrate lyase/malate synthase	CE32565	271	15	26	14	14	26
methylcrotonyl-CoA carboxylase	CE00136	212	15	26	10	18	22
polyadenylate-binding protein	CE36227	86	7	17	9	**13**	**35**
proteasome alpha subunit (PAS-3)	CE30307	74	26	14	13	**14**	**27**
protein CE32871	CE32871	374	22	26	12	**13**	**21**
protein F46H5.3	CE33098	275	**22**	**26**	12	13	21
protein F46H5.3	CE33098	226	20	18	11	3	**13**
protein K07C5.4	CE06114	390	12	15	9	8	28
T-complex protein 1 (subunit zeta)	CE01234	517	26	30	12	9	26
tubulin (alpha-2 chain)	CE09692	314	15	23	7	18	**34**
vacuolar ATP synthase (subunit A)	CE22210	218	22	28	10	11	11
vigilin	CE23530	1063	16	11	7	15	**31**
vinculin	CE31398	336	16	20	11	**14**	**38**

Cluster 6

Protein	Acc No	Cys	L2	L4	Day 2	Day 8	Day 15
40S ribosomal protein S21	CE30779	57	38	34	26	43	42
40S ribosomal protein S23	CE05747	90	17	27	22	32	39
glutamyl-tRNA synthetase	CE06580	377	14	26	22	34	33
neprilysin	CE43217	170	66	**46**	22	**37**	62
nucleoside diphosphate kinase	CE09650	109	36	35	28	36	47
nucleoside diphosphate kinase	CE09650	117	37	36	30	45	54
serine hydroxymethyltransferase MEL-32	CE01130	391	63	34	31	60	44

Cluster 7

Protein	Acc No	Cys	L2	L4	Day 2	Day 8	Day 15
adenylate kinase	CE29198	53	61	63	57	**50**	59
paramyosin	CE42754	297	81	59	56	60	56
phosphoinositide 3-kinase AGE-1	CE23506	710	54	56	50	72	72
vitellogenin-2	CE41109	1489/1498	**69**	65	63	63	71

Suppl. Table 4-2 continued

Cluster 8

Protein	Acc No	Cys	L2	L4	Day 2	Day 8	Day 15
chitinase	CE32592	738/747	96	94	68	**78**	91
DNA polymerase (subunit delta)	CE09308	1043	74	79	77	69	78
protein C44B12.5	CE16921	178/189/ 192/193	**90**	**92**	77	91	87
vitellogenin-4	CE26817	206	81	85	63	75	77
vitellogenin-6	CE28594	218	81	87	71	71	75
vitellogenin-6	CE28594	468	83	89	65	74	80
vitellogenin-6	CE28594	1569	**81**	88	69	76	75

bold values are calculated using the CTWC algorithm (http://ctwc.weizmann.ac.il/).

Suppl. Table 4-3 Oxidation status of *C. elegans* proteins during lifespan of WT worms

Protein	Acc No	Cys	N2 L2		N2 L4		N2 Day 2		N2 Day 8		N2 Day 15	
			ox.	stdv	ox.	stdv	ox.	stdv	ox.	stdv	ox.	stdv
2-oxoglutarate dehydrogenase	CE28486	947	17	4	14	3	12	3	21	15		
40S ribosomal protein S12	CE26896	114	20	1	30	5	13	4	24	2	34	6
40S ribosomal protein S14	CE00821	140	9	1	15	3	5	2	15	4	15	3
40S ribosomal protein S17	CE26948	35	7	3	7	2	5	2	9	6	7	3
40S ribosomal protein S19	CE13265	99	5	3	7	3	4	1	5	2	6	5
40S ribosomal protein S21	CE30779	57	38	7	34	6	26	8	43	12	42	8
40S ribosomal protein S23	CE05747	90	17	1	27	4	22	3	32	6	39	12
40S ribosomal protein S25	CE04691	95	6	2	10	5	6	3	14	10	14	7
40S ribosomal protein S28	CE21842	22	10	2	20	3	6	3	16	2	29	4
40S ribosomal protein S3	CE01810	99/104					34	5	7	1		
40S ribosomal protein S3a	CE00664	199	12	1	13	3	13	2	16	5	15	6
40S ribosomal protein S5	CE06360	161	0	1	10	3	3	0	6	4	14	17
40S ribosomal protein S5	CE06360	178	5	3	5	3	3	2	5	3	4	3
40S ribosomal protein S6	CE24592	83	8	5	5	4	3	1			6	4
40S ribosomal protein SA	CE00854	107	19	13	8	5	2	2	22	7	4	2
40S ribosomal protein SA	CE00854	163	13	4	17	6	12	2	12	5	19	8
60S ribosomal protein L11	CE07033	28/32					18	3	35	9		
60S ribosomal protein L12	CE17986	141	18	0	3	1	8	2	19	4		
60S ribosomal protein L22	CE04102	27	6	2	8	2	6	2	9	3	19	5
60S ribosomal protein L4	CE07669	216	10	3	10	8	7	4	8	6	9	6
aconitase	CE32436	29	6	4	12	1	6	1	13	2	14	3
aconitase	CE32436	288			28	13	18	1				
actin-2	CE13150	258	19	8	23	6	16	3	24	6	30	9
adenylate kinase	CE29198	53	61	12	63	1	57	6			59	0
alcohol dehydrogenase	CE12212	114			20	9	47	1				
aldehyde dehydrogenase	CE39486	93							25	5		
ANC-1	CE33588	1632			80	12	84	6	70	6	76	15
annexin	CE01431	112	12	10	7	4	5	2	6	4	5	3
aspartyl-tRNA synthetase	CE00015	233			27	8	6	2	13	10	17	11
ATP synthase (subunit alpha)	CE36263	202	10	6	17	15	6	2	12	8	12	8
ATP synthase (subunit beta)	CE29950	119	14	5	19	2	25	3	31	2	32	2
attractin	CE41899	263/265	90	6	96	3	94	4	98	2	97	1
calponin	CE09767	22	2	0	9	7	3	1	2	2		
CDC-48.2	CE05402	696	24	3	35	3	26	6	34	13	36	16
CDC-48.2	CE05402	577	11	3	16	1	8	3	10	2	11	4
chitinase	CE32592	738/747	96	6	94	5	68	1			91	2
citrate synthase	CE00513	434	14	2			8	3	1	1		
clathrin (heavy chain)	CE00480	353	4	3	2	2	2	1	4	3	1	1
COPI coatomer (subunit beta)	CE18673	688	7	11	12	4	8	4	9	6	9	9
COPI coatomer (subunit gamma)	CE06451	806	15	11	13	3	15	4	12	8	17	5
COPII coatomer (subunit SAR-1)	CE07622	174	23	7	23	5	10	2	27	4	25	7
cyclin (ZK353.1)	CE34452	92	89	9	94	6	96	3				
degenerin (ASIC-1)	CE40185	659/661			87	16	98	2	94	9	100	1
degenerin (DEL-1)	CE05547	180/182	13	8	16	3	14	3	11	3	11	4
DHHC-type Zn-finger protein	CE42532	134/137/ 138/139			8	11	8	3	4	4	6	3
DIM-1	CE04038	234	11	2	18	5	8	3	18	4	33	14
DNA polymerase (subunit delta)	CE09308	1043	74	14	79	3	77	7	69	13	78	7

Suppl. Table 4-3 WT continued

Protein	Acc No	Cys	N2 L2		N2 L4		N2 Day 2		N2 Day 8		N2 Day 15	
			ox.	stdv	ox.	stdv	ox.	stdv	ox.	stdv	ox.	stdv
DNA repair protein RAD-50	CE21149	1174	**13**	2	**14**	3	**12**	3	**12**	5	**21**	4
dynamin GTPase	CE07832	430	**2**	3	**5**	3	**4**	2			**3**	0
dynein light chain 1	CE00788	56			**2**	2	**26**	7	**13**	7	**17**	8
egg-laying defective protein 27	CE31287	227	**15**	19	**2**	3	**1**	0	**6**	7	**1**	1
elongation factor 1-alpha	CE01270	152	**10**	3	**15**	5	**10**	4	**9**	4	**16**	8
elongation factor 1-alpha	CE01270	411	**9**	3	**10**	3	**6**	3	**10**	3	**13**	3
elongation factor 2	CE15900	598	**14**	2	**25**	7	**14**	7	**23**	13	**23**	4
elongation factor 2	CE15900	745	**7**	5	**7**	4	**5**	3	**7**	3	**10**	5
endonuclease III	CE44645	48	**4**	3	**10**	10	**5**	5	**10**	4	**10**	6
forkhead transcription factor	CE02683	265	**90**	8	**97**	5	**96**	4	**81**	9	**92**	11
fructose-bisphosphate	CE16341	178/198	**5**	2	**4**	3	**23**	8				
glutamyl-tRNA synthetase	CE06580	377	**14**	5	**26**	5	**22**	2	**34**	2	**33**	3
glutathione S-transferase	CE00302	52	**8**	5	**4**	1	**4**	1	**5**	3	**2**	1
glycine decarboxylase	CE06652	232	**0**	4	**5**	3	**3**	1	**10**	8	**8**	9
glycosyl transferase	CE31185	97	**29**	13	**23**	10	**20**	2	**26**	15	**28**	11
GTP-binding protein (TAG-210)	CE14708	54	**20**	1			**7**	6				
heat shock protein 60	CE42184	106	**8**	7	**8**	3	**4**	3	**8**	2	**8**	5
heat shock protein 70	CE09682	307	**4**	3	**3**	1	**3**	1	**3**	1	**3**	1
heat shock protein 70	CE09682	243	**31**	2	**5**	4	**4**	2	**10**	2	**9**	4
heat shock protein 70	CE08631	587			**9**	15	**12**	5	**17**	15		
heat shock protein Hsp-12.2	CE00072	61	**11**	3	**12**	4	**9**	2	**10**	6	**19**	9
helicase (C28H8.3)	CE29195	669	**18**	2	**15**	4	**10**	5	**12**	2	**18**	7
heparan sulfate proteoglycan	CE37074	1245	**6**	10			**3**	4	**2**	3	**10**	9
HIS-40	K03A1.1	63	**96**	3	**96**	4	**96**	1	**96**	3	**88**	12
integrin (subunit beta)	CE01102	445	**80**	14			**94**	6	**83**	11		
intermediate filament B	CE02618	367	**5**	4	**10**	5	**5**	4	**8**	4	**6**	5
isocitrate dehydrogenase (subunit alpha)	CE34018	208	**8**	2	**11**	2	**8**	5			**6**	3
isocitrate dehydrogenase (subunit alpha)	CE34018	343/351					**26**	4	**14**	8		
isocitrate lyase/malate synthase	CE32565	218	**15**	3	**16**	6	**9**	4	**14**	8	**17**	6
isocitrate lyase/malate synthase	CE32565	271	**15**	6	**26**	12	**14**	6	**14**	6	**26**	7
LIN-28	CE24879	168/171/181	**7**	2	**13**	2	**9**	2	**11**	2	**18**	5
lysozyme	CE06003	80	**83**	16	**93**	3	**78**	6				
methylcrotonyl-CoA	CE00136	212	**15**	4	**26**	5	**10**	6	**18**	3	**22**	2
mitochondrial ADP/ATP carrier protein ANT-1.4	CE12898	146	**8**	6	**6**	5	**5**	2	**13**	12		
MUA-3	CE37256	2258	**10**	5	**14**	1	**28**	3	**5**	5	**4**	3
myosin-2	CE31619	970					**3**	1	**9**	2		
myosin-2	CE31619	708	**8**	6	**15**	6	**14**	2			**20**	16
myosin-2	CE31619	1932	**15**	1	**11**	5	**7**	4				
myosin-3	CE34936	707	**18**	2	**21**	2	**26**	3	**39**	6	**37**	11
myosin-4	CE06253	259	**9**	7	**8**	5	**6**	4	**8**	7	**8**	3
myosin-4	CE06253	700	**16**	9	**18**	8	**19**	5	**14**	8	**12**	8
NADH-ubiquinone	CE10972	124/129	**4**	0	**2**	7	**1**	1			**6**	8
neprilysin	CE43217	170	**66**	4			**22**	6			**62**	6
NHP2 like protein	CE02283	93	**14**	4	**25**	4	**20**	4	**21**	5	**26**	5
nucleoside diphosphate kinase	CE09650	109	**36**	4	**35**	6	**28**	4	**36**	13	**47**	8

Suppl. Table 4-3 WT continued

Protein	Acc No	Cys	N2 L2		N2 L4		N2 Day 2		N2 Day 8		N2 Day 15	
			ox.	stdv	ox.	stdv	ox.	stdv	ox.	stdv	ox.	stdv
nucleoside diphosphate kinase	CE09650	117	**37**	5	**36**	2	**30**	5	**45**	3	**54**	13
papilin PPN-1	CE17536	477					**98**	3				
paramyosin	CE42754	297	**81**		**59**	15	**56**	10	**60**	14	**56**	7
phosphatase 2A	CE30997	150	**7**	2	**11**	6	**5**	4	**7**	4	**12**	8
phosphatidylglycerol-phosphate synthase	CE09617	14	**96**	1	**99**	3	**95**	4	**89**	6	**93**	5
phosphoenolpyruvate carboxykinase	CE36359	9			**18**	3	**10**	2	**19**	8	**21**	9
phosphoinositide 3-kinase AGE-1	CE23506	710	**54**	4	**56**	4	**50**	12	**72**	12	**72**	5
polyadenylate-binding protein	CE36227	86	**7**	4	**17**	9	**9**	3				
proliferating cell nuclear antigen	CE14512	197	**21**	4	**19**	4	**13**	1	**15**	5	**18**	7
proteasome alpha subunit (PAS-3)	CE30307	74	**26**	6	**14**	2	**13**	1				
protein B0361.2	CE33549	242	**11**	8	**14**	1	**10**	2	**10**	6	**5**	4
protein C08F11.11	CE17388	34			**96**	2	**94**	2	**92**	5	**93**	2
protein C08F11.11	CE17388	81			**99**	1	**99**	0	**96**	6	**99**	1
protein C44B12.5	CE16921	178/189/ 192/193					**77**	1	**91**	2	**87**	4
protein CE32871	CE32871	374	**22**	3	**26**	3	**12**	3				
protein F37C4.5	CE33640	53	**21**	7	**18**	4	**18**	5	**32**	2		
protein F46H5.3	CE33098	226	**20**	0	**18**	3	**11**	4	**3**	2		
protein F46H5.3	CE33098	304	**14**	12	**9**	4	**4**	1	**5**	2	**6**	3
protein F46H5.3	CE33098	275					**12**	7	**13**	4	**21**	2
protein K04G2.6	CE06100	234	**17**	9	**13**	13	**5**	3	**6**	3	**20**	9
protein K07C5.4	CE06114	390	**12**	4	**15**	3	**9**	5	**8**	2	**28**	8
protein T13F3.6	CE39775	83			**71**	9	**77**	4				
protein W07G4.4	CE03794	187					**48**	5			**28**	11
protein Y57G11C.15	CE14954	13	**2**	1	**4**	2	**3**	2	**5**	3	**2**	3
pyruvate carboxylase	CE09072	637	**2**	1	**9**	3	**8**	2	**11**	8	**8**	6
pyruvate carboxylase	CE09072	371	**18**	11	**21**	5	**22**	2	**15**	9	**32**	5
RETR-1	CE41402	478	**14**	3	**16**	1	**8**	1	**20**	4	**14**	5
ribonucleoprotein ROP-1	CE15613	185	**8**	3	**14**	6	**5**	3	**9**	7	**10**	8
RNA helicase CGH-1	CE00839	336					**22**	4	**28**	8	**45**	10
RNA helicase CGH-1	CE00839	49	**15**	15	**11**	3	**11**	3	**9**	8	**8**	3
RNA helicase GLH-1	CE25121	417					**30**	2				
RNA helicase HEL-1	CE32593	161	**16**	9	**12**	2	**11**	5	**18**	8	**20**	7
S-adenosylhomocysteine hydrolase	CE17154	280	**9**	8	**11**	11	**5**	2	**9**	8	**12**	10
serine hydroxymethyltransferase	CE01130	391	**63**	3	**34**	4	**31**	4	**60**	13	**44**	3
small molecules methylase (C28H8.7)	CE01829	224	**2**	3	**2**	2	**12**	1	**23**	4	**26**	6
SMC4	CE03287	740					**62**	1	**35**	13	**57**	4
SURF family member SFT-4	CE06987	39	**13**	15	**8**	4	**6**	3	**8**	3	**15**	12
T-complex protein 1 (subunit beta)	CE16437	445	**6**	2	**9**	4	**4**	1	**12**	8	**13**	3
T-complex protein 1 (subunit theta)	CE44228	35	**13**	11	**8**	3	**3**	1	**8**	4	**10**	3
T-complex protein 1 (subunit zeta)	CE01234	517	**26**	5	**30**	4	**12**	2	**9**	10	**26**	14

Suppl. Table 4-3 WT continued

Protein	Acc No	Cys	N2 L2		N2 L4		N2 Day 2		N2 Day 8		N2 Day 15	
			ox.	stdv	ox.	stdv	ox.	stdv	ox.	stdv	ox.	stdv
T-complex protein 1 (subunit zeta)	CE01234	171	**7**	5			**4**	1				
translation initiation factor 2 (subunit beta)	CE16227	138	**11**	7	**9**	4	**5**	2	**9**	5	**9**	1
translation initiation factor 5A	CE37787	111	**17**	3	**18**	3	**27**	6	**33**	6	**47**	2
transthyretin-like protein TTR-2	CE00475	98/105	**95**	5	**88**	8	**93**	4	**98**	8	**94**	4
transthyretin-like protein TTR-6	CE14325	91/98			**87**	4	**97**	3	**82**	16	**93**	4
troponin T	CE04994	219	**13**	9	**6**	4	**3**	1	**10**	9	**9**	12
tubulin (alpha-2 chain)	CE09692	314	**15**	7	**23**	6	**7**	2	**18**	5		
tubulin (beta-2 chain)	CE00913	239	**10**	5	**13**	1	**5**	2	**21**	9		
tubulin (gamma chain)	CE00224	252	**96**	0	**89**	3	**92**	8	**96**	2	**97**	1
ubiquitin-conjugating enzyme E2	CE03482	85	**6**	0	**8**	7	**9**	1	**8**	3	**11**	11
UNC-87	CE36924	472			**68**	6	**40**	2	**38**	5	**54**	6
UNC-89	CE37702	4588			**12**	1	**4**	3	**2**	0	**3**	1
vacuolar ATP synthase (subunit A)	CE22210	521	**7**	1	**14**	3	**10**	2	**15**	14	**7**	0
vacuolar ATP synthase (subunit A)	CE22210	218	**22**	6	**28**	5	**10**	2	**11**	5	**11**	4
vacuolar ATP synthase (subunit A)	CE22210	266	**31**	4			**36**	9	**24**	2		
vacuolar ATP synthase (subunit B)	CE04424	94	**6**	2	**10**	3	**5**	2	**8**	3	**9**	3
vacuolar ATP synthase (subunit B)	CE04424	33	**7**	6	**10**	6	**1**	1			**12**	8
vacuolar proton pump (subunit G)	CE10604	104	**6**	3	**12**	8	**3**	3	**5**	10	**12**	8
vigilin	CE23530	1063	**16**	8	**11**	4	**7**	4	**15**	6		
vigilin	CE23530	666	**23**	12	**24**	8	**17**	3				
vinculin	CE31398	336	**16**	7	**20**	7	**11**	7				
vitellogenin-2	CE41109	627			**9**	8	**10**	5	**11**	8	**18**	4
vitellogenin-2	CE41109	1489/ 1498			**65**	18	**63**	10	**63**	9	**71**	2
vitellogenin-3	CE20900	626					**10**	2	**14**	1	**76**	9
vitellogenin-4	CE26817	206			**85**	4	**63**	5	**75**	4	**77**	8
vitellogenin-4	CE26817	1474			**19**	1	**5**	1	**4**	2	**2**	2
vitellogenin-6	CE28594	218			**87**	7	**71**	2	**71**	14	**75**	6
vitellogenin-6	CE28594	384			**8**	1	**4**	2	**5**	2	**7**	6
vitellogenin-6	CE28594	468			**89**	5	**65**	4	**74**	12	**80**	8
vitellogenin-6	CE28594	655			**19**	3	**13**	4	**18**	8	**20**	9
vitellogenin-6	CE28594	1364			**8**	7	**22**	3	**16**	8	**17**	6
vitellogenin-6	CE28594	1417					**22**	8	**27**	1	**25**	8
vitellogenin-6	CE28594	1514					**27**	4				
vitellogenin-6	CE28594	1569			**88**	5	**69**	15	**76**	4	**75**	9
vitellogenin-6	CE28594	1479/ 1482					**90**	8				
vitellogenin-6	CE28594	1645					**16**	6	**13**	7	**10**	11
WDR-23	CE23620	73			**3**	1	**3**	3	**5**	3	**4**	2
ZNF9	CE21045	37/40	**25**	1					**17**	5		

Suppl. Table 4-3 Oxidation status of *C. elegans* proteins during lifespan of *daf-2* deletion worms

Protein	Acc No	Cys	*daf-2* L2		*daf-2* L4		*daf-2* Day 2		*daf-2* Day 8		*daf-2* Day 15	
			ox.	stdv	ox.	stdv	ox.	stdv	ox.	stdv	ox.	stdv
2-oxoglutarate dehydrogenase	CE28486	947	**17**	1	**13**	10	**21**	8				
40S ribosomal protein S12	CE26896	114	**15**	1	**13**	6	**18**	5			**31**	6
40S ribosomal protein S14	CE00821	140	**17**	11	**13**	5	**11**	6	**19**	9	**14**	2
40S ribosomal protein S17	CE26948	35	**5**	4	**2**	1	**8**	4			**8**	4
40S ribosomal protein S19	CE13265	99	**5**	2	**4**	2	**5**	2	**5**	3	**5**	2
40S ribosomal protein S21	CE30779	57	**34**	7	**29**	6	**34**	14	**36**	9	**39**	8
40S ribosomal protein S23	CE05747	90	**25**	6	**26**	4	**26**	19	**13**	9	**39**	4
40S ribosomal protein S25	CE04691	95	**7**	1	**7**	3	**8**	2	**7**	6	**13**	4
40S ribosomal protein S28	CE21842	22	**13**	4	**9**	1	**15**	6	**18**	8	**12**	7
40S ribosomal protein S3	CE01810	99/104			**15**	16	**9**	8				
40S ribosomal protein S3a	CE00664	199	**12**	3	**12**	7	**15**	6	**17**	1	**14**	3
40S ribosomal protein S5	CE06360	161	**5**	3	**6**	1	**9**	8	**9**	4	**10**	11
40S ribosomal protein S5	CE06360	178	**5**	3	**5**	4	**7**	4	**6**	3	**4**	5
40S ribosomal protein S6	CE24592	83	**16**	8	**19**	9	**6**	6			**15**	14
40S ribosomal protein SA	CE00854	107	**8**	4	**4**	4	**2**	2			**10**	3
40S ribosomal protein SA	CE00854	163	**13**	6	**10**	5	**15**	8	**19**	7	**15**	2
60S ribosomal protein L11	CE07033	28/32	**12**	2							**18**	5
60S ribosomal protein L12	CE17986	141	**11**	5	**1**	0	**20**	1				
60S ribosomal protein L22	CE04102	27	**9**	3	**9**	4	**10**	3	**22**	6	**15**	9
60S ribosomal protein L4	CE07669	216	**11**	3	**8**	4	**10**	8	**10**	7	**7**	3
aconitase	CE32436	29	**12**	8	**5**	1	**11**	9	**9**	2	**10**	1
aconitase	CE32436	288										
actin-2	CE13150	258	**20**	6	**15**	6	**27**	10	**20**	5	**23**	8
adenylate kinase	CE29198	53			**56**	12						
alcohol dehydrogenase	CE12212	114	**33**	1	**36**	3	**49**	15				
aldehyde dehydrogenase	CE39486	93			**12**	1					**16**	5
ANC-1	CE33588	1632			**88**	6	**80**	4	**75**	5	**91**	3
annexin	CE01431	112	**5**	1	**5**	5	**4**	1	**8**	5	**9**	7
aspartyl-tRNA synthetase	CE00015	233	**37**	3	**18**	4	**12**	4			**11**	7
ATP synthase (subunit alpha)	CE36263	202	**9**	3	**9**	7	**9**	4	**9**	4	**13**	10
ATP synthase (subunit beta)	CE29950	119	**26**	2	**18**	6	**21**	7			**15**	2
attractin	CE41899	263/265	**93**	6	**99**	1			**85**	6	**96**	2
calponin	CE09767	22	**6**	1	**8**	8	**6**	0	**6**	6		
CDC-48.2	CE05402	696	**32**	7	**27**	5	**43**	17	**34**	8	**33**	3
CDC-48.2	CE05402	577	**10**	3	**9**	2	**14**	9	**9**	3	**11**	4
chitinase	CE32592	738/747	**97**	1								
citrate synthase	CE00513	434	**8**	2			**15**	11	**5**	3	**4**	3
clathrin (heavy chain)	CE00480	353	**6**	2	**2**	1	**3**	3	**7**	7	**5**	1
COPI coatomer (subunit beta)	CE18673	688	**7**	6	**8**	4	**17**	7	**11**	13	**14**	4
COPI coatomer (subunit gamma)	CE06451	806	**9**	4	**10**	4	**12**	1	**17**	6	**12**	2
COPII coatomer (subunit SAR-1)	CE07622	174	**17**	11	**22**	6	**13**	8	**25**	3	**24**	5
cyclin (ZK353.1)	CE34452	92	**98**	2	**88**	3	**93**	12				
degenerin (ASIC-1)	CE40185	659/661							**94**	7	**95**	4
degenerin (DEL-1)	CE05547	180/182	**8**	2	**12**	6	**13**	7			**34**	2
DHHC-type Zn-finger protein	CE42532	134/137/ 138/139			**10**	6	**5**	9	**6**	2	**17**	6
DIM-1	CE04038	234	**13**	7	**14**	6	**17**	6	**27**	3	**28**	8
DNA polymerase (subunit delta)	CE09308	1043	**82**	6	**77**	4	**89**	3	**71**	5	**44**	7

Suppl. Table 4-3 *daf-2* continued

Protein	Acc No	Cys	*daf-2* L2		*daf-2* L4		*daf-2* Day 2		*daf-2* Day 8		*daf-2* Day 15	
			ox.	stdv	ox.	stdv	ox.	stdv	ox.	stdv	ox.	stdv
DNA repair protein RAD-50	CE21149	1174	**18**	5	**9**	3	**18**	10	**18**	2	**22**	6
dynamin GTPase	CE07832	430	**8**	1	**5**	3	**14**	13			**2**	8
dynein light chain 1	CE00788	56					**12**	0			**22**	9
egg-laying defective protein 27	CE31287	227	**1**	1	**1**	0	**1**	0	**3**	2	**9**	8
elongation factor 1-alpha	CE01270	152	**12**	4	**15**	11	**14**	5	**11**	8	**12**	6
elongation factor 1-alpha	CE01270	411	**10**	3	**7**	3	**10**	6	**10**	3	**10**	2
elongation factor 2	CE15900	598	**12**	9	**6**	8	**19**	2	**15**	5		
elongation factor 2	CE15900	745	**8**	4	**6**	3	**7**	4	**8**	4	**8**	4
endonuclease III	CE44645	48	**11**	10	**4**	0	**12**	7	**7**	1	**3**	1
forkhead transcription factor	CE02683	265	**99**	4	**91**	12	**93**	5				
fructose-bisphosphate	CE16341	178/198	**17**	3	**8**	6	**16**	7	**16**	10	**15**	22
glutamyl-tRNA synthetase	CE06580	377	**19**	4	**16**	1	**32**	15	**21**	3	**19**	6
glutathione S-transferase	CE00302	52	**6**	4	**2**	1	**13**	13	**4**	3	**8**	0
glycine decarboxylase	CE06652	232	**3**	4	**3**	4	**6**	4	**7**	3	**11**	10
glycosyl transferase	CE31185	97	**20**	5	**17**	8			**29**	3	**27**	7
GTP-binding protein (TAG-210)	CE14708	54			**6**	9	**10**	2			**17**	8
heat shock protein 60	CE42184	106	**6**	3	**10**	6	**7**	4	**9**	3	**11**	10
heat shock protein 70	CE09682	307	**3**	1	**2**	1	**2**	1	**3**	1	**3**	2
heat shock protein 70	CE09682	243	**7**	5	**7**	4	**9**	3	**8**	4	**8**	1
heat shock protein 70	CE08631	587										
heat shock protein Hsp-12.2	CE00072	61	**12**	3	**6**	4	**15**	7			**10**	4
helicase (C28H8.3)	CE29195	669	**14**	4	**11**	4	**15**	7	**15**	1	**13**	2
heparan sulfate proteoglycan	CE37074	1245	**3**	0	**16**	6	**7**	0			**10**	8
HIS-40	K03A1.1	63			**96**	2	**97**	6	**91**	4	**91**	0
integrin (subunit beta)	CE01102	445	**80**	4	**84**	4	**85**	2	**92**	3	**85**	5
intermediate filament B	CE02618	367	**9**	8	**3**	1			**7**	1		
isocitrate dehydrogenase (subunit alpha)	CE34018	208	**7**	5	**11**	8	**13**	11	**7**	3		
isocitrate dehydrogenase (subunit alpha)	CE34018	343/351										
isocitrate lyase/malate synthase	CE32565	218	**12**	4	**9**	3	**13**	10	**14**	4	**15**	6
isocitrate lyase/malate synthase	CE32565	271	**9**	5	**12**	3	**15**	8	**25**	10	**19**	9
LIN-28	CE24879	168/171/181	**14**	4	**12**	3	**10**	2	**12**	5	**16**	6
lysozyme	CE06003	80	**91**	5	**86**	11	**89**	2				
methylcrotonyl-CoA	CE00136	212	**12**	6	**21**	5	**27**	13	**16**	7	**22**	2
mitochondrial ADP/ATP carrier protein ANT-1.4	CE12898	146	**7**	4	**10**	8	**9**	6	**11**	5	**8**	3
MUA-3	CE37256	2258	**4**	3	**14**	2	**23**	7			**5**	3
myosin-2	CE31619	970	**54**	6	**12**	5						
myosin-2	CE31619	708	**11**	5	**9**	3	**11**	6			**9**	4
myosin-2	CE31619	1932	**8**	5	**15**	5	**9**	6				
myosin-3	CE34936	707	**21**	6	**24**	4	**25**	7			**29**	6
myosin-4	CE06253	259	**10**	3	**6**	3	**6**	6	**8**	4	**5**	4
myosin-4	CE06253	700	**15**	11	**13**	7	**12**	9	**11**	5	**11**	4
NADH-ubiquinone	CE10972	124/129	**8**	4			**17**	2				
neprilysin	CE43217	170	**72**	8	**66**	7	**10**	1			**43**	9
NHP2 like protein	CE02283	93	**24**	7	**16**	1	**29**	9	**26**	14	**20**	7
nucleoside diphosphate kinase	CE09650	109	**34**	5	**29**	3	**37**	8	**40**	3	**47**	11

Suppl. Table 4-3 *daf-2* continued

Protein	Acc No	Cys	*daf-2* L2		*daf-2* L4		*daf-2* Day 2		*daf-2* Day 8		*daf-2* Day 15	
			ox.	stdv	ox.	stdv	ox.	stdv	ox.	stdv	ox.	stdv
nucleoside diphosphate kinase	CE09650	117	**30**	9	**29**	4	**23**	1	**45**	5	**45**	14
papilin PPN-1	CE17536	477	**99**	0			**100**	0	**98**	2	**87**	11
paramyosin	CE42754	297	**99**	2	**75**	13	**62**	19	**55**	9	**53**	13
phosphatase 2A	CE30997	150	**8**	2	**10**	1	**12**	9	**7**	5	**7**	6
phosphatidylglycerol-phosphate synthase	CE09617	14	**97**	4	**98**	1	**98**	1	**93**	5	**93**	6
phosphoenolpyruvate carboxykinase	CE36359	9	**20**	2	**11**	3	**15**	4	**23**	0	**23**	3
phosphoinositide 3-kinase AGE-1	CE23506	710	**64**	9	**60**	2	**59**	16	**81**	10	**74**	14
polyadenylate-binding protein	CE36227	86	**12**	1	**14**	3	**12**	6				
proliferating cell nuclear antigen	CE14512	197	**25**	14			**13**	2	**15**	3	**20**	6
proteasome alpha subunit (PAS-3)	CE30307	74										
protein B0361.2	CE33549	242	**11**	1	**9**	1	**14**	9	**12**	8	**8**	7
protein C08F11.11	CE17388	34					**93**	2	**84**	5	**93**	1
protein C08F11.11	CE17388	81			**98**	2	**99**	0	**92**	11	**97**	2
protein C44B12.5	CE16921	178/189/ 192/193									**82**	8
protein CE32871	CE32871	374	**17**	2	**27**	4	**38**	9				
protein F37C4.5	CE33640	53	**29**	9	**17**	4	**22**	7				
protein F46H5.3	CE33098	226	**16**	8	**18**	5	**13**	5	**9**	0	**14**	5
protein F46H5.3	CE33098	304	**8**	4	**5**	1	**5**	2	**9**	6	**6**	2
protein F46H5.3	CE33098	275			**23**	2	**20**	7	**11**	4	**11**	2
protein K04G2.6	CE06100	234			**11**	2	**15**	10	**12**	1	**15**	2
protein K07C5.4	CE06114	390	**14**	3	**13**	3	**15**	8	**20**	10	**13**	6
protein T13F3.6	CE39775	83										
protein W07G4.4	CE03794	187									**7**	1
protein Y57G11C.15	CE14954	13	**2**	1	**3**	4	**3**	4	**12**	11	**1**	1
pyruvate carboxylase	CE09072	637	**8**	1	**8**	4	**9**	6	**10**	1	**7**	3
pyruvate carboxylase	CE09072	371	**19**	5	**25**	10	**21**	7	**14**	8	**35**	10
RETR-1	CE41402	478	**14**	9	**5**	3	**12**	7	**6**	1	**12**	1
ribonucleoprotein ROP-1	CE15613	185	**7**	4	**6**	2	**8**	7	**9**	3	**8**	3
RNA helicase CGH-1	CE00839	336			**19**	13	**27**	6	**33**	2	**41**	2
RNA helicase CGH-1	CE00839	49			**17**	5	**9**	7	**8**	5	**8**	6
RNA helicase GLH-1	CE25121	417					**43**	10			**44**	2
RNA helicase HEL-1	CE32593	161	**17**	9	**14**	5	**14**	9	**14**	5	**24**	7
S-adenosylhomocysteine hydrolase	CE17154	280	**7**	5	**13**	8	**8**	5	**9**	8	**14**	9
serine hydroxymethyltransferase	CE01130	391	**69**	11	**37**	14			**42**	12	**43**	2
small molecules methylase (C28H8.7)	CE01829	224	**3**	2	**4**	3	**9**	3	**12**	4	**7**	7
SMC4	CE03287	740	**24**	3	**37**	2	**35**	11	**39**	2	**41**	13
SURF family member SFT-4	CE06987	39	**9**	7	**5**	2	**9**	5	**9**	2	**13**	11
T-complex protein 1 (subunit beta)	CE16437	445	**9**	3	**9**	3	**10**	2	**11**	5	**9**	3
T-complex protein 1 (subunit theta)	CE44228	35	**6**	1	**5**	2	**7**	3	**6**	8	**13**	3
T-complex protein 1 (subunit zeta)	CE01234	517	**22**	2	**12**	0	**11**	6			**7**	6

Suppl. Table 4-3 *daf-2* continued

Protein	Acc No	Cys	*daf-2* L2		*daf-2* L4		*daf-2* Day 2		*daf-2* Day 8		*daf-2* Day 15	
			ox.	stdv	ox.	stdv	ox.	stdv	ox.	stdv	ox.	stdv
T-complex protein 1 (subunit zeta)	CE01234	171			**9**	4						
translation initiation factor 2 (subunit beta)	CE16227	138	**9**	2	**6**	1	**7**	6	**14**	8	**7**	1
translation initiation factor 5A	CE37787	111	**14**	2	**20**	8	**37**	4	**21**	6		
transthyretin-like protein TTR-2	CE00475	98/105	**98**	6	**94**	3	**91**	4	**90**	2	**92**	1
transthyretin-like protein TTR-6	CE14325	91/98	**87**	3	**95**	5	**94**	0	**99**	3	**91**	3
troponin T	CE04994	219	**3**	0	**7**	5	**5**	3	**7**	4	**7**	3
tubulin (alpha-2 chain)	CE09692	314			**24**	4						
tubulin (beta-2 chain)	CE00913	239										
tubulin (gamma chain)	CE00224	252	**98**	1			**97**	3			**93**	5
ubiquitin-conjugating enzyme E2	CE03482	85	**6**	4	**4**	1	**10**	1				
UNC-87	CE36924	472	**57**	6	**54**	2	**62**	1	**33**	7	**34**	1
UNC-89	CE37702	4588	**9**	3	**7**	4	**2**	2	**6**	7	**6**	9
vacuolar ATP synthase (subunit A)	CE22210	521	**13**	7	**11**	5	**14**	6	**15**	5	**18**	2
vacuolar ATP synthase (subunit A)	CE22210	218	**22**	10	**13**	3	**8**	6	**17**	6	**21**	2
vacuolar ATP synthase (subunit A)	CE22210	266	**45**	11	**25**	9	**40**	14	**30**	2		
vacuolar ATP synthase (subunit B)	CE04424	94	**7**	1	**6**	2	**9**	1	**11**	3	**8**	2
vacuolar ATP synthase (subunit B)	CE04424	33			**4**	3	**11**	14	**8**	6	**10**	7
vacuolar proton pump (subunit G)	CE10604	104	**10**	5	**4**	4	**4**	3	**9**	7	**14**	8
vigilin	CE23530	1063	**6**	7	**5**	10	**12**	1	**9**	13		
vigilin	CE23530	666	**19**	2	**16**	2	**24**	5	**26**	8		
vinculin	CE31398	336	**14**	5	**12**	2	**30**	6			**16**	8
vitellogenin-2	CE41109	627			**6**	6	**13**	12	**9**	10	**14**	3
vitellogenin-2	CE41109	1489/ 1498			**50**	5	**60**	10	**67**	5	**65**	3
vitellogenin-3	CE20900	626					**14**	3	**16**	9	**75**	6
vitellogenin-4	CE26817	206			**75**	5	**73**	8	**71**	3	**74**	6
vitellogenin-4	CE26817	1474			**13**	5	**5**	2	**11**	8	**1**	1
vitellogenin-6	CE28594	218			**87**	4	**75**	3	**70**	4	**73**	5
vitellogenin-6	CE28594	384			**11**	2	**6**	3	**7**	5	**7**	3
vitellogenin-6	CE28594	468			**67**	11	**70**	17	**81**	10	**78**	8
vitellogenin-6	CE28594	655			**20**	4	**16**	7	**16**	9	**18**	1
vitellogenin-6	CE28594	1364			**6**	5	**21**	10	**18**	3	**18**	5
vitellogenin-6	CE28594	1417					**57**	10	**19**	10	**33**	11
vitellogenin-6	CE28594	1514										
vitellogenin-6	CE28594	1569			**84**	11	**75**	5	**77**	5	**69**	9
vitellogenin-6	CE28594	1479/ 1482					**89**	3			**83**	1
vitellogenin-6	CE28594	1645	**10**	3			**7**	2	**13**	2	**29**	9
WDR-23	CE23620	73	**2**	3	**6**	4	**5**	4	**4**	2	**4**	3
ZNF9	CE21045	37/40	**38**	3							**16**	12

Suppl. Table 4-3 Oxidation status of *C. elegans* proteins during lifespan of *daf-16* deletion worms

Protein	Acc No	Cys	*daf-16* L2		*daf-16* L4		*daf-16* Day 2		*daf-16* Day 8		*daf-16* Day 15	
			ox.	stdv	ox.	stdv	ox.	stdv	ox.	stdv	ox.	stdv
2-oxoglutarate dehydrogenase	CE28486	947	**20**	9	**20**	5	**11**	3				
40S ribosomal protein S12	CE26896	114	**21**	8	**23**	8			**32**	6	**32**	12
40S ribosomal protein S14	CE00821	140	**13**	2	**25**	8	**12**	4	**13**	1	**16**	4
40S ribosomal protein S17	CE26948	35	**7**	1	**13**	3	**9**	4	**3**	1	**7**	1
40S ribosomal protein S19	CE13265	99	**6**	2	**10**	4	**5**	1	**4**	2	**4**	1
40S ribosomal protein S21	CE30779	57	**36**	11	**49**	12	**28**	11	**36**	5	**40**	7
40S ribosomal protein S23	CE05747	90	**29**	9	**38**	2	**18**	10	**25**	0	**18**	2
40S ribosomal protein S25	CE04691	95	**6**	1	**9**	2	**10**	3	**12**	10	**9**	3
40S ribosomal protein S28	CE21842	22	**13**	2	**19**	5	**9**	3	**12**	7	**18**	4
40S ribosomal protein S3	CE01810	99/104	**14**	3	**6**	6	**9**	6				
40S ribosomal protein S3a	CE00664	199	**12**	4	**19**	2	**20**	9	**13**	8	**16**	4
40S ribosomal protein S5	CE06360	161	**4**	4	**7**	5	**11**	9	**4**	3	**6**	2
40S ribosomal protein S5	CE06360	178	**5**	3	**8**	6	**8**	9	**5**	6	**3**	1
40S ribosomal protein S6	CE24592	83	**4**	1	**13**	12	**6**	3			**2**	0
40S ribosomal protein SA	CE00854	107	**12**	7	**20**	9	**24**	10	**17**	10	**5**	2
40S ribosomal protein SA	CE00854	163	**14**	4	**20**	5	**13**	6	**15**	4	**16**	6
60S ribosomal protein L11	CE07033	28/32	**10**	1	**20**	1			**16**	8	**31**	15
60S ribosomal protein L12	CE17986	141	**9**	4	**16**	1					**18**	9
60S ribosomal protein L22	CE04102	27	**8**	2	**11**	4	**5**	6	**11**	9	**12**	9
60S ribosomal protein L4	CE07669	216	**10**	4	**11**	6	**11**	10	**6**	5	**11**	6
aconitase	CE32436	29	**13**	6	**13**	2	**12**	7	**5**	0	**9**	3
aconitase	CE32436	288					**27**	7	**26**	7	**30**	8
actin-2	CE13150	258	**23**	4	**25**	8	**16**	6	**17**	2	**19**	4
adenylate kinase	CE29198	53	**43**	3	**52**	11	**47**	2	**67**	4	**84**	9
alcohol dehydrogenase	CE12212	114			**46**	1						
aldehyde dehydrogenase	CE39486	93										
ANC-1	CE33588	1632					**88**	6	**66**	11	**75**	11
annexin	CE01431	112	**3**	1	**8**	2	**3**	2	**3**	0	**3**	0
aspartyl-tRNA synthetase	CE00015	233			**10**	7	**20**	14	**7**	2	**32**	10
ATP synthase (subunit alpha)	CE36263	202	**12**	9	**17**	10	**6**	3	**5**	2	**7**	3
ATP synthase (subunit beta)	CE29950	119	**19**	6	**33**	6	**24**	7	**28**	11	**19**	11
attractin	CE41899	263/265	**92**	6	**97**	2	**97**	4	**98**	0	**94**	6
calponin	CE09767	22	**4**	4	**9**	6	**4**	4	**5**	4	**4**	2
CDC-48.2	CE05402	696	**33**	9	**48**	6	**28**	9	**31**	11	**31**	10
CDC-48.2	CE05402	577	**10**	5	**16**	2	**9**	3	**8**	0	**11**	3
chitinase	CE32592	738/747					**84**	9	**82**	11	**83**	6
citrate synthase	CE00513	434			**5**	6						
clathrin (heavy chain)	CE00480	353	**3**	4	**5**	5	**3**	3	**3**	2	**4**	2
COPI coatomer (subunit beta)	CE18673	688	**15**	7	**7**	8	**14**	3	**9**	1	**6**	5
COPI coatomer (subunit gamma)	CE06451	806	**14**	5	**13**	3	**16**	4	**7**	3	**12**	6
COPII coatomer (subunit SAR-1)	CE07622	174	**22**	3	**30**	11	**16**	5	**15**	3	**22**	11
cyclin (ZK353.1)	CE34452	92	**92**	2	**97**	1	**88**	1	**92**	1	**87**	8
degenerin (ASIC-1)	CE40185	659/661	**94**	1	**94**	4	**100**	1	**94**	9	**93**	2
degenerin (DEL-1)	CE05547	180/182	**13**	2	**19**	3	**21**	4	**15**	2	**17**	5
DHHC-type Zn-finger protein	CE42532	134/137/ 138/139			**5**	6	**2**	5	**2**	1	**3**	4
DIM-1	CE04038	234	**18**	9	**18**	5	**12**	3	**12**	3	**16**	10
DNA polymerase (subunit delta)	CE09308	1043	**75**	9	**79**	6	**80**	9	**74**	4	**82**	7

Suppl. Table 4-3 *daf-16* continued

Protein	Acc No	Cys	*daf-16* L2		*daf-16* L4		*daf-16* Day 2		*daf-16* Day 8		*daf-16* Day 15	
			ox.	stdv	ox.	stdv	ox.	stdv	ox.	stdv	ox.	stdv
DNA repair protein RAD-50	CE21149	1174	**14**	7	**24**	3	**17**	7	**13**	4	**17**	3
dynamin GTPase	CE07832	430	**5**	2	**22**	1	**5**	8	**4**	4	**16**	5
dynein light chain 1	CE00788	56					**24**	4			**27**	7
egg-laying defective protein 27	CE31287	227	**3**	2	**5**	3	**13**	19	**5**	4	**18**	13
elongation factor 1-alpha	CE01270	152	**14**	7	**13**	7	**14**	7	**10**	2	**11**	5
elongation factor 1-alpha	CE01270	411	**8**	3	**13**	5	**6**	3	**7**	2	**11**	2
elongation factor 2	CE15900	598	**23**	2	**30**	9	**16**	8	**27**	10	**34**	13
elongation factor 2	CE15900	745	**6**	3	**8**	5	**5**	3	**5**	2	**8**	2
endonuclease III	CE44645	48	**12**	8	**14**	11	**8**	6	**12**	9	**9**	8
forkhead transcription factor	CE02683	265	**93**	6	**96**	2	**95**	5	**93**	10	**95**	5
fructose-bisphosphate	CE16341	178/198	**5**	4	**3**	9	**16**	3	**8**	3	**22**	22
glutamyl-tRNA synthetase	CE06580	377	**16**	7	**29**	2	**19**	1	**25**	2	**25**	3
glutathione S-transferase	CE00302	52	**7**	3	**3**	1			**5**	1	**1**	2
glycine decarboxylase	CE06652	232	**3**	5	**10**	7	**6**	3	**1**	1	**4**	4
glycosyl transferase	CE31185	97	**24**	3	**30**	9	**17**	10	**21**	2	**13**	1
GTP-binding protein (TAG-210)	CE14708	54										
heat shock protein 60	CE42184	106	**8**	2	**8**	5	**9**	4	**7**	3	**9**	2
heat shock protein 70	CE09682	307	**3**	1	**3**	1	**2**	1	**2**	1	**3**	1
heat shock protein 70	CE09682	243	**11**	9	**18**	4	**8**	4	**10**	6	**3**	2
heat shock protein 70	CE08631	587	**15**	7	**11**	6			**28**	1	**22**	4
heat shock protein Hsp-12.2	CE00072	61	**13**	4	**15**	11	**9**	5	**9**	2	**7**	3
helicase (C28H8.3)	CE29195	669	**11**	3	**23**	2	**9**	6	**10**	0	**16**	6
heparan sulfate proteoglycan	CE37074	1245	**27**	8	**24**	4	**27**	6	**19**	1	**18**	4
HIS-40	K03A1.1	63	**95**	1	**97**	4	**94**	1	**95**	0	**95**	5
integrin (subunit beta)	CE01102	445	**87**	5	**90**	1			**96**	7		
intermediate filament B	CE02618	367	**3**	1	**7**	5	**4**	2	**7**	7	**5**	3
isocitrate dehydrogenase (subunit alpha)	CE34018	208	**14**	8	**13**	5	**9**	5	**10**	5	**7**	5
isocitrate dehydrogenase (subunit alpha)	CE34018	343/351									**9**	2
isocitrate lyase/malate synthase	CE32565	218	**15**	6	**20**	12	**18**	12	**13**	6	**26**	10
isocitrate lyase/malate synthase	CE32565	271	**19**	8	**19**	6	**15**	2	**21**	9	**12**	2
LIN-28	CE24879	168/171/181	**10**	3	**15**	4	**11**	5	**9**	3	**33**	6
lysozyme	CE06003	80	**86**	11	**87**	13	**87**	1				
methylcrotonyl-CoA	CE00136	212	**22**	10	**23**	10	**21**	3	**17**	4	**22**	10
mitochondrial ADP/ATP carrier protein ANT-1.4	CE12898	146	**8**	3	**6**	2	**10**	8	**8**	4	**7**	1
MUA-3	CE37256	2258	**6**	3	**24**	5	**14**	13	**16**	11	**10**	4
myosin-2	CE31619	970			**16**	0	**7**	11			**34**	0
myosin-2	CE31619	708	**13**	1	**16**	8	**14**	7	**18**	5	**17**	8
myosin-2	CE31619	1932	**8**	1	**12**	4	**13**	3	**10**	5	**22**	7
myosin-3	CE34936	707	**20**	12	**27**	9	**23**	8	**36**	8	**16**	5
myosin-4	CE06253	259	**6**	5	**8**	4	**7**	4	**14**	3	**9**	8
myosin-4	CE06253	700	**18**	11	**23**	6	**16**	3	**22**	13	**14**	5
NADH-ubiquinone	CE10972	124/129	**4**	3	**2**	0	**4**	2	**4**	6	**5**	7
neprilysin	CE43217	170	**58**	11	**35**	11					**63**	16
NHP2 like protein	CE02283	93	**20**	11	**23**	2	**19**	11	**14**	5	**15**	5
nucleoside diphosphate kinase	CE09650	109	**35**	4	**39**	4	**25**	10	**32**	4	**42**	14

Suppl. Table 4-3 *daf-16* continued

Protein	Acc No	Cys	*daf-16* L2		*daf-16* L4		*daf-16* Day 2		*daf-16* Day 8		*daf-16* Day 15	
			ox.	stdv	ox.	stdv	ox.	stdv	ox.	stdv	ox.	stdv
nucleoside diphosphate kinase	CE09650	117	**31**	9	**34**	11	**27**	7	**33**	3	**34**	11
papilin PPN-1	CE17536	477							**99**	2	**97**	1
paramyosin	CE42754	297	**83**	16	**64**	19	**71**	6	**59**	11	**71**	16
phosphatase 2A	CE30997	150	**10**	5	**11**	8	**8**	1	**6**	3	**7**	2
phosphatidylglycerol-phosphate synthase	CE09617	14	**94**	2	**94**	4	**98**	1	**98**	3	**95**	3
phosphoenolpyruvate carboxykinase	CE36359	9	**9**	3	**22**	1	**11**	4	**24**	13	**8**	1
phosphoinositide 3-kinase AGE-1	CE23506	710	**63**	6	**54**	17			**66**	10	**74**	5
polyadenylate-binding protein	CE36227	86	**13**	4	**9**	2	**5**	2	**9**	2	**13**	3
proliferating cell nuclear antigen	CE14512	197	**22**	3			**12**	6	**9**	2	**21**	6
proteasome alpha subunit (PAS-3)	CE30307	74	**21**	3	**23**	1	**17**	8	**18**	8	**8**	0
protein B0361.2	CE33549	242	**8**	1	**6**	5	**13**	7	**8**	5	**10**	5
protein C08F11.11	CE17388	34			**95**	8			**90**	3	**93**	3
protein C08F11.11	CE17388	81			**98**	1	**93**	10	**99**	0	**99**	1
protein C44B12.5	CE16921	178/189/ 192/193					**90**	11	**78**	7	**94**	9
protein CE32871	CE32871	374	**23**	4	**33**	8	**22**	6	**21**	4	**16**	8
protein F37C4.5	CE33640	53	**40**	7	**33**	4	**16**	6	**23**	10	**25**	5
protein F46H5.3	CE33098	226	**11**	1	**15**	4	**18**	11	**11**	4	**7**	5
protein F46H5.3	CE33098	304	**6**	3	**7**	2	**11**	11	**5**	3	**6**	2
protein F46H5.3	CE33098	275							**10**	1	**8**	3
protein K04G2.6	CE06100	234	**13**	4	**5**	3	**5**	0	**2**	1	**6**	1
protein K07C5.4	CE06114	390	**14**	5	**16**	3	**10**	6	**12**	6	**9**	1
protein T13F3.6	CE39775	83										
protein W07G4.4	CE03794	187					**31**	7	**38**	15	**20**	17
protein Y57G11C.15	CE14954	13	**3**	1	**5**	3	**2**	2	**3**	3	**6**	4
pyruvate carboxylase	CE09072	637	**6**	4	**22**	7	**13**	5	**5**	1	**6**	2
pyruvate carboxylase	CE09072	371	**28**	6	**27**	8	**25**	10	**24**	8	**14**	10
RETR-1	CE41402	478	**23**	3	**15**	4	**10**	4	**5**	5	**10**	0
ribonucleoprotein ROP-1	CE15613	185	**8**	3	**11**	4	**7**	3	**5**	2	**13**	5
RNA helicase CGH-1	CE00839	336			**22**	13	**22**	8	**27**	3	**17**	6
RNA helicase CGH-1	CE00839	49	**9**	10	**9**	5	**11**	13	**12**	7	**4**	2
RNA helicase GLH-1	CE25121	417										
RNA helicase HEL-1	CE32593	161	**16**	4	**16**	8	**13**	2	**18**	2	**15**	5
S-adenosylhomocysteine hydrolase	CE17154	280	**18**	12	**15**	12	**7**	5	**8**	6	**17**	10
serine hydroxymethyltransferase	CE01130	391	**57**	13	**67**	13	**48**	14	**48**	15	**47**	6
small molecules methylase (C28H8.7)	CE01829	224	**4**	4	**5**	4	**7**	4	**16**	1	**1**	1
SMC4	CE03287	740			**49**	13	**50**	11	**34**	6	**55**	10
SURF family member SFT-4	CE06987	39	**13**	11	**11**	2	**11**	2	**10**	9	**4**	5
T-complex protein 1 (subunit beta)	CE16437	445	**13**	4	**8**	2	**5**	4	**10**	1	**7**	4
T-complex protein 1 (subunit theta)	CE44228	35	**7**	1	**7**	5	**5**	3	**6**	7	**10**	5
T-complex protein 1 (subunit zeta)	CE01234	517	**17**	13	**24**	7			**10**	7	**17**	5

Suppl. Table 4-3 *daf-16* continued

Protein	Acc No	Cys	*daf-16* L2		*daf-16* L4		*daf-16* Day 2		*daf-16* Day 8		*daf-16* Day 15	
			ox.	stdv	ox.	stdv	ox.	stdv	ox.	stdv	ox.	stdv
T-complex protein 1 (subunit zeta)	CE01234	171	**6**	6	**8**	0	**9**	10	**5**	4	**6**	0
translation initiation factor 2 (subunit beta)	CE16227	138	**8**	1	**9**	3	**9**	2	**8**	3	**7**	7
translation initiation factor 5A	CE37787	111	**18**	3	**28**	11	**14**	2	**22**	9	**26**	2
transthyretin-like protein TTR-2	CE00475	98/105	**91**	4	**92**	8	**92**	2	**96**	4	**97**	2
transthyretin-like protein TTR-6	CE14325	91/98	**89**	7	**87**	6	**89**	10	**94**	5	**95**	2
troponin T	CE04994	219	**11**	15	**7**	8	**4**	3	**13**	6	**16**	9
tubulin (alpha-2 chain)	CE09692	314	**26**	10	**29**	12			**16**	3	**12**	1
tubulin (beta-2 chain)	CE00913	239	**15**	1	**16**	9			**11**	3	**5**	7
tubulin (gamma chain)	CE00224	252	**95**	9	**95**	5	**96**	2	**97**	3	**98**	2
ubiquitin-conjugating enzyme E2	CE03482	85	**6**	5	**8**	6	**8**	2	**9**	5	**5**	1
UNC-87	CE36924	472	**66**	1	**65**	14			**52**	6	**45**	11
UNC-89	CE37702	4588			**1**	1	**1**	1	**8**	7	**3**	2
vacuolar ATP synthase (subunit A)	CE22210	521	**12**	7	**24**	3	**16**	1	**11**	5	**7**	0
vacuolar ATP synthase (subunit A)	CE22210	218	**27**	7	**34**	7	**17**	9	**18**	4	**17**	8
vacuolar ATP synthase (subunit A)	CE22210	266	**43**	11	**32**	13	**35**	14	**37**	9	**30**	3
vacuolar ATP synthase (subunit B)	CE04424	94	**6**	2	**9**	5	**7**	3	**6**	1	**9**	3
vacuolar ATP synthase (subunit B)	CE04424	33	**0**	1	**6**	6	**5**	10	**6**	7	**8**	9
vacuolar proton pump (subunit G)	CE10604	104	**8**	12	**5**	4	**3**	5	**1**	3	**4**	6
vigilin	CE23530	1063	**14**	6	**20**	6	**10**	9	**16**	6	**4**	4
vigilin	CE23530	666	**31**	10	**21**	5	**22**	0			**19**	9
vinculin	CE31398	336	**13**	8	**14**	3	**16**	6	**25**	4	**24**	5
vitellogenin-2	CE41109	627			**10**	9	**14**	10	**9**	6	**19**	3
vitellogenin-2	CE41109	1489/ 1498					**72**	11	**63**	8	**77**	4
vitellogenin-3	CE20900	626					**9**	5	**67**	10	**77**	7
vitellogenin-4	CE26817	206			**84**	3	**78**	9	**70**	5	**75**	10
vitellogenin-4	CE26817	1474					**12**	12	**7**	2	**5**	5
vitellogenin-6	CE28594	218					**81**	9	**74**	13	**74**	4
vitellogenin-6	CE28594	384			**5**	2	**7**	5	**3**	2	**4**	1
vitellogenin-6	CE28594	468					**72**	15	**70**	12	**84**	1
vitellogenin-6	CE28594	655			**23**	8	**14**	4	**18**	3	**16**	4
vitellogenin-6	CE28594	1364					**31**	12	**17**	4	**34**	3
vitellogenin-6	CE28594	1417					**17**	12	**41**	5	**26**	1
vitellogenin-6	CE28594	1514			**48**	4	**52**	2				
vitellogenin-6	CE28594	1569			**88**	6	**82**	10	**68**	9	**75**	13
vitellogenin-6	CE28594	1479/ 1482							**84**	9	**61**	14
vitellogenin-6	CE28594	1645			**5**	3	**26**	11	**36**	9	**34**	13
WDR-23	CE23620	73	**2**	2	**3**	2	**1**	1	**2**	1	**4**	3
ZNF9	CE21045	37/40	**23**	13	**28**	11			**16**	12		

5 Review: -THE REDOXOME- PROTEOMIC ANALYSIS OF CELLULAR REDOX NETWORKS

Maike Thamsen[1], Ursula Jakob[1,2]

Curr Opin Chem Biol, *in press*

[1]Department of Molecular, Cellular, and Developmental Biology and [2]Program in Cellular and Molecular Biology, University of Michigan, Ann Arbor, MI, USA

5.1 Abstract

Redox-regulated proteins play fundamentally important roles not only during the defense of organisms against oxidative stress conditions but also as targets of cellular signaling events. This realization has spurred the development of proteomic techniques geared towards characterizing the redoxome; proteins with highly reactive cysteine residues, whose thiol oxidation state controls the function of the proteins, and by extension, the pathways they are part of. We will here summarize the most recent advances made in the field of redox proteomic analyses, aimed to elucidate the cellular redox networks that appear to control pro- and eukaryotic organisms.

5.2 Introduction

Cellular redox conditions set the pace for many processes, ranging from gene expression and protein translation to metabolism, proteostasis, cell signaling and apoptosis (Halliwell & Gutteridge, 2007). Thus it is not surprising that perturbations in redox homeostasis are associated with many different disease conditions, including cancer, type 2 diabetes, cardiovascular and neurodegenerative diseases, and aging (Stadtman, 2001; Valko *et al.*, 2007). Alterations in the cellular redox status or in the levels of specific reactive oxygen species (ROS) or nitrogen species (RNS) are most often sensed by proteins with redox-reactive cysteine residues, whose thiol oxidation states exert control over the activity of the proteins (Brandes *et al.*, 2009; Klomsiri *et al.*, 2010; Paulsen & Carroll, 2010). High levels of ROS are produced by cells of the innate immune system in response to bacterial infections, are found at sites of chronic inflammation, or are generated during many disease conditions, such as ischemic stroke (Miller & Britigan, 1997; Allen & Bayraktutan, 2009; Reuter *et al.*, 2010). High ROS levels trigger rapid oxidative activation of anti-oxidant transcription factors, including OxyR, Yap1p and Nrf2 (Antelmann & Helmann, 2010), activate redox-regulated chaperones, such as Hsp33 and peroxiredoxin (Jang *et al.*, 2004; Winter *et al.*, 2008), and alter the function of many redox-senitive metabolic enzymes, like GAPDH, to re-route metabolic fluxes important for the restoration of redox homeostasis (Brandes *et al.*, 2009). Low levels of ROS

are instead continuously produced by NADPH oxidases, by proteins of the mitochondrial electron transport chain and during oxidative protein folding in the endoplasmic reticulum (Veal *et al.*, 2007). At this low level, ROS act as signaling molecules to mediate localized signaling events via the oxidative modification of redox sensitive key players, including phosphatases (*e.g.,* phosphatase and tensin homologue, PTEN) and kinases (*e.g.,* JNK, PKC) (Tonks, 2005; Veal *et al.*, 2007; Dalle-Donne *et al.*, 2009).

The types of oxidative thiol modifications that affect redox-sensitive cysteines depend on the local protein environment of the thiol groups and the prevailing redox conditions. An increase in the ratio of oxidized to reduced glutathione (GSSG to GSH), for instance, leads most often to S-glutathionylation (-S-S-G). Presence of hydrogen peroxide (H_2O_2), peroxynitrite ($ONOO^-$) or hypochlorous acid (HOCl) commonly causes sulfenic (-SOH) acid formation (Dalle-Donne *et al.*, 2009; Burgoyne & Eaton, 2010). Although stable sulfenic acid formation has been demonstrated to occur in a number of redox sensitive proteins (*e.g.,* NADH peroxidase, GAPDH), their highly reactive nature often leads to further oxidation reactions with nearby thiols to form disulfide bonds (S-S) (Yeh *et al.*, 1996). Alternatively, sulfenic acids are further oxidized to sulfinic ($-SO_2H$) or sulfonic acids ($-SO_3H$) (Fig. 5-1). Due to the largely irreversible nature of these overoxidation reactions, however, these thiol modifications usually play only minor roles in controlling redox-regulated proteins and serve as biomarkers for oxidative protein damage (Dalle-Donne *et al.*, 2005). Presence of RNS has been shown to lead to S-nitrosylation (S-NO) in a large subset of redox-sensitive proteins (Foster *et al.*, 2009; Burgoyne & Eaton, 2010) (Fig. 5-1). Most oxidative thiol modifications are fully reversible *in vivo* and dedicated, highly conserved systems exist, which control the redox status of proteins and maintain the cellular redox homeostasis. Members of the thioredoxin family facilitate the reduction of sulfenated, nitrosylated and disulfide-bonded proteins (Koharyova & Kolarova, 2008), while glutaredoxins, such as Grx-1 reduce mixed disulfides with glutathione (Fig. 5-1) (Gallogly & Mieyal, 2007). Recently, a highly conserved class of sulfinic acid reductases (*i.e.,* sulfiredoxins) has been identified, which reduce overoxidized type 2 peroxiredoxins (Rhee *et al.*, 2007) and moonlight as de-glutathionylation enzymes (Findlay *et al.*, 2006). This ability to rapidly and reversibly modify structurally and/or functionally important cysteine thiols makes redox regulation an excellent mechanism to regulate protein activity on a posttranslational level. With the development of highly quantitative redox proteomic methods, which we will summarize below, we have now the possibility to globally identify these redox-regulated proteins, collectively called "*the redoxome*" (Chiappetta *et al.*, 2010), and further characterize the many redox-sensitive networks that appear to exist in the cell.

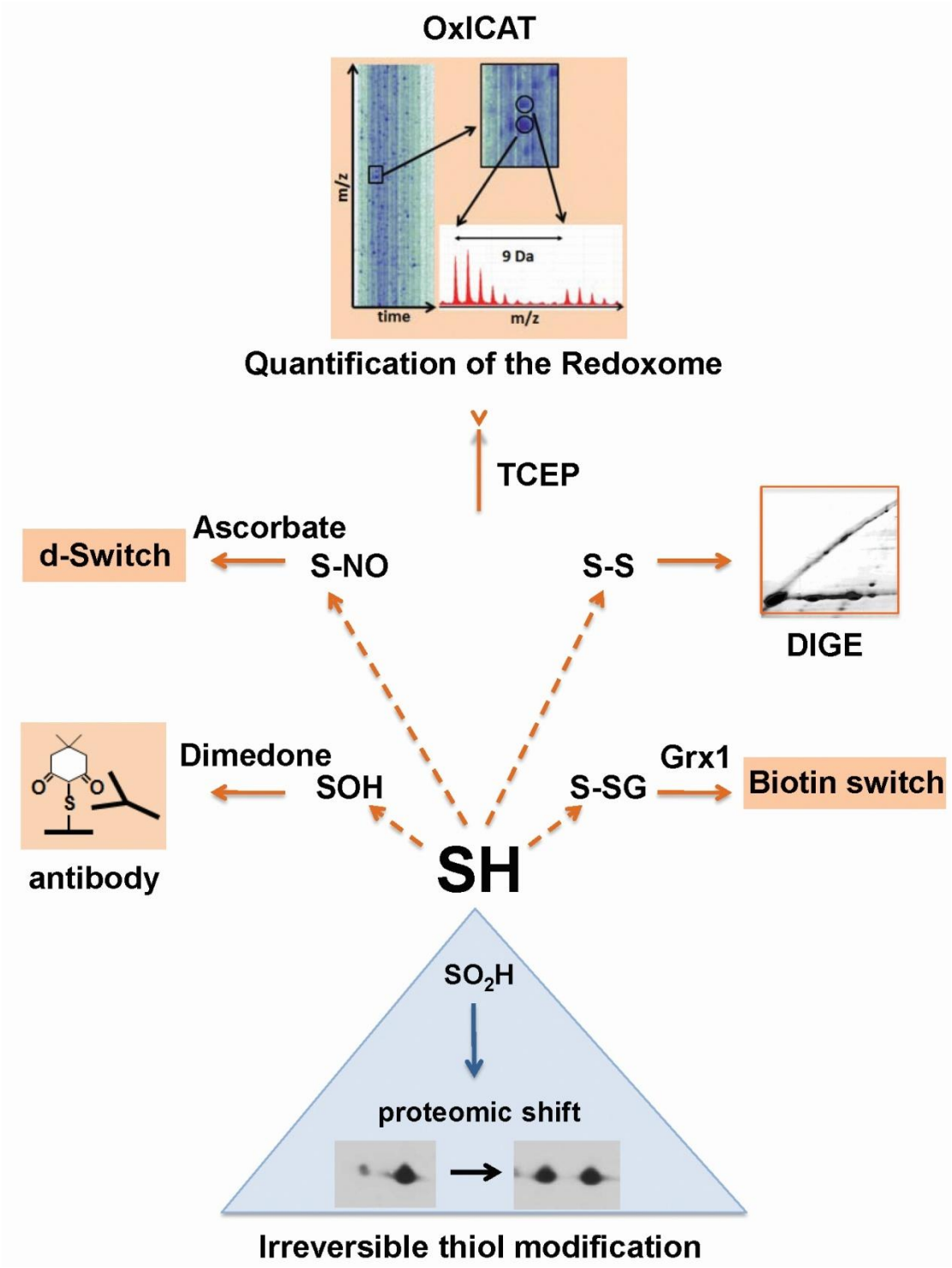

Figure 5-1 Select detection methods for oxidative cysteine modifications
Reversible oxidative thiol modifications include cysteine sulfenic acid (-SOH), which can be specifically labeled with dimedone or dimedone derivatives, and either visualized using dimedone specific antibodies, or enriched and subsequently identified (Leonard *et al.*, 2009; Seo & Carroll, 2009). Proteins containing disulfide bonds (-S-S-) can be visualized using diagonal gel electrophoresis (DIGE), in which proteins are first separated under non-reducing conditions, followed by a separation under reducing conditions in the second dimension (Leichert & Jakob, 2006). The biotin switch assay (see Fig. 2 for details) is commonly used for the detection of S-nitrosylated (-S-NO) and S-glutathionylated (-S-SG) proteins (Burgoyne & Eaton, 2010). Very recently, a quantitative mass spectrometric biotin switch assay termed "d-Switch" was introduced, which quantifies S-nitrosylations using mass

spectrometry (Sinha *et al.*, 2010). OxICAT, a quantitative mass spectrometric method, monitors the absolute oxidation status of hundreds of different protein thiols in a single experiment (Leichert *et al.*, 2008). Irreversible oxidation of cysteines to sulfinic acids (-SO_2H) can be visualized and quantified as shifts in the isoelectric point of proteins on 2D gels.

5.3 Detection and *in vivo* relevance of sulfenic acids

Sulfenic acids are highly reactive precursors for most known stable oxidative thiol modifications, and thus play a central role in redox-regulatory processes (Kettenhofen & Wood, 2010). In recent years, a number of innovative techniques have been developed to detect and identify proteins that show increased sulfenic acid formation (Kettenhofen & Wood, 2010). Some of the methods rely on the *ex vivo* reduction of sulfenic acids with arsenite, a variation of the biotin switch assay (BSA) that is outlined in detail below (Burgoyne & Eaton). Other methods make use of fluorescent- or affinity-tagged dimedone (5,5-dimethyl-1,3-cyclohexanedione) derivatives, which specifically alkylate and thereby tag sulfenic acids. Subsequent enrichment of the tagged proteins from complex samples allows their mass spectrometric identification (Nelson *et al.*, 2010). Another very powerful approach has recently been introduced by the Carroll lab, who developed DAz-2 (4-(3-azidopropyl)cyclohexane-1,3-dione), a highly membrane permeable dimedone derivative, which can be used to trap sulfenic acids as they form in the cell (Leonard *et al.*, 2009). DAz-2 labeled proteins were conjugated to phosphine-biotin via their azide group, purified and identified using LC-MS/MS. By using this method in HeLa cells, nearly all previously known sulfenic acid containing proteins were confirmed and more than 170 new candidate proteins were identified (Leonard *et al.*, 2009). In contrast to these methods, which rely on the interaction of protein sulfenic acids with small alkylating reagents, a protein-based assay was recently introduced as well (Takanishi *et al.*, 2007). This assay makes use of a small His-tagged peptide, derived from the oxidative stress transcription factor Yap1, which contains one highly reactive cysteine. This cysteine traps sulfenic acids in other proteins by forming intermolecular disulfides. Ni-affinity chromatography serves to purify and enrich the proteins, which are identified upon DTT-mediated release from the Yap1-peptide. Using targeted expression of the Yap1p-peptide, this approach opens up the possibility to detect protein sulfenic acids even in distinct sub-cellular compartments (Takanishi *et al.*, 2007). In addition, a sulfenic acid-specific antibody is now available, which allows the detection and profiling of sulfenic acids using protein microarrays and the direct visualization of sulfenic acids as they develop in the cell using microscopy (Seo & Carroll, 2009).

Taken together, detection of sulfenic acid-containing proteins has come a long way. However, a few major limitations still remain; the main concern is the instability of sulfenic acids, which makes them hard to trap. Identification of sulfenic acid containing proteins often requires their enrichment, which obscures any information about the extent to which a protein is actually sulfenated in the cell. Thus, the development of quantitative differential sulfenic acid trapping techniques is needed to distinguish between reduced, sulfenated or stably oxidatively modified cysteines within a protein population. Only then will we be able to differentiate between proteins that use sulfenic acid formation as final oxidation product, and proteins that use it as transient intermediate on their way to more stable oxidative thiol modifications. This distinction is crucial for our understanding of what sequence or structural features in proteins mediate the redox sensitivity of cysteine thiols and support the formation of stable oxidative modifications.

5.4 Biotin Switch Assay – Recent Advances to a Powerful Approach

Although semi-quantitative by nature, the biotin switch assay has greatly contributed to the elucidation of many redox-sensitive pathways in pro- and eukaryotic cells (Foster *et al.*, 2009; Burgoyne & Eaton, 2010). Countless S-nitrosylated, sulfenated proteins and S-glutathionylated proteins have been pulled out of complex protein mixtures by this approach. Originally introduced by Jaffrey and Snyder to identify S-nitrosylated proteins (Jaffrey & Snyder, 2001), and subsequently modified and optimized by numerous groups (see below), the principle behind this method is surprisingly simple (Fig. 5-2); free cysteines in complex protein mixtures are first alkylated using the reversible, thiol-specific alkylation reagent methyl methanethiosulfonate (MMTS) (Jaffrey & Snyder, 2001). Existing oxidative thiol modifications are then reduced and switched for the stable biotin, hence the name. The crucial step lies in the choice of reducing agents, which mediates the biotin switch; incubation with ascorbate/$CuCl_2$ (Wang *et al.*, 2008) or siapinic acid, an apparently more S-nitrosylation-selective reductant (Kallakunta *et al.*), is used to specifically reduce and subsequently label S-nitrosylated proteins. Arsenite has been shown to specifically liberate sulfenated cysteines (Saurin *et al.*, 2004) while incubation of the alkylated protein mixture with glutaredoxin (Grx) triggers the specific reduction of S-glutathionylated cysteines (Shelton *et al.*, 2005) (Fig. 5-2). The biotin-tagged proteins are then either visualized by western blot and/or enriched for by affinity purification and subsequently identified (Burgoyne & Eaton, 2010).

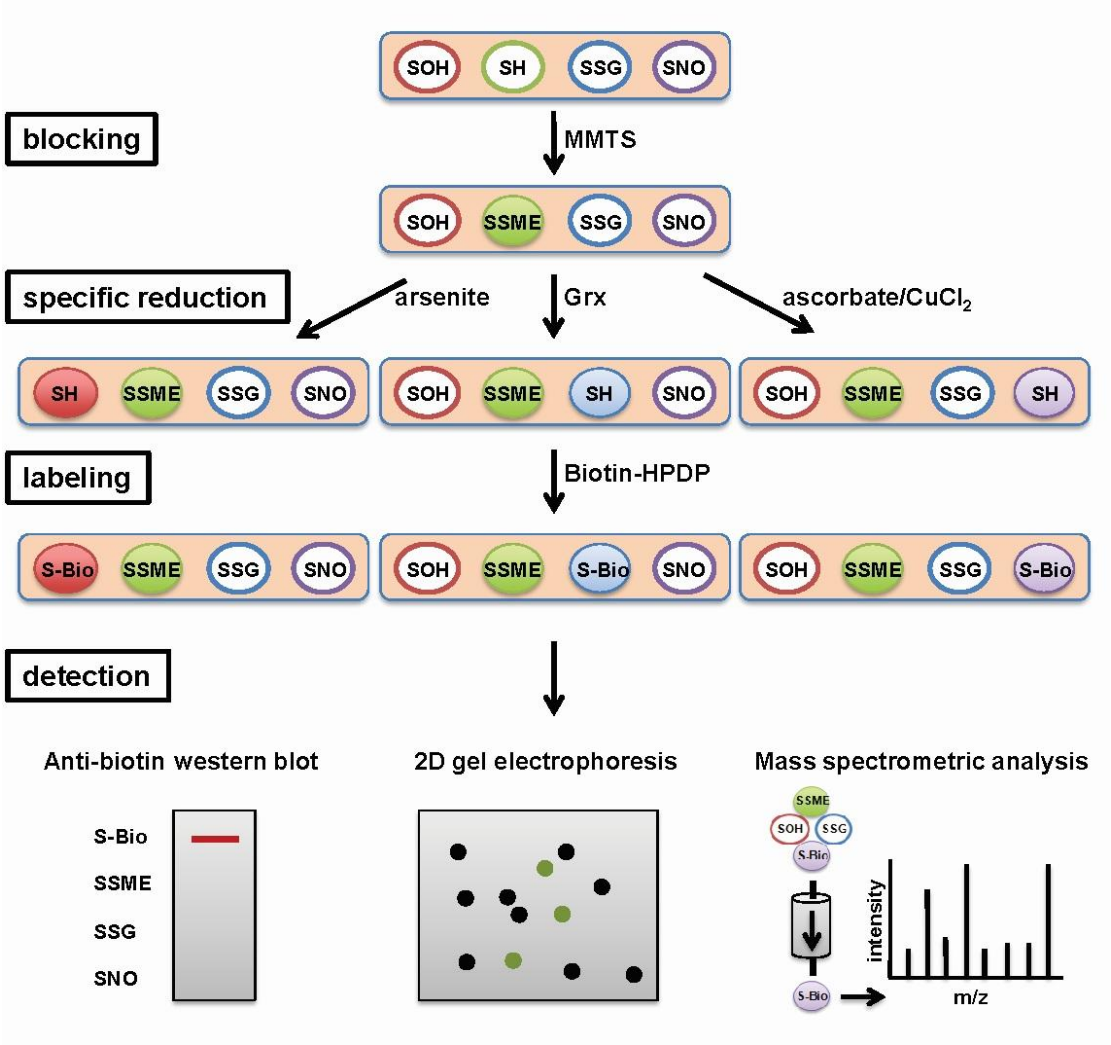

Figure 5-2 Detection of specific cysteine modifications - the biotin switch assay
To detect sulfenated, nitrosated or glutathionylated proteins in cell lysates, samples are first incubated with the reversible thiol-alkylating reagent MMTS to block all free thiols. Then, depending on the type of cysteine modification present, proteins are either incubated with arsenite to reduce sulfenic acids, with ascorbate to reduce S-nitrosylations or with the small protein glutaredoxin (Grx) to reduce S-glutathionylated cysteines. These cysteine thiols are subsequently labeled with biotin-HPDP, thus tagging only those proteins, which originally contained the thiol modification. Proteins are then separated on 1D or 2D gels and biotinylated proteins are detected by western blot analysis using antibodies against biotin, or enriched by affinity chromatography and identified by MS analysis.

The realization that numerous important proteins and cellular pathways are regulated by S-nitrosylation drove the development of many variations on the biotin switch assay theme, some simply to increase sensitivity and detection of S-nitrosylated proteins, others to aid in the identification of the affected cysteines and the quantification of S-nitrosylation. The fluorescence-switch method, for instance, uses fluorescein-5-maleimide instead of biotin to label, visualize and identify nitrosylated proteins in endothelial cells using 2D gels (Tello *et al.*, 2009). The irreversible biotinylation procedure (*i.e.,* IDP) introduced the use of the irreversible isotope-coded affinity tag (ICAT) labeling to identify S-

nitrosylated cysteines using LC-MS/MS (Huang & Chen). In SNO-SID (*i.e.,* S-NO identification), a proteolytic cleavage step was introduced to enrich for only those peptides that previously carried the modification, an advance that led to the identification of nearly 70 nitrosylated peptides in rat cerebellum lysates (Hao *et al.*, 2006). The related SNO-RAC technique went a step further by incorporating quantitative iTRAQ tags to the purified peptides, which allowed the first quantitative comparison of nitrosylation profiles in various samples (Forrester *et al.*, 2009). Finally, in 2010, the *d-Switch* method was introduced, which allows the quantification of S-nitrosylation at distinct sites in proteins using a differential thiol trapping approach combined with quantitative mass spectrometry (see below) (Sinha *et al.*).

Although the biotin switch assay has been instrumental in identifying many oxidatively modified proteins in complex protein mixtures, its development has seen its share of challenges. Ascorbate, for instance, appears to reduce not only S-nitrosylations but also "soft" cysteine modifications, including sulfenic acids and even disulfide bonds (Giustarini *et al.*, 2008), and was found to require $CuCl_2$ to increase its sensitivity (Wang *et al.*, 2008). The reversible thiol blocking reagent MMTS has been suggested to not only alkylate cysteines but to potentially even introduce oxidative thiol modifications into proteins (Karala & Ruddock, 2007). These concerns illustrate how methods, as simple as they initially seem, require constant re-evaluation and improvement, and warrant the careful verification of identified oxidative thiol modifications by alternative strategies. Despite these labor pains, however, it is now clear that S-nitrosylated and S-glutathionylated proteins are involved in dozens of different cell signaling pathways, a realization that would not have been possible without this powerful method.

5.5 The Quantitative Redoxome – Determining the Thiol Oxidation State *in vivo*

One major advance in determining the *in vivo* thiol oxidation status of proteins came with the introduction of acid-trapping techniques, where cells are lysed with acids like trichloroacetic acid (Hansen & Winther, 2009). Since rates of thiol-disulfide exchange reactions decrease 10-fold for each pH unit below the cysteine's pK_a value, low pH incubation effectively "freezes" the *in vivo* thiol oxidation status and prevents oxidation artifacts during cell lysis. Subsequent modification of all accessible thiol groups and comparison with the thiol oxidation status of proteins in control samples has contributed significantly to the view that proteins can undergo reversible thiol modifications *in vivo.* However, many of these initial studies failed to identify the affected cysteine(s), and, even

more importantly, none were able to determine the absolute oxidation status of the cysteines. Yet this information is crucial to evaluate how oxidative thiol modification might affect the structure or function of the respective protein, and to assess whether a large enough population of any given protein is affected to make a physiological impact in the cell. One major advance came with the establishment of differential thiol labeling techniques, in which all reduced cysteines are first labeled with one alkylating agent, while all oxidized cysteines are, after their reduction, labeled with either another variant of the same reagent or a different alkylating reagent (Leichert & Jakob, 2004; Riederer & Riederer, 2007) (Fig. 5-3). In combination with 2D gels, this strategy provided information about the relative amount of oxidized protein over total protein, and redox changes could be expressed as fold-changes in oxidation status. This semi-quantitative technology has been successfully used to identify many redox sensitive proteins in bacteria, yeast and higher organisms, to determine the substrate proteins of many pro- and eukaryotic oxidoreductases, and to monitor changes in the redox status of proteins in response to disease conditions and aging (Leichert & Jakob, 2004; Le Moan *et al.*, 2006; Marino *et al.*, 2010; Perez *et al.*, 2010).

An important recent advance came with the realization by us and others that the highly quantitative ICAT, which comes in an isotopically light 12C-ICAT form and a 9 Da heavier 13C-ICAT form, is a thiol specific-trapping reagent and thus suitable for a quantitative redox proteomic approach (Leichert *et al.*, 2008; Go *et al.*, 2009) (Fig. 5-3). In this method, which we termed OxICAT, reduced cysteines are labeled with light ICAT, while all previously oxidized cysteines are upon reduction labeled with heavy ICAT. This differential labeling causes a mass difference of 9 Da or multiples of 9 Da depending on the number of oxidized cysteines. The biotin-moiety of the ICAT reagent allows the enrichment of only cysteine-containing peptides, which are then separated by HPLC and identified using MS and tandem MS analysis (Fig. 5-3). Mass spectrometric analysis not only provides the identification of the peptide and of the redox sensitive cysteine, but at the same time, delivers the exact oxidation status of the cysteine-containing peptides. Because both light and heavy labeled peptides are chemically identical, they co-elute from the HPLC and fly to the same extent in the mass spectrometer. Thus, mass peaks that are precisely 9 Da or multiples of 9 Da apart correspond to the reduced and oxidized species of the peptide, with the respective peak areas reflecting their true *in vivo* distribution (Fig. 5-3). By using the OxICAT method (Leichert *et al.*, 2008), the absolute oxidation status of thousands of individual thiols can be monitored and quantified in a single experiment. OxICAT is widely applicable and has been used to determine the steady-state redox status of high abundance

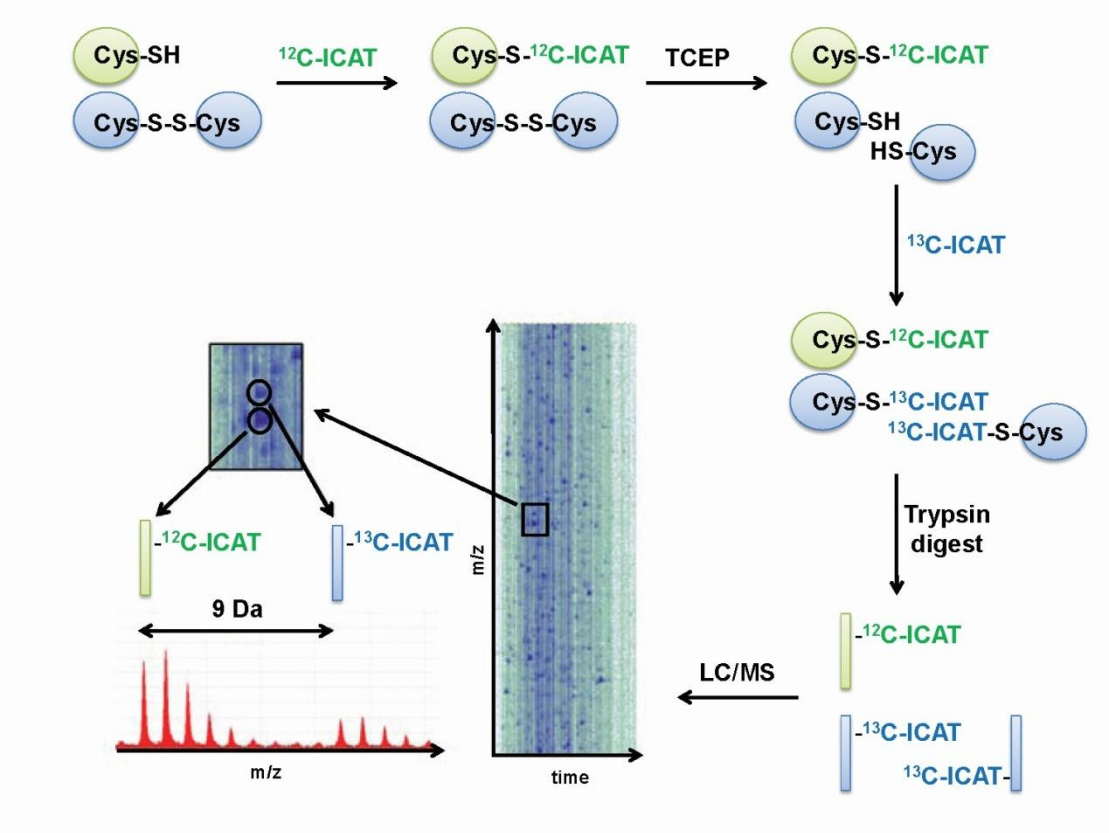

Figure 5-3 OxICAT – Identification of the redoxome
Cells or tissues are harvested on TCA to maintain the *in vivo* thiol redox status of the proteins. Protein samples are incubated with light ^{12}C-ICAT under protein-denaturing conditions to label all reduced protein thiols. Light ICAT is removed, and, after reduction with the general reductant TCEP, all previously oxidized proteins are labeled with the 9 Da heavier ^{13}C-ICAT. The differentially labeled proteins are digested with trypsin, enriched by affinity chromatography, separated by HPLC (LC) and identified by MS and tandem MS analysis. A graphical representation of an LC/MS run is shown. The cysteine-containing peptide of a protein that was partially oxidized *in vivo* co-elutes as an ICAT pair from the HPLC (inset). Analysis of the mass spectrum reveals two mass peaks, which are precisely 9 Da apart, corresponding to the light and heavy-labeled version of the peptide. Because the ICAT-labeled peptides are chemically identical, their behavior in the mass spec is identical and the relative signal intensity of the two peaks can be used to determine the absolute oxidation status of the cysteine *in vivo*. Tandem MS analysis is then used to identify the peptide and the cysteine(s) affected.

proteins in the nucleus, to identify oxidation-sensitive proteins in uni- and multicellular organisms (*e.g., E. coli*, *C. elegans*), and to characterize and determine the redox sensitivity of defined proteins both *in vitro* and *in vivo* (Leichert *et al.*, 2008) (Go *et al.*, 2009; Yi *et al.*, 2009; Kumsta *et al.*, 2010). While this method is very powerful and provides the exact oxidation states for thousands of peptides at the same time, many of which can be identified by MS/MS analysis, its analysis is time-consuming. An slightly less quantitative alternative is the comparative ICAT-analysis, which assesses the relative oxidation status of protein thiols between samples (Sethuraman *et al.*, 2004; Fu *et al.*, 2008; Hagglund *et al.*, 2008). Reduced cysteines from one sample are labeled with light ICAT, while the reduced cysteines of the other sample are labeled with heavy ICAT. Like in other quantitative proteomics approaches,

the samples are then mixed in equal ratios and any deviation from the expected equal signal intensity of ICAT pairs is interpreted as a potential change in the oxidation status of the corresponding peptide. However, since alterations in the steady-state peptide concentration lead to similar results, additional control experiments are necessary to confirm the redox sensitivity of the identified proteins.

5.6 Conclusions

Over the last decade, tremendous progress in the field of redox proteomics has been made. Hundreds of proteins have been identified, which use reversible thiol modifications to adjust their functions to the prevailing redox conditions and ROS levels in the cell, coining the term "Redoxome" (Chiappetta *et al.*, 2010). By developing methods for the identification and quantification of oxidative cysteine modifications, many new insights in the field of redox-regulation have been gained. It is now clear that complex cellular pathways can be controlled by the redox status of as little as one single cysteine (*e.g.,* active site cysteine in GAPDH), and that disturbances of the cellular redox homeostasis have severe physiological consequences, associated with an increasing number of pathological conditions. By applying these new quantitative tools to model systems and disease models, we have now the opportunity to ask more sophisticated questions about cause and effects of redox alterations, aimed to improve antioxidant therapies and intervention strategies with the ultimate goal to maintain cellular redox homeostasis.

5.7 References

Allen CL & Bayraktutan U (2009) Oxidative stress and its role in the pathogenesis of ischaemic stroke. *Int J Stroke* **4**, 461-470.

Antelmann H & Helmann JD (2010) Thiol-based redox switches and gene regulation. *Antioxid Redox Signal*.

Brandes N, Schmitt S & Jakob U (2009) Thiol-based redox switches in eukaryotic proteins. *Antioxid Redox Signal* **11**, 997-1014.

Burgoyne JR & Eaton P (2010) A rapid approach for the detection, quantification, and discovery of novel sulfenic acid or S-nitrosothiol modified proteins using a biotin-switch method. *Methods Enzymol* **473**, 281-303.

Chiappetta G, Ndiaye S, Igbaria A, Kumar C, Vinh J & Toledano MB (2010) Proteome screens for Cys residues oxidation: the redoxome. *Methods Enzymol* **473**, 199-216.

Dalle-Donne I, Rossi R, Colombo G, Giustarini D & Milzani A (2009) Protein S-glutathionylation: a regulatory device from bacteria to humans. *Trends Biochem Sci* **34**, 85-96.

Dalle-Donne I, Scaloni A, Giustarini D, Cavarra E, Tell G, Lungarella G, Colombo R, Rossi R & Milzani A (2005) Proteins as biomarkers of oxidative/nitrosative stress in diseases: the contribution of redox proteomics. *Mass Spectrom Rev* **24**, 55-99.

Forrester MT, Thompson JW, Foster MW, Nogueira L, Moseley MA & Stamler JS (2009) Proteomic analysis of S-nitrosylation and denitrosylation by resin-assisted capture. *Nat Biotechnol* **27**, 557-559.

Foster MW, Hess DT & Stamler JS (2009) Protein S-nitrosylation in health and disease: a current perspective. *Trends Mol Med* **15**, 391-404.
Fu C, Hu J, Liu T, Ago T, Sadoshima J & Li H (2008) Quantitative analysis of redox-sensitive proteome with DIGE and ICAT. *J Proteome Res* **7**, 3789-3802.
Gallogly MM & Mieyal JJ (2007) Mechanisms of reversible protein glutathionylation in redox signaling and oxidative stress. *Curr Opin Pharmacol* **7**, 381-391.
Giustarini D, Dalle-Donne I, Colombo R, Milzani A & Rossi R (2008) Is ascorbate able to reduce disulfide bridges? A cautionary note. *Nitric Oxide* **19**, 252-258.
Go YM, Pohl J & Jones DP (2009) Quantification of redox conditions in the nucleus. *Methods Mol Biol* **464**, 303-317.
Hagglund P, Bunkenborg J, Maeda K & Svensson B (2008) Identification of thioredoxin disulfide targets using a quantitative proteomics approach based on isotope-coded affinity tags. *J Proteome Res* **7**, 5270-5276.
Halliwell B & Gutteridge JMC (2007) *Free radicals in biology and medicine*, 4th ed. Oxford ; New York: Oxford University Press.
Hansen RE & Winther JR (2009) An introduction to methods for analyzing thiols and disulfides: Reactions, reagents, and practical considerations. *Anal Biochem* **394**, 147-158.
Hao G, Derakhshan B, Shi L, Campagne F & Gross SS (2006) SNOSID, a proteomic method for identification of cysteine S-nitrosylation sites in complex protein mixtures. *Proc Natl Acad Sci U S A* **103**, 1012-1017.
Huang B & Chen C Detection of protein S-nitrosation using irreversible biotinylation procedures (IBP). *Free Radic Biol Med* **49**, 447-456.
Jaffrey SR & Snyder SH (2001) The biotin switch method for the detection of S-nitrosylated proteins. *Sci STKE* **2001**, pl1.
Jang HH, Lee KO, Chi YH, Jung BG, Park SK, Park JH, Lee JR, Lee SS, Moon JC, Yun JW, Choi YO, Kim WY, Kang JS, Cheong GW, Yun DJ, Rhee SG, Cho MJ & Lee SY (2004) Two enzymes in one; two yeast peroxiredoxins display oxidative stress-dependent switching from a peroxidase to a molecular chaperone function. *Cell* **117**, 625-635.
Kallakunta VM, Staruch A & Mutus B Sinapinic acid can replace ascorbate in the biotin switch assay. *Biochim Biophys Acta* **1800**, 23-30.
Karala AR & Ruddock LW (2007) Does s-methyl methanethiosulfonate trap the thiol-disulfide state of proteins? *Antioxid Redox Signal* **9**, 527-531.
Kettenhofen NJ & Wood MJ (2010) Formation, Reactivity, and Detection of Protein Sulfenic Acids. *Chem Res Toxicol*.
Klomsiri C, Karplus PA & Poole LB (2010) Cysteine-Based Redox Switches in Enzymes. *Antioxid Redox Signal*.
Koharyova M & Kolarova M (2008) Oxidative stress and thioredoxin system. *Gen Physiol Biophys* **27**, 71-84.
Kumsta C, Thamsen M & Jakob U (2010) Effects of Oxidative Stress on Behavior, Physiology, and the Redox Thiol Proteome of Caenorhabditis elegans. *Antioxid Redox Signal*.
Le Moan N, Clement G, Le Maout S, Tacnet F & Toledano MB (2006) The Saccharomyces cerevisiae proteome of oxidized protein thiols: contrasted functions for the thioredoxin and glutathione pathways. *J Biol Chem* **281**, 10420-10430.
Leichert LI, Gehrke F, Gudiseva HV, Blackwell T, Ilbert M, Walker AK, Strahler JR, Andrews PC & Jakob U (2008) Quantifying changes in the thiol redox proteome upon oxidative stress *in vivo*. *Proc Natl Acad Sci U S A* **105**, 8197-8202.
Leichert LI & Jakob U (2004) Protein thiol modifications visualized *in vivo*. *PLoS Biol* **2**, e333.
Leichert LI & Jakob U (2006) Global methods to monitor the thiol-disulfide state of proteins *in vivo*. *Antioxid Redox Signal* **8**, 763-772.
Leonard SE, Reddie KG & Carroll KS (2009) Mining the thiol proteome for sulfenic acid modifications reveals new targets for oxidation in cells. *ACS Chem Biol* **4**, 783-799.
Marino SM, Li Y, Fomenko DE, Agisheva N, Cerny RL & Gladyshev VN (2010) Characterization of surface-exposed reactive cysteine residues in Saccharomyces cerevisiae. *Biochemistry* **49**, 7709-7721.
Miller RA & Britigan BE (1997) Role of oxidants in microbial pathophysiology. *Clin Microbiol Rev* **10**, 1-18.

Nelson KJ, Klomsiri C, Codreanu SG, Soito L, Liebler DC, Rogers LC, Daniel LW & Poole LB (2010) Use of dimedone-based chemical probes for sulfenic acid detection methods to visualize and identify labeled proteins. *Methods Enzymol* **473**, 95-115.

Paulsen CE & Carroll KS (2010) Orchestrating redox signaling networks through regulatory cysteine switches. *ACS Chem Biol* **5**, 47-62.

Perez VI, Pierce A, de Waal EM, Ward WF, Bokov A, Chaudhuri A & Richardson A (2010) Detection and quantification of protein disulfides in biological tissues a fluorescence-based proteomic approach. *Methods Enzymol* **473**, 161-177.

Reuter S, Gupta SC, Chaturvedi MM & Aggarwal BB (2010) Oxidative stress, inflammation, and cancer: How are they linked? *Free Radic Biol Med*.

Riederer IM & Riederer BM (2007) Differential protein labeling with thiol-reactive infrared DY-680 and DY-780 maleimides and analysis by two-dimensional gel electrophoresis. *Proteomics* **7**, 1753-1756.

Saurin AT, Neubert H, Brennan JP & Eaton P (2004) Widespread sulfenic acid formation in tissues in response to hydrogen peroxide. *Proc Natl Acad Sci U S A* **101**, 17982-17987.

Seo YH & Carroll KS (2009) Profiling protein thiol oxidation in tumor cells using sulfenic acid-specific antibodies. *Proc Natl Acad Sci U S A* **106**, 16163-16168.

Sethuraman M, McComb ME, Huang H, Huang S, Heibeck T, Costello CE & Cohen RA (2004) Isotope-coded affinity tag (ICAT) approach to redox proteomics: identification and quantitation of oxidant-sensitive cysteine thiols in complex protein mixtures. *J Proteome Res* **3**, 1228-1233.

Shelton MD, Chock PB & Mieyal JJ (2005) Glutaredoxin: role in reversible protein s-glutathionylation and regulation of redox signal transduction and protein translocation. *Antioxid Redox Signal* **7**, 348-366.

Sinha V, Wijewickrama GT, Chandrasena RE, Xu H, Edirisinghe PD, Schiefer IT & Thatcher GR Proteomic and mass spectroscopic quantitation of protein S-nitrosation differentiates NO-donors. *ACS Chem Biol* **5**, 667-680.

Sinha V, Wijewickrama GT, Chandrasena RE, Xu H, Edirisinghe PD, Schiefer IT & Thatcher GR (2010) Proteomic and mass spectroscopic quantitation of protein S-nitrosation differentiates NO-donors. *ACS Chem Biol* **5**, 667-680.

Stadtman ER (2001) Protein oxidation in aging and age-related diseases. *Ann N Y Acad Sci* **928**, 22-38.

Takanishi CL, Ma LH & Wood MJ (2007) A genetically encoded probe for cysteine sulfenic acid protein modification *in vivo*. *Biochemistry* **46**, 14725-14732.

Tello D, Tarin C, Ahicart P, Breton-Romero R, Lamas S & Martinez-Ruiz A (2009) A "fluorescence switch" technique increases the sensitivity of proteomic detection and identification of S-nitrosylated proteins. *Proteomics* **9**, 5359-5370.

Tonks NK (2005) Redox redux: revisiting PTPs and the control of cell signaling. *Cell* **121**, 667-670.

Valko M, Leibfritz D, Moncol J, Cronin MT, Mazur M & Telser J (2007) Free radicals and antioxidants in normal physiological functions and human disease. *Int J Biochem Cell Biol* **39**, 44-84.

Veal EA, Day AM & Morgan BA (2007) Hydrogen peroxide sensing and signaling. *Mol Cell* **26**, 1-14.

Wang X, Kettenhofen NJ, Shiva S, Hogg N & Gladwin MT (2008) Copper dependence of the biotin switch assay: modified assay for measuring cellular and blood nitrosated proteins. *Free Radic Biol Med* **44**, 1362-1372.

Winter J, Ilbert M, Graf PC, Ozcelik D & Jakob U (2008) Bleach activates a redox-regulated chaperone by oxidative protein unfolding. *Cell* **135**, 691-701.

Yeh JI, Claiborne A & Hol WG (1996) Structure of the native cysteine-sulfenic acid redox center of enterococcal NADH peroxidase refined at 2.8 A resolution. *Biochemistry* **35**, 9951-9957.

Yi L, Jenkins PM, Leichert LI, Jakob U, Martens JR & Ragsdale SW (2009) Heme regulatory motifs in heme oxygenase-2 form a thiol/disulfide redox switch that responds to the cellular redox state. *J Biol Chem* **284**, 20556-20561